D6.2 From hazard to risk: models for the DEMOs - Part 6 -France -Brague catchment

Guillaume Piton, S. Dupire, Alexandre Mas, Roxane Marchal, David Moncoulon, Thomas Curt, Z.X. Wang, T. Onfroy, Jean-Marc Tacnet

Deliverable 6.2

From hazard to risk: models for the DEMOs

PART 6

France – Brague catchment

Pages: 215 – 344

CONTENTS

LIST OF FIGURES

LIST OF TABLES

An assessment framework for the estimation of nature-based solutions efficiency for flood hazard reduction in the Brague catchment

Abstract

Flash floods and torrential floods occur frequently in the Brague catchment, the last extreme event in Oct. 2015 was a large-scale disaster. Located in Southern France, the Brague catchment is challenged by flood hazards threatening residential and economic areas. Those living in flood-prone areas face the risk of severe damage to their infrastructures due to torrential floods eventually aggravated after forest wildfire, and those living outside flooded areas have to cope with runoff hazards. These natural disasters, although they are natural drivers of ecology and geomorphology, generate large losses to economy and human lives. Flood and fire risk analysis combined to nature-based solutions (NBS) are an opportunity to reduce vulnerability and to assess the value of NBS. This report aims at presenting the methodology developed in the Brague DEMO to assess the potential efficiency of nature-based solutions. The main strategies that will be investigated are a series of NBS spread along the river corridor in the lowlands where the largest number of assets and people is concentrated. However, a significant part of the catchment is still occupied by forests and a study of forest fire hazards and possible cascading consequences on floods in the lowlands will also be performed in order to raise the awareness of the current flood reduction ecosystem service of forests. The report is organized as follows: (i) fire hazards, (ii) hydrology (rainfall and runoff modelling), (iii) hydraulics, (iv) exposure based on insurance flood claims and (v) integrated flood protection schemes (assessment and portfolio of NBS).

Keywords: torrent, flood, wildfire, hazard, Brague, hydrology, hydraulics, NBS

1 Introduction

This chapter synthetizes the essence of following chapters.

1.1 General information

The Mediterranean Brague catchment is located in the Alpes-Maritimes Department and the Provences-Alpes-Côte-d'Azur region in South of France. It covers an area of 69 km². The floods of the Brague river have serious impact in the lowland, namely Biot and Antibes. NAIAD Deliverable 6.1 reviewed general information on catchment land use, hazards and assets
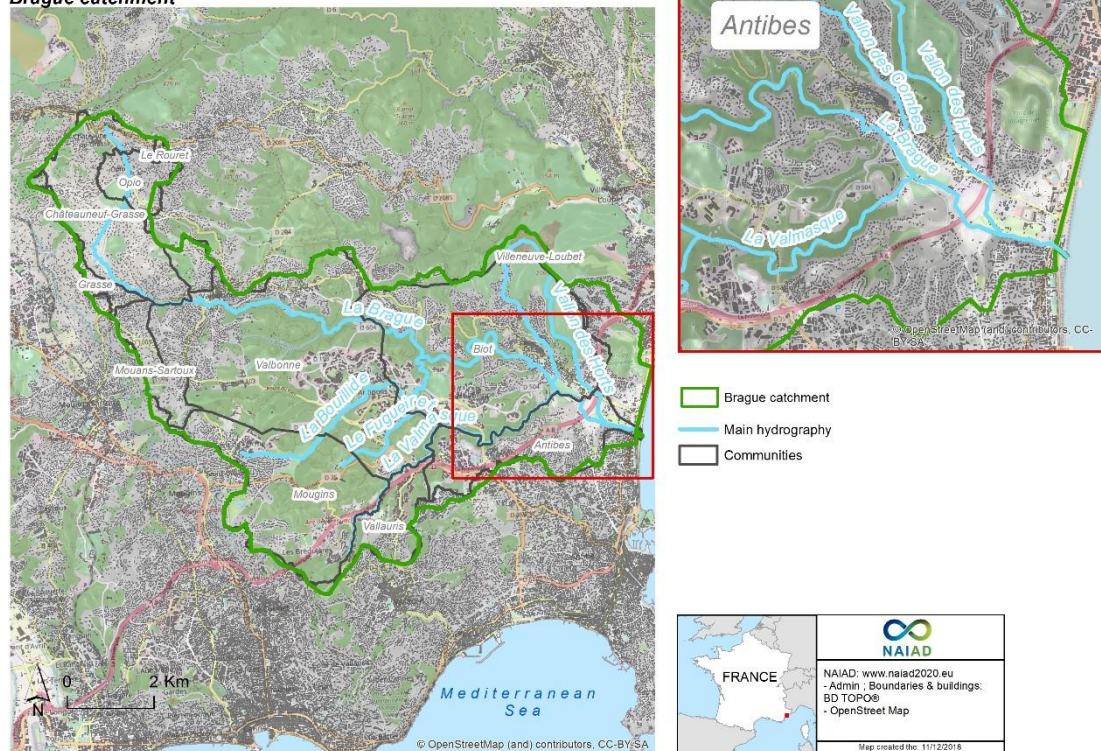
Figure 1 : Map of the Brague catchment

1.2 Wildfire hazards

Wildfire hazards were assessed in order to appraise the vulnerability of the flood protection ecosystem services to their main local natural threat. Using a multi-criteria method aggregating hydro-meteo and forest indicators, forest wildfire hazards were appraised as high on "average years" and extremely high on the whole catchment on "dry and hot years". A temporally increasing trend towards higher frequency of wildfire-prone days has also been detected.

Firefighters' data demonstrated that wildfire events are indeed common in the catchment but annual burnt areas remain low thanks to their efforts. However, the firefighters' capacities are limited and insufficient during particularly dry and hot years, when they are overwhelmed. This resulted in the occurrence of a few years when amount of burnt areas cumulated to more than 100 ha. Three wild fire scenarios were created based on expert assessment for later analysis of cascading hazards on floods and erosions: an average fire activity, a large fire activity as historically observed and a mega fire of the biggest continuous forest units of the catchment.

1.3   General information on flood risks

The Brague catchment is challenged by the exposure to intense flash and torrential floods generating large losses. In addition to these risks, surface water runoff also represents a strong risk. In the objective to understand flood risks, the 2015 October event is one of the best examples. The following table (Table 1) synthetizes the main consequences of the largest flood hitting the Brague catchment in the last decades. This disaster is used as reference disaster against which one would like to raise protective measures.

Table 1: Extrapolated costs for the Brague catchment of Oct. 2015 event (Source: Caisse Centrale de Réassurance, insurance database)

Features	Oct. 2015 disaster
Event name	Floods in South-East of France the 3rd October 2015 (code: G_201510_ICB_SUD_EST)
Hydro-Meteorological aspects	A depression has been developed in the Mediterranean Sea in the afternoon of the 3 October, generating violent thunderstorm in South-East of France. Large rainfalls (70 to 100mm in 24h), hail and strong winds (>100km/h) were recorded.
	20 people died during the event, 9 died within the communities of the Brague catchment.
	4 departments have been touched, within these departments, 10 communities were the most affected, including Biot, Antibes, Villeneuve-Loubet, Mougins, Vallauris.
Number of municipalities "NatCat" declaration	All damaged Departments: 68 Brague catchment: 11
Insured damages (M€)	Total event: M€520 Brague catchment: M€200 (extrapolated costs)
Number of claims & average costs (€) in Brague catchment	Total: 1410 & €30 900 Residential: 1141 & €21 500 Professional: 269 & €70 700

The experience proves that all assets located in flooded areas do not experience damages. This is related to what is sometimes called the exposure, which considers that only a certain percentage of assets is actually damaged. The reasons can be multiple, e.g. first floor elevation above the flood level, garden walls diverting the flows but neglected in the models, etc. An analysis of the CCR database and cross control with several flood mapping results were performed to analyse this exposure.

The experience proves that all assets located in flooded areas do not experience damages. This is related to what is sometimes called the exposure, which considers that only a certain percentage of assets is actually damaged. The reasons can be multiple, e.g. first floor elevation above the flood level, garden walls diverting the flows but neglected in the models, etc. An analysis of the CCR database and cross control with several flood mapping results were performed to analyse this exposure.

1.4 Hydrological modelling

A typical hydrological study has been performed with a state-of-the-art method called Shyreg that has been compared to existing data from technical reports as well as distributed runoff simulations using the CCR model chain. Special emphasis was put on reconstructing the Oct. 2015 event for new analysis and use in hydraulic models.

The hydrological functioning of catchment is strongly linked to its morphology, the soils features and the land use. Although the catchment morphology and the average soils features are assumed to remain stable over relevant time scales, the land use can change more frequently, for instance due to wildfire, urbanization, and/or changed forest management practices.

Changes in land use can lead to an increase or decrease in runoff and flood risk. To understand the impact of land use changes on the flood risk, the hydrological regime of France Mediterranean region catchments, where a significant change in land use was observed, were studied. This study, coupled with a literature review, provides information on the possible evolution of flood risk associated with the land use change.

The bibliography review proves that no sharp and obvious hydrological response was observed after land use changes, only more or less significant responses were reported in the literature. Consistently, our study of severely burned catchments in the south of France did not show any noticeable change in mean flows. However, further investigation of flood dynamics, remains to be conducted.

These results are incorporated into the Brague DEMO study. For this catchment, a method has been established to estimate floods of several return period at the sub-catchment scale. These design floods are used in a hydraulic model to map their impact in terms of flooded area and

associated potential costs. This approach, based on hydrological modelling, will make it possible to test different climate change scenarios (input of the method) and the effect of land use evolution (parameters of the method). These protection scenarios, based on conventional and nature-based solutions, will be used in later NAIAD deliverables and papers to rank the factors related to the evolution of the risk, but also to trial and test their robustness against external changes and to evaluate their potentials to reduce risks and their consequences.

1.5   Hydraulics

Two methods were used to appraise the hydraulics of the Brague catchment:

- A simple "0D" analysis focusing on flood in the town of Biot was first performed and a way to deal with it proposed. It offered a straightforward and educational protocol to quantify flood-mitigation capacities of protection strategies, targeted for effectiveness analysis and decision-making. It is based on the concept of flood-excess volume (FEV) i.e., volume exceeding a threshold and generating flood damage. The central question is: what fraction of FEV is reduced, and at what cost, by particular flood-mitigation measure?
- An accurate 2D depth-averaged modelling approach was also employed to study flood hazards in a much more detailed way. The software was selected for its capacity to compute the transport of large woody pieces. The data used to build and calibrate the model, particularly a campaign of data acquisition dedicated to large wood transport processes, was described. The calibration of the model is still in progress, hence only its principle has been described so far.

1.6   Protection strategies

Finally, comprehensive and integrated flood protection scenarios were tailored to the Brague lowlands, i.e., the Biot and Antibes municipalities. Three strategies were defined, the measures and works' locations were mapped and their implementations in the model defined theoretically but are still to be performed. This actual implementation will be performed during the last year of the NAIAD project and presented in subsequent deliverables. The three strategies were:

- o An NBS-based strategy with intermediate ambition that was likely feasible on the short term. It avoided houses and industrial building removal but widened the river bed and corridor wherever possible.
- o An NBS-based strategy of much higher ambition but with a higher impact on real estates and assets and thus likely feasible on a longer term.
- o A strategy based on large retention basins with a cumulated retention volume of more than 1 Mm^3 in order to deal with events similar to Oct. 2015.

These three protection strategies will be studied, modelled and evaluated in the later stages of the NAIAD project in order to perform cost-benefit analysis and multi-criteria assessment of their benefits, drawbacks and co-benefits.

2 Wildfires assessment methods

2.1 Time and spatial scales

A conceptual framework for depicting controls on fire at different scales is presented in Figure 2, which combines the traditional two "fire triangles" - Flame and Wildfire, with a broader scaled Fire Regime triangle. This framework was introduced and further developed by Moritz et al. (2005) and (2011). The scale of interest for the Brague catchment DEMO site is between the Wildfire and Fire Regime scales. In order to accurately characterize wildfire hazard in this DEMO the following information is needed: 1) Fire history for the area and vegetation affected, 2) Spatio-temporal analysis of the trends in the climate/weather component of fire hazard (fire weather hazard), 3) Estimation of the probability to experience an annual burned surface greater than or equal to different thresholds.
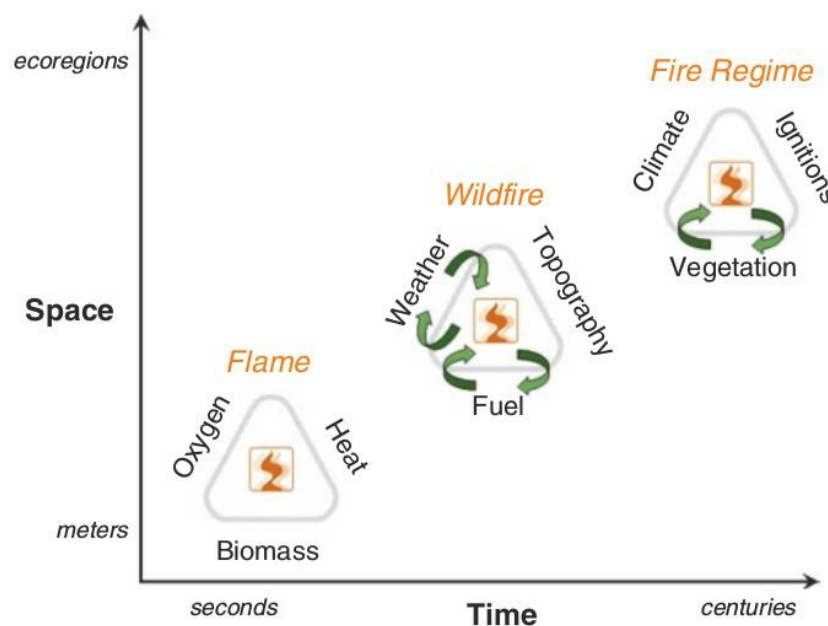
Figure 2 : Controls on fire at different scales of space and time. This framework adds a fire regime triangle (upper right) to the traditional triangles used to characterize combustion (lower left) and the fire environment (middle). Arrows represent feedbacks between fire and the forces controlling fire at different scales.

2.2   Vegetation types and fire history

2.2.1   Vegetation types

Brague catchment DEMO site is highly urbanized with about half of the territory covered by urbanized areas (Table 2) and the other half by vegetation.

Table 2 : Land cover on the DEMO site (extracted from Corine Land Cover and the IGN BDForet)

Land cover	Area [ha]	Proportion [%]
Total vegetation area	3295	47.3
Urban area	3300	47.3
Agricultural area	370	5.4
Total area	6965	100

Only four different forest types (the first four of Table 3) cover 91% of the vegetated surfaces and consequently, 90% of the fire activity. Forests are mainly located in the central area of the DEMO (black circle in Figure 3) where about 80% of the total vegetated area is located. This central forest entity has a limited number of discontinuities (mainly rivers and roads) and is surrounded by urban areas. This configuration may favour the ignitions of fires and their propagations over large surfaces.
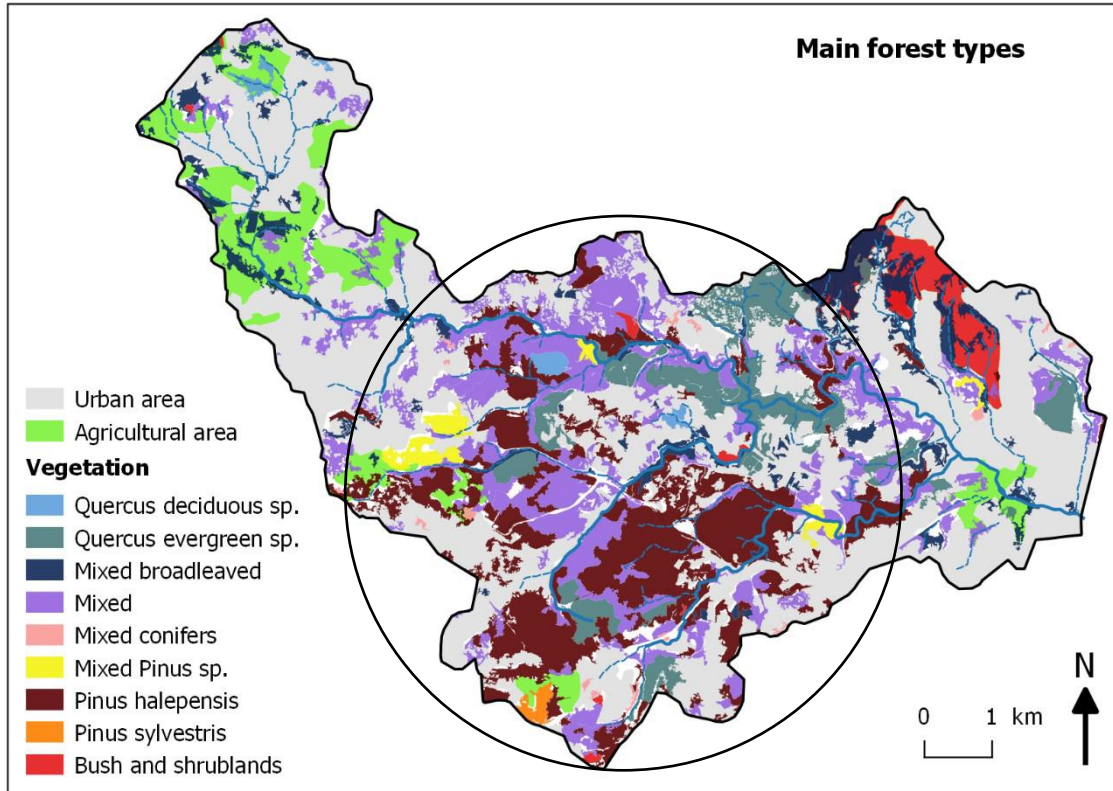
Figure 3 : Map of the land cover on the DEMO site (extracted from Corine Land Cover and the IGN BDForet)

Table 3 : Main forest types and fire activity

Forest type	Area [ha]	% of vegetation area [%]	% number of fires	% of the total burned surface
Mixed	**1112**	**33.8**	**39.2**	**36.9**
Pinus halepensis	**1017**	**30.9**	**24.2**	**25.7**
Quercus evergreen sp.	**448**	**13.6**	**5.3**	**7.8**
Mixed broadleaved	**415**	**12.6**	**20.6**	**20.5**
Bush and shrublands	149	4.5	3.0	1.8
Mixed Pinus sp.	75	2.3	2.0	2.3
Quercus deciduous sp.	41	1.2	2.0	2.3
Mixed conifers	21	0.6	3.4	1.5
Pinus sylvestris	17	0.5	0.4	1.3

2.2.2 Fire history

In 1973 the authorities launched the Prométhée (2018) database for the Mediterranean are, subject to many fires. The database collects data on wildland and forest fires with the indication of date, hour, size, and location on a 2x2 km grid.

The fire history analysis of the Brague catchment for the period between 1973 and 2016 returned 656 vegetation fires together contributing a total of 737 ha of burned surface. Moreover, the results suggest (Figure 4) that there is a dominant season for fires in the area which last from June to September (66% of the fires, 70% of the burned surfaces). It has to be noted than 7 forest fires that happened during this high season are responsible for 50% of the total burned areas in the last 44 years. A lower wildfire season can also be detected around the months of March and April (12% of the number of fires and 15% of the burned surface).
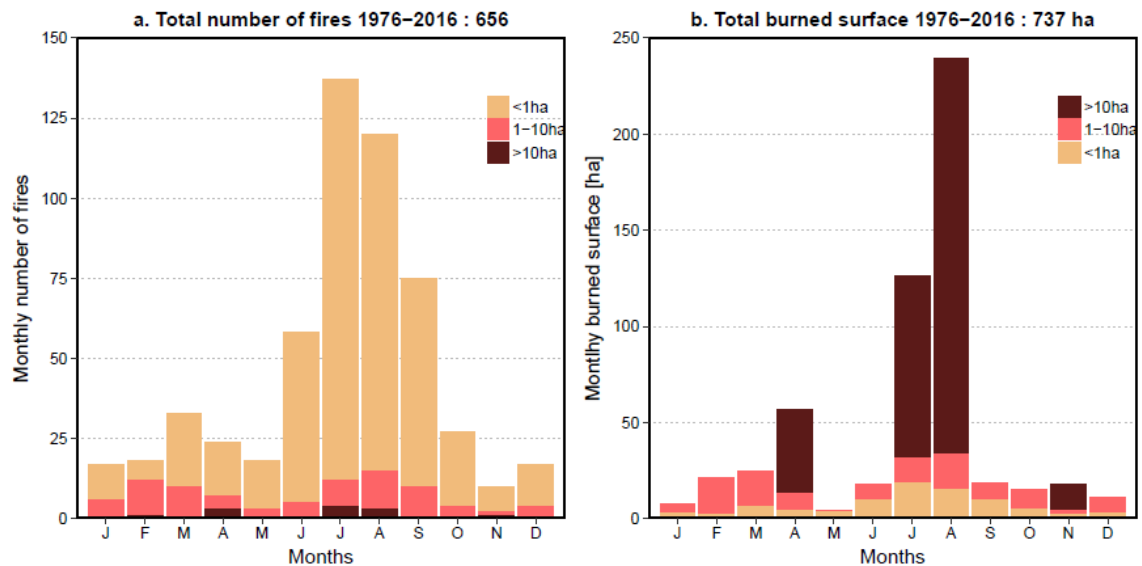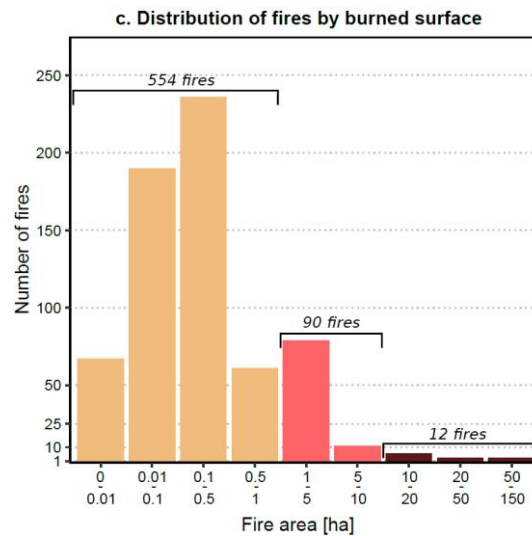
Figure 4 : Brague wildfire on the period 1976-2016: monthly distribution of (a) the number of fires, (b) burned surfaces and (c) distribution of burned surfaces in numbers.

The distribution of burned surfaces by fire events (Figure 4c) shows that most of the fires (85%) are quite small in area (<1ha) and cannot be responsible for a high loss of the forest cover. Only 12 forest fires covering at least 10ha and 3 events with at least 50ha burnet have been recorded in the 44-year period. Thus, moderate to large fires are not very common in the DEMO site.

The spatial distributions of annual fire frequency and burned surface ratio (burned surface divided by forest area) are shown in Figure 5. During the period 1981-2016, the average annual fire frequency is of 0.1 fire/year/km² with higher values observed at the centre of the DEMO site. The burned surface ratio observed over the 36-year period is relatively low (<5%) for 75% of the vegetated area.
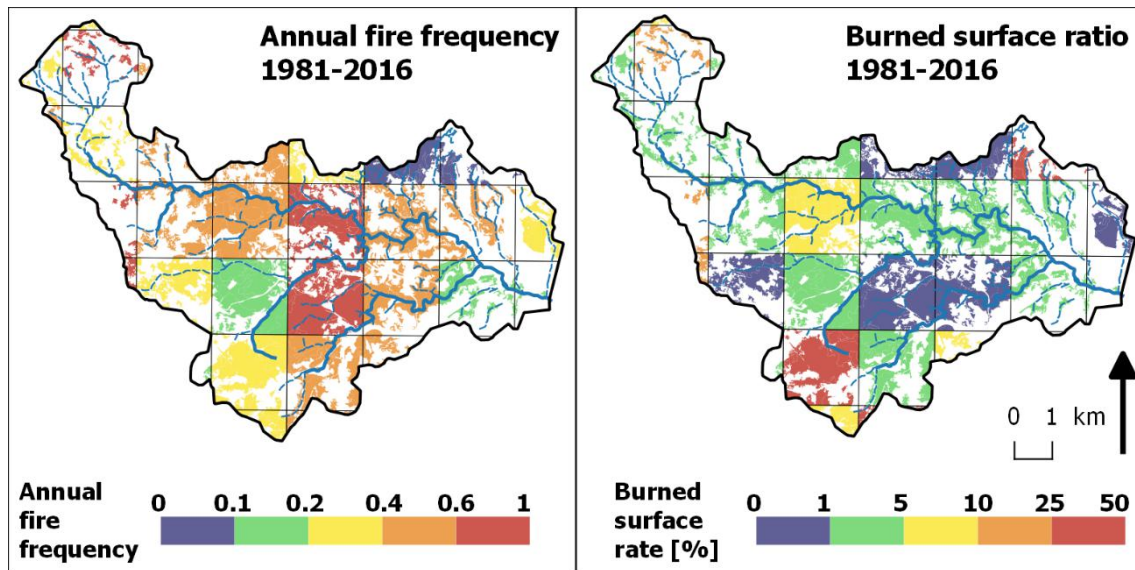
Figure 5 : Annual fire frequency and burned surface ratio for each square of the 2x2 km Prométhée grid during the period 1981-2016.

Table 4 : Proportion of the full catchment vegetation area according to fire frequency and burned surface ratio

Annual fire frequency	% of vegetation area [%]	Burned surface ratio	% of vegetation area [%]
<0.1	4.2	<1%	25.9
0.1-0.2	13.9	1-5%	50.6
0.2-0.4	18.4	5-10%	9.4
0.4-0.6	46.5	10-25%	2.4
0.6-1	17.0	25-50%	11.7

2.3   Fire weather hazard modelling

The climatic component of forest fires (fire weather hazard) drives the ease of fire ignition and propagation. Its spatio-temporal trends have been analysed on the DEMO site. The overall method is taken from Dupire et al. (2017).

2.3.1   Climatic data

The climatic data used in this study were taken from the Safran analysis system implemented by Météo France (Vidal et al. 2010). Safran computes vertical profiles of precipitation, temperature,

humidity, wind speed and cloudiness every day at noon (precipitation) or every 6 h (other variables).

2.3.2   Fire weather indices

At local scale and on a daily basis weather controls the moisture of fuels, thus their potential for ignition and propagation of fire. Consequently, many methods and indices have been produced to assess the daily wildfire risk based on meteorological data (Van Wagner 1987, Amatulli et al. 2013).

In this analysis, we used the Canadian Fire Weather Danger Rating System (hereafter "CFFDRS", see Van Wagner, 1987) defined by six daily meteorological-based indices, each one measuring a different aspect of fire danger (Figure 6).
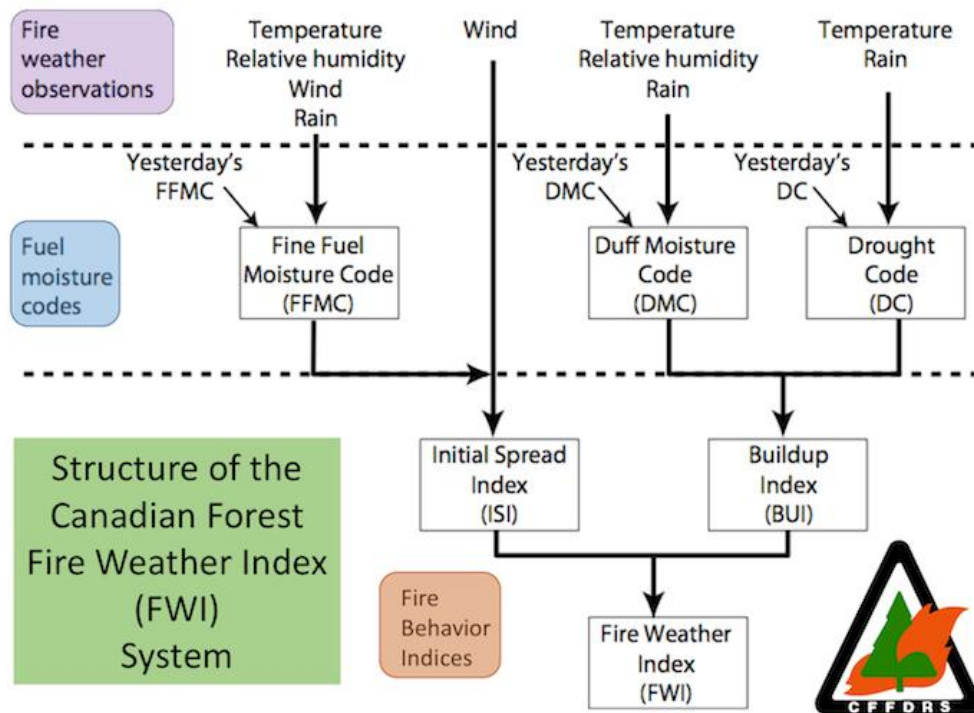
Figure 6 : Structure of the Canadian Fire Weather Danger Rating System (CFFDRS) indices

All CFFDRS indices were computed and their ranges of variation and statistical links with fire activity were compared. We finally focused on FWI and FFMC that performed better than the other indices. Moreover, the two indices are complementary as FWI is very integrative and indicates well the overall fire danger and the potential intensity of fire. FFMC detects minor

changes in fuel moisture content of surface fuels which are the first most likely to ignite and to burn.

2.3.3   Levels of fire weather danger

The analysis of the distribution of FWI and FFMC values on the days with a fire records in the Prométhée database was carried out in order to link fire activity with fire weather indices values (Figure 7). It allows the definition of 4 levels of fire weather danger according to 3 thresholds as proposed in Dupire et al. (2017).
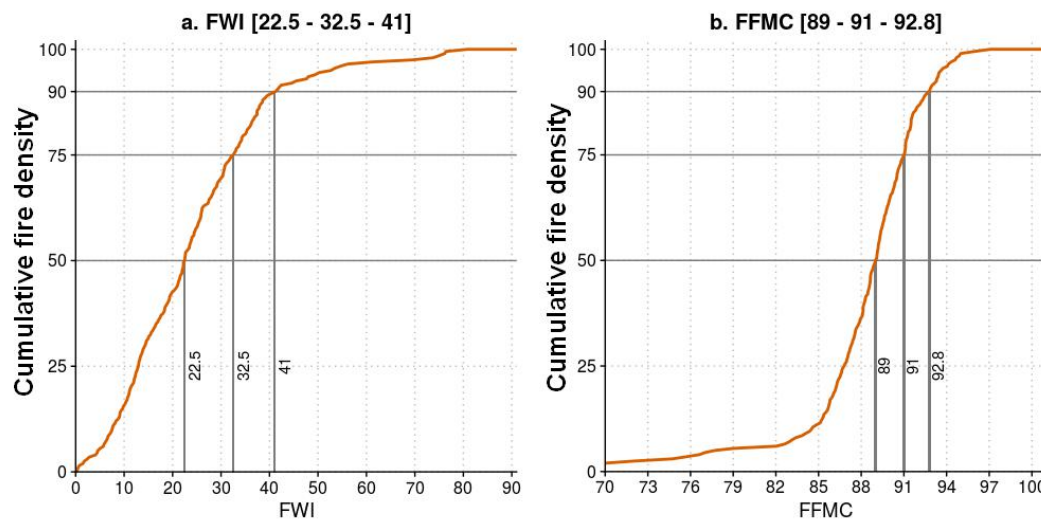
Figure 7 : Empirical cumulated distribution function curves of the (a) Fire Weather Index (FWI) and (b) Fine Fuel Moisture Code (FFMC) values encountered on the days of fire recorded in the Prométhée database. Figures in brackets represent the different thresholds defining the fire weather danger levels.

For the Brague catchment DEMO site, the different levels of fire weather danger are presented in Table 5.

Table 5 : Thresholds used for the definition of fire weather danger

Level of fire weather danger	FWI values	FFMC values
Low	< 22.5	< 89
Moderate	[22.5 – 32.5[	[89 – 91[
High	[32.5 –41[	[91 – 92.8[
Extreme	≥ 41	≥ 92.8

2.3.4   Spatio-temporal trends of fire weather hazard and link to fire activity

When analysing the number of days per year belonging to each fire weather danger class in the period 1973-2015, one can observe a temporal trend (Figure 8). The cumulated number of days per year with Fire Weather Index (FWI) and Fine Fuel Moisture Code (FFMC) values belonging to Moderate, High or Extreme ranges increased by 1.2 and 2.2 days/year, respectively. Despite an overall increasing trend of fire weather danger (on both FWI and FFMC indicators), the number of recorded fires does not present a significant trend over the period 1973-2015. The burned surface even follows an opposite trend with a reduction over the same period. This is due to an efficient firefighting strategy since the 90's with a systematic suppression of all ignitions occurring during the fire season (June to September).

On extremely dry years (e.g. 2003, 1986, 1974), some limitations of this fire suppression strategy are revealed, since these are the years with a peak in the annual burned surface and sometimes in the number of fires.

Figure 8 : Annual number of days with Fire Weather Index (FWI) and Fine Fuel Moisture Code (FFMC) exceeding thresholds, number of fires and burned surface on Brague catchment DEMO over the period 1973-2015. The temporal linear trend is shown with a dashed line if significant (the sum of all days of moderate to extreme fire weather is taken into account for FFMC and FWI temporal trends).

The values of FWI and FFMC for the average and extreme summers as well as their temporal linear trends are mapped in

Figure 9. Both FWI and FFMC already reach high values during a normal summer, but the entire DEMO site can experiment very high fire weather danger during extreme years. The fire weather danger increased in the entire area over the period 1973-2015, regardless of FWI or FFMC. Uphill areas (North-West of the maps) showed higher increases than downhill ones which is a common observation in the South-East of France (Dupire et al. 2017).
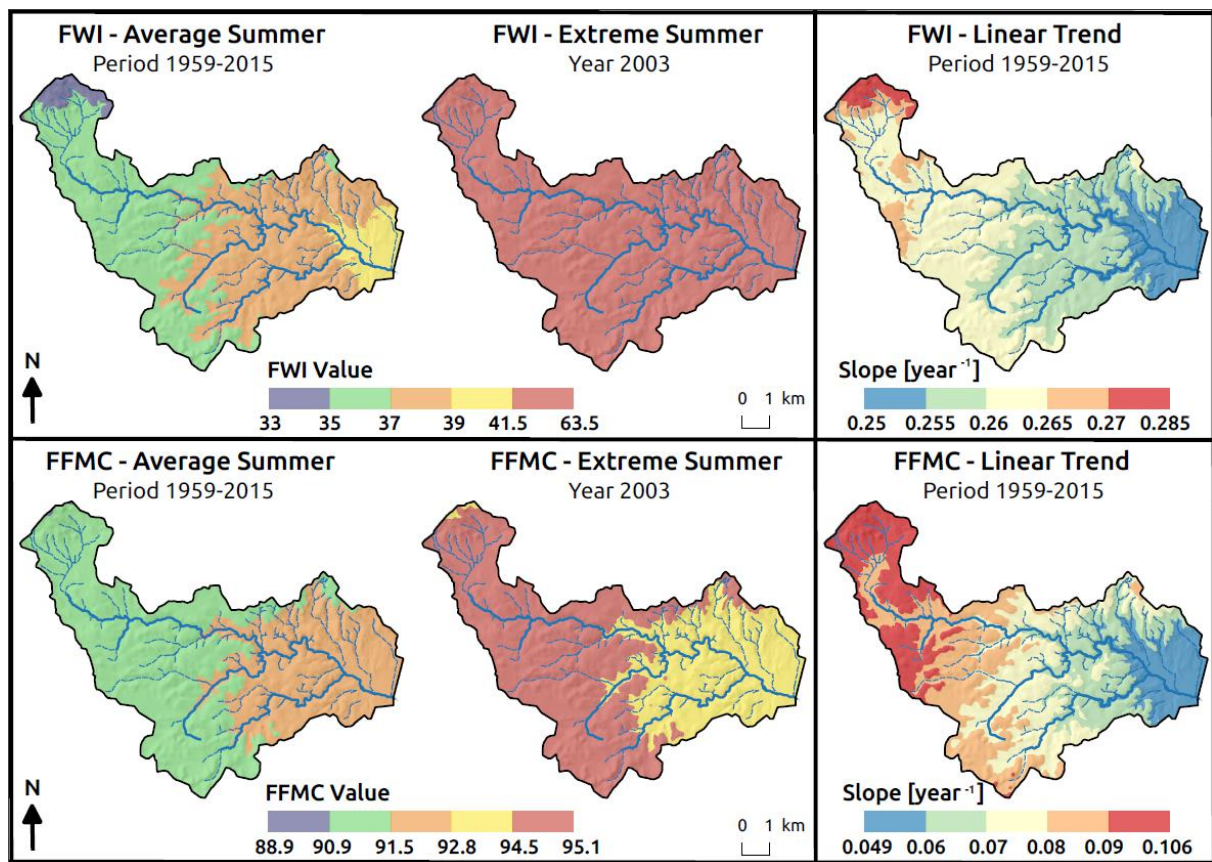
Figure 9 : Spatio-temporal evolution of Fire Weather Index (FWI) and Fine Fuel Moisture Code (FFMC) in Brague catchment DEMO

2.4   Fire scenarios for cascading effect assessment on hydrological processes

Three wildfire scenarios are defined in Table 4 with their associate annual burned surface and return period. Return periods were computed with extRemes R packages (Gilleland and Katz 2016) using a generalized Pareto model on the burned surface of the 656 fires on record from the DEMO area.

The first scenario corresponds to the average fire activity observed in the period 1973-2015 and the annual burned surface considered is 5.5ha for the whole DEMO area (median value of the annual burned surface). The return period associated to this scenario is 2 years (95% confidence interval in [1.5-3.5] years).

Table 6 : Proposed wildfire hazard scenarios

Forest fire scenario	Base of the choice	Annual burned surface [ha]	Return Period Year [95% ci]
Average fire activity 1973-2015	Median value of annual burned surface	5.5 ha	2 [1.5 – 3.5]
Big fire activity	95th percentile	100 ha	60 [27-100]
Mega-fire	Area of the 2 biggest continuous forest entities (Fig.8)	700 ha	720 [215-1200]

The second scenario corresponds to the highest fire activity observed in the period 1973-2015. The annual burned surface considered is 100ha for the whole DEMO area (95th percentile of the annual burned surface). The return period associated to this scenario is 60 years (95% confidence interval in [27-100] years).

Finally, the third scenario corresponds to a theoretical exceptional fire activity. The annual burned surface considered is 700ha for the whole DEMO area, which corresponds to the average area of the two biggest continuous forest entities of the area (Figure 10). The return period associated to this scenario is 720 years (95% confidence interval in [215-1200] years). Therefore, the uncertainty regarding the return period of this scenario is quite important.
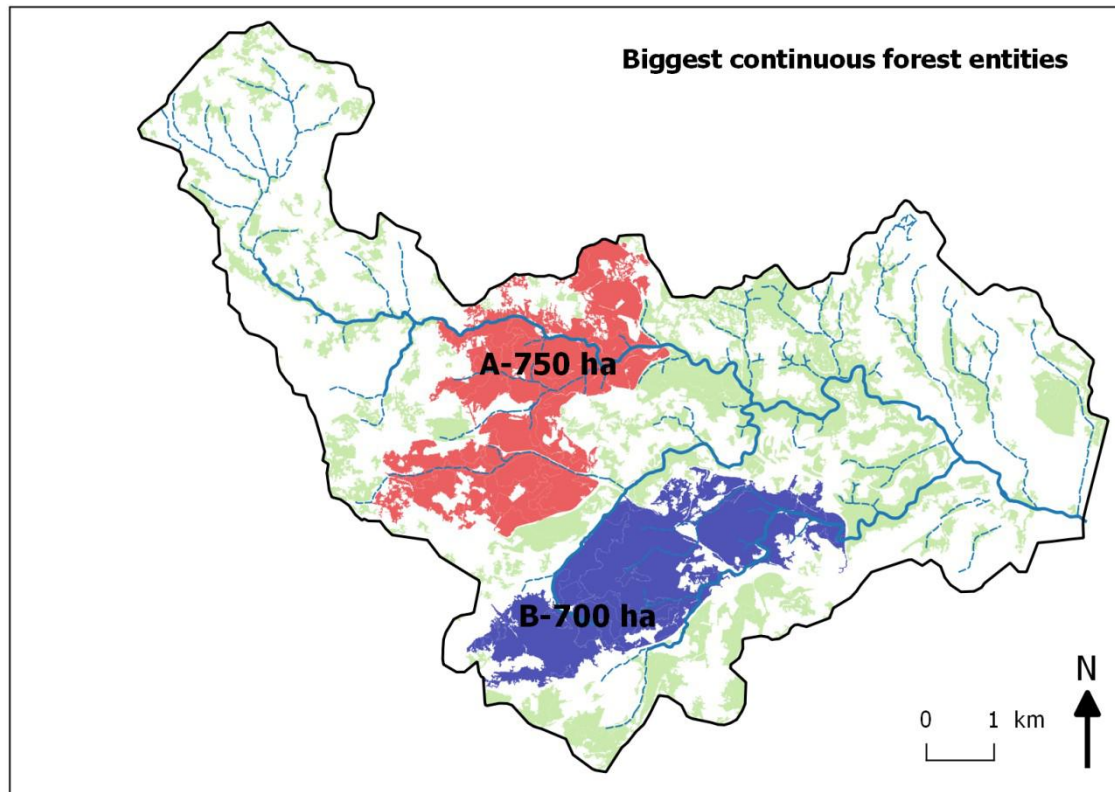
Figure 10 : Map of the two biggest continuous forest entities within the Brague DEMO catchment

Using those scenarios, cascading hazards of flash floods will be studied.

The changes of hydrology due to wildfire are studied in §6.1, but on-going review and analysis are additionally in progress to provide eventual changes in sediment and large wood supplies.

3 Hydrology

3.1 Rainfall modelling

3.1.1 Rainfall intensities from rain gauges

Cabinet Merlin (2016a) re-analysed the rainfall data of the Nice Airport Météo France station and provided duration – probability values as reported in the next Table 7.

Table 7 : Rainfall in mm depending on their time return and duration from Cabinet Merlin (2016a)

Duration (min)	5 years	10 years	20 years	T30 years	T50 years	T100 years
15	20.7	23.9	27.2	29.0	31.3	34.6
30	28.9	33.7	38.5	41.2	44.8	49.9
60	40.4	47.3	54.5	58.5	64.0	71.8
90	49.2	57.8	66.8	71.9	78.9	88.9
120	56.5	66.6	77.2	83.2	91.5	103.4
240	62.4	73.8	86.0	93.6	103.8	118.8
360	69.9	82.1	95.0	103.0	113.6	129.1
720	84.8	98.5	112.7	121.4	132.6	148.8
1440	102.9	118.2	133.6	142.9	154.8	171.5
2880	124.8	141.8	158.5	168.3	180.6	197.7

These data are provided here for information, but were not used in our analysis which relies on the SHYREG modelling approach (see later).

3.1.2 Oct. 3rd 2015 radar rainfalls

For the October 2015 event, 128mm of rainfall in 24h has been recorded in Antibes (

Figure 11). Antibes (06), Biot (06), Valbonne (06), Vallauris (06) have been impacted by urban runoff generating large damages.
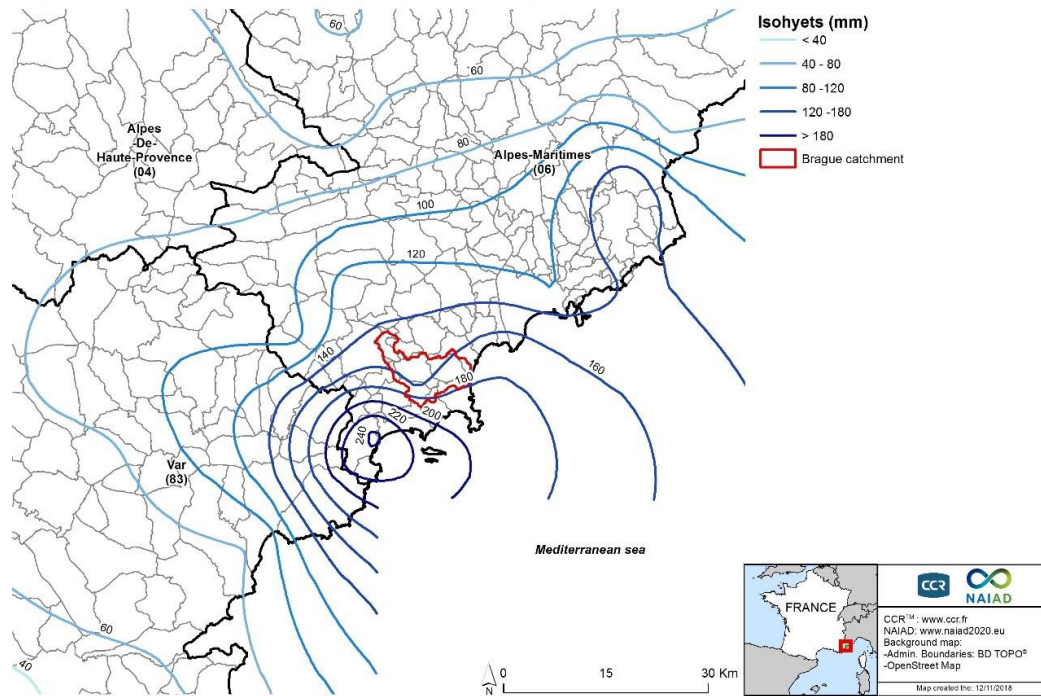
Figure 11 : The October 2015 isohyets for the related thunderstorm, the Brague catchment is displayed in red.

Some radar data are available and reported in Cabinet Merlin (2016b) and Préfécture des Alpes-Maritimes (2016) as exemplified in the next Figure 12.
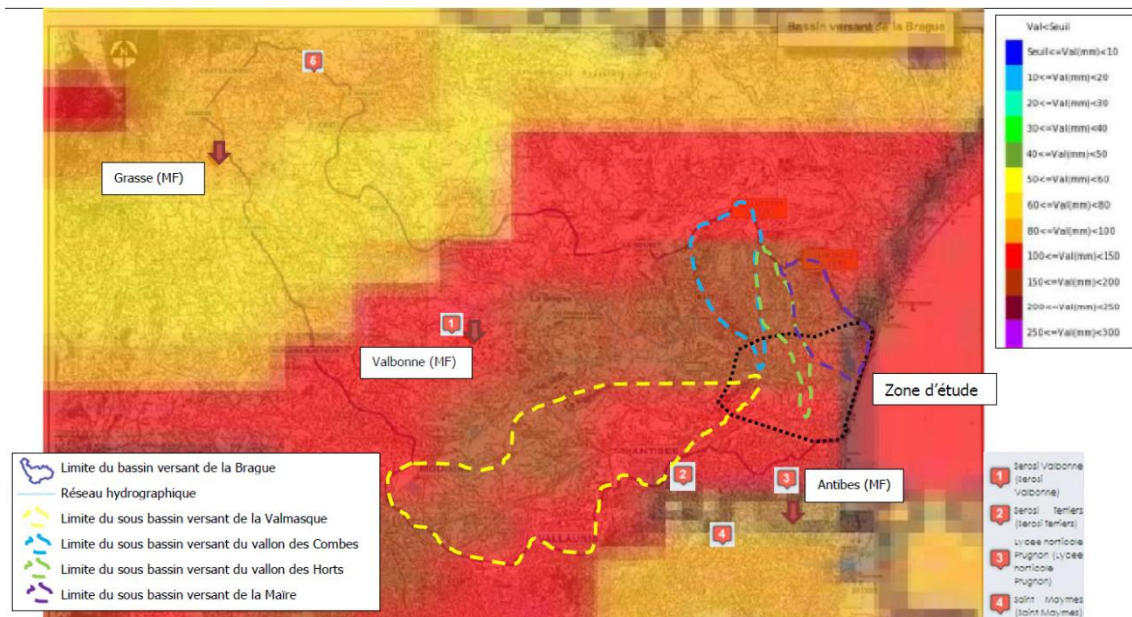
*Figure 12 : Rainfall height on Oct. 3rd between 20:00 and 23:00, location of sub-catchments, taken from **Cabinet Merlin (2016b)**.*

Préfécture des Alpes-Maritimes (2016) additionally reports that overall, the 68km² catchment of the Brague experienced 138 mm of rainfall between Oct. 3rd 18:00 and Oct. 4th 01:00 and more precisely, 126 mm between 20:00 and 22:15 (2h15) and 81 mm in 1h between 20:15 and 21:15. All those values are higher than the 100 year return period values reported in the last Table 7. Such a rainfall was equivalent to 8.6 Mm^3 of which roughly half flowed down to the sea within a day and the rest flowed more slowly, infiltrated or evaporated later.

3.1.3 Stochastic rainfall generator used in the Shyreg method

A method using a stochastic rainfall generator coupled with rainfall-runoff model was used to compute hydrographs of given probability of exceedance. This method called SHYREG is the fruit of a long-lasting research effort. Its presentation is split between the rainfall generator below and the rainfall-runoff module presented in §3.3.4.

The rainfall hourly stochastic generator was calibrated on the whole continental and over-seas France territories (Arnaud et al. 2006, 2008). The data have been extracted for the Brague area (Figure 13 & Figure 14). Their use is detailed in §3.3.4.
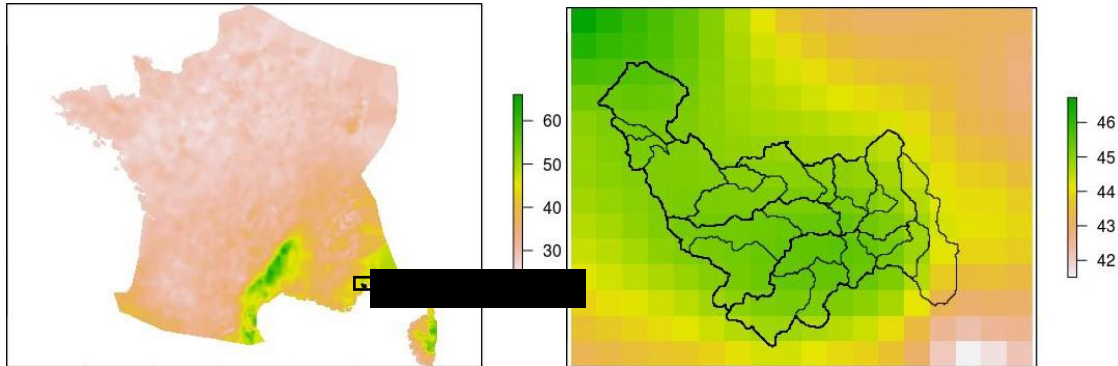
Figure 13 : Regional parameter of the rainfall generator in the Brague DEMO area, example of the PJMAX-Summer parameter.
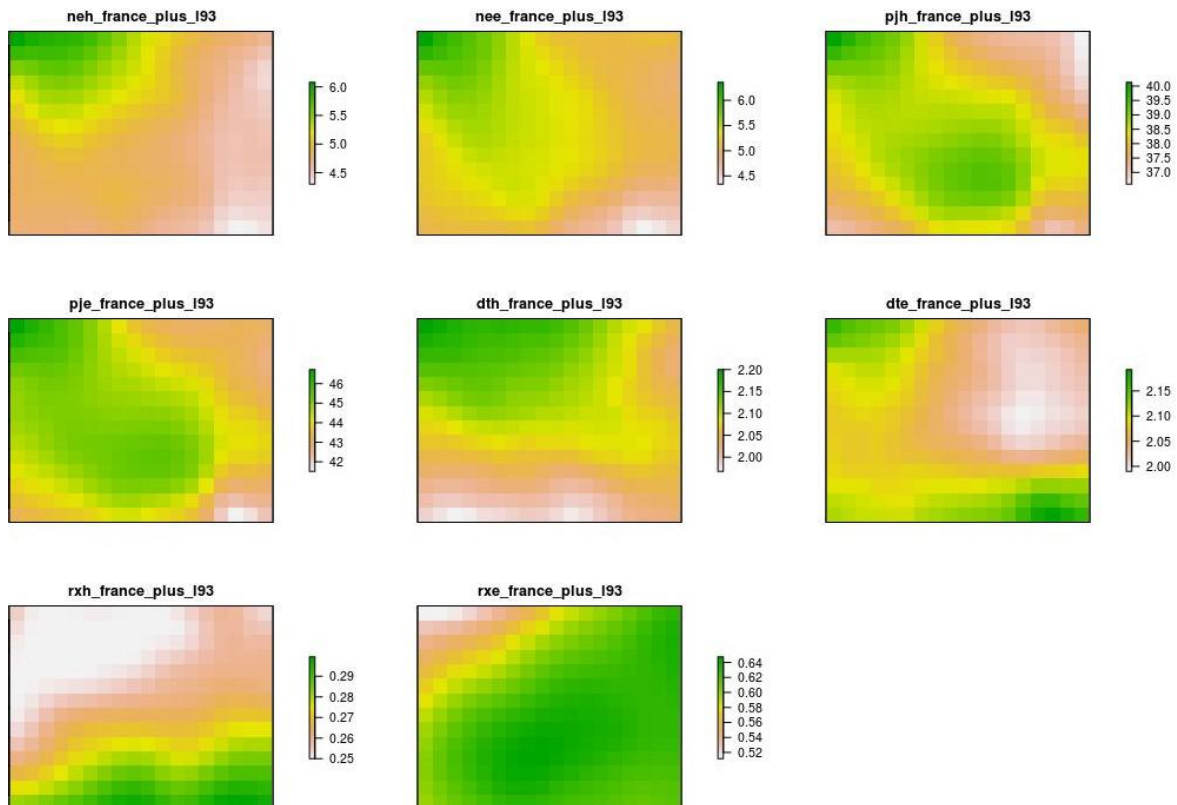
Figure 14 : Maps of the rainfall generator parameters in the Brague DEMO area.

3.2   Surface runoff methods

The Brague catchment is exposed to flash flood hazards and surface water runoff and the objective is to model and understand the surface runoff hazard and the related damages (D6.3). First, the flood claims analysis of the 2015-October event highlights that 60% of the claims are related to runoff hazard and 40% are related to river flooding hazard (chapter 0). CCR defines runoff hazard as *"hazard occurring outside flood-prone areas and generating flood claims explained by surface flow"*.

This analysis revealed the importance of runoff modelling to explain *what, where and why* flood claims are located outside the flood-prone areas. Then, the CCR surface-runoff model has been launched on the 2015-October event input data.

3.2.1   Initial model

The ARTEMIS CCR flood model is based on three coupled models (Figure 15): a hazard unit to simulate events and to identify damaged areas (topic related to NAIAD Deliverable D6.2); a vulnerability unit to localise risks (topic related to NAIAD Deliverable D6.3); and a damage unit focusing on damage curves linking hazard to damage (NAIAD Deliverable D6.3).
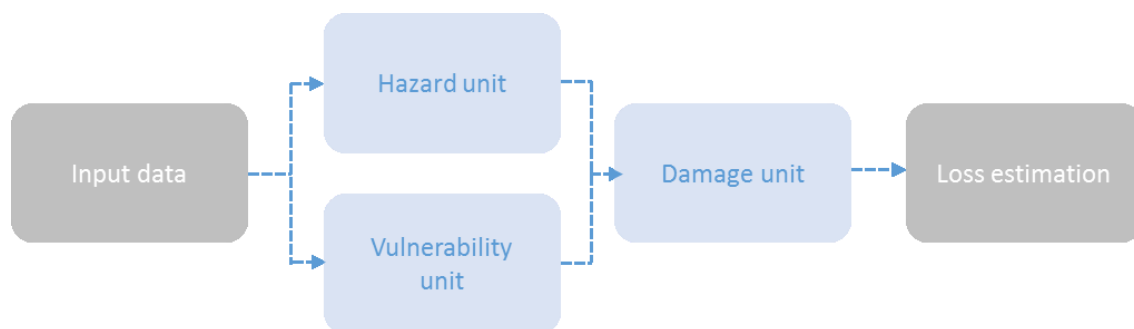
Figure 15: Global explanation of ARTEMIS flood model.

CCR understands flood hazard as overflow, runoff due to intense rainfall, inland flooding and marine submersion. The CCR flood model is both:
- a deterministic model to estimate the losses of real past events and
- a probabilistic model to simulate a stochastic event set.

It covers the entire France, combining river overflow and surface water runoff (Moncoulon et al. 2014).

An event is defined by its location (watershed) and its duration (in hours). The model simulates the hazard and the damages for each single event (real or fictive event). The river routing and overflow model estimates the main rivers flow from the rainfall/runoff output data and a 1D propagation model on the rivers meshes. In case of river banks overflowing, the flooded area is determined on the 25m digital elevation model. The rainfall runoff model is a 2D spatialized production and transfer model based on hourly spatialized rainfall data. It uses a 30 sec time-step, a 25m altitude grid (BD Alti IGN), Météo-France pluviometry data and Corine Land Cover data (Figure 16).

For each single event, two specific hazard maps are generated:
- Maximum level of water (m) on each single cell for inundation areas
- Maximum water runoff (m3/s) on each single cell for run-off hazard

For the stochastic event set, each single event hazard map is combined with the others to create a probabilistic exposure map. Overflow and runoff maps are validated by comparison with the address-based claims data at the catchment scale.

The Brague River is strongly influenced by rapid water level changes from flash floods as stressed in §3.3.

By using climatic and geographical input data, the hazard unit characterises the intensity of the phenomena and estimates the extent of related affected areas.
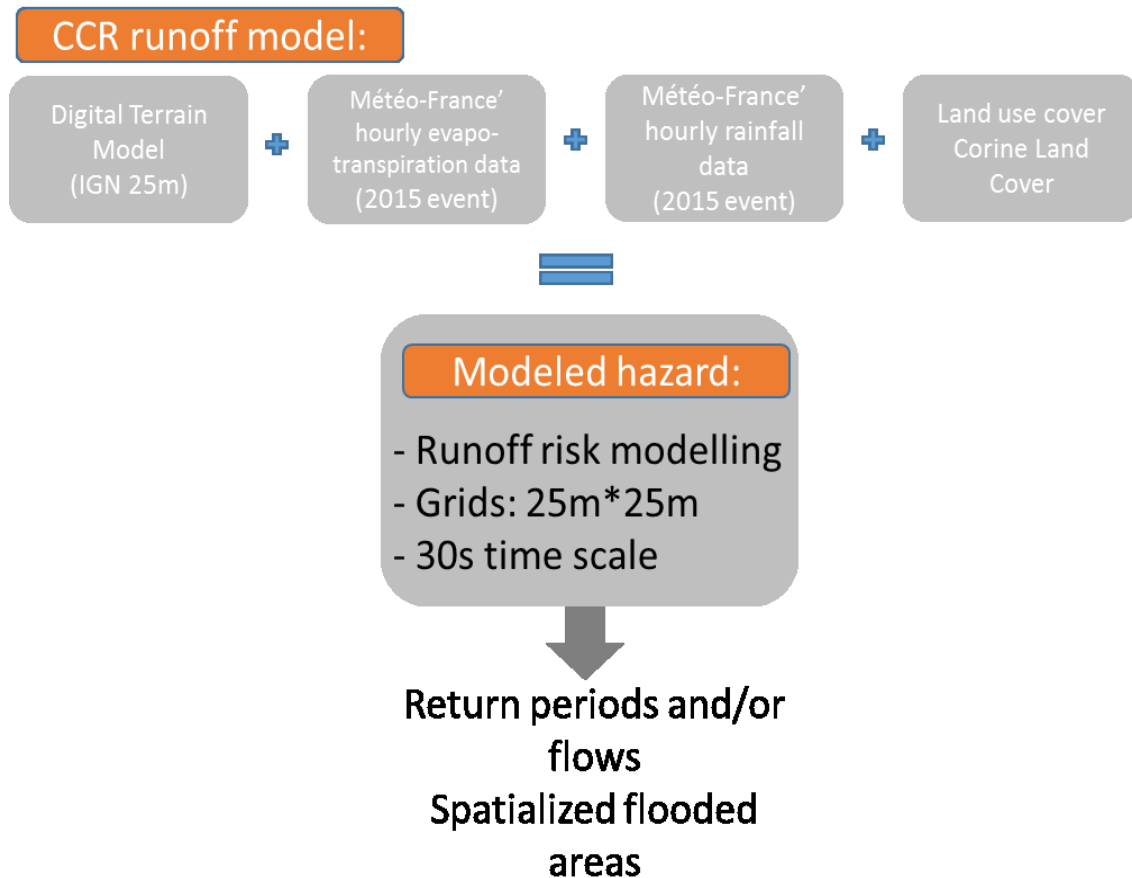
Figure 16: Explanation of CCR runoff model.

3.2.2   Enhancement brought by the NAIAD project

To calibrate the CCR runoff model, CCR selected the most characteristic torrential flood event in the Brague catchment: the October 2015 event (

Figure 11). The objective is to understand the runoff hazard at the catchment scale and then link it to the 2015-flood claims to generate cost/flow relation as the main input to NAIAD Deliverable 6.3. To ensure short calculation times when running the mode for the entire country, the current runoff model calculates DTM slopes only once.

The results of this modelling are presented in §5 along with a cross control with claim locations.

Within NAIAD, the Brague catchment is small; the model has been tuned to calculate slopes taking into account water heights in each cell. This method sprawls water along short watercourses, instead of being stuck in the banks.

The model was run on the October 2015 flood event. Model inputs are the radar rainfall (Météo France) values collected for the events and the Corine Land Cover data. The runoff modelling has been applied thanks to the rainfall/overflow ARTEMIS CCR model, with runoff coefficients specific to the CCR model for the simulation on the Corine Land Cover and detailed runoff coefficients for the adapted-land cover.

Another enhancement is the use of local land use cover data as input to the CCR model, the inventory of the land use realised since 1999 by the CRIGE PACA.

3.3 River discharges

3.3.1 Discharge measurement data

The Brague river has been equipped with a hydrological station since 1981 (N. Y5605210 "La Brague à Biot [Plan Saint-Jean]" and data is available at http://www.hydro.eaufrance.fr, catchment size 41 km²). The discharge and stage measurements are provided in Figure 17.
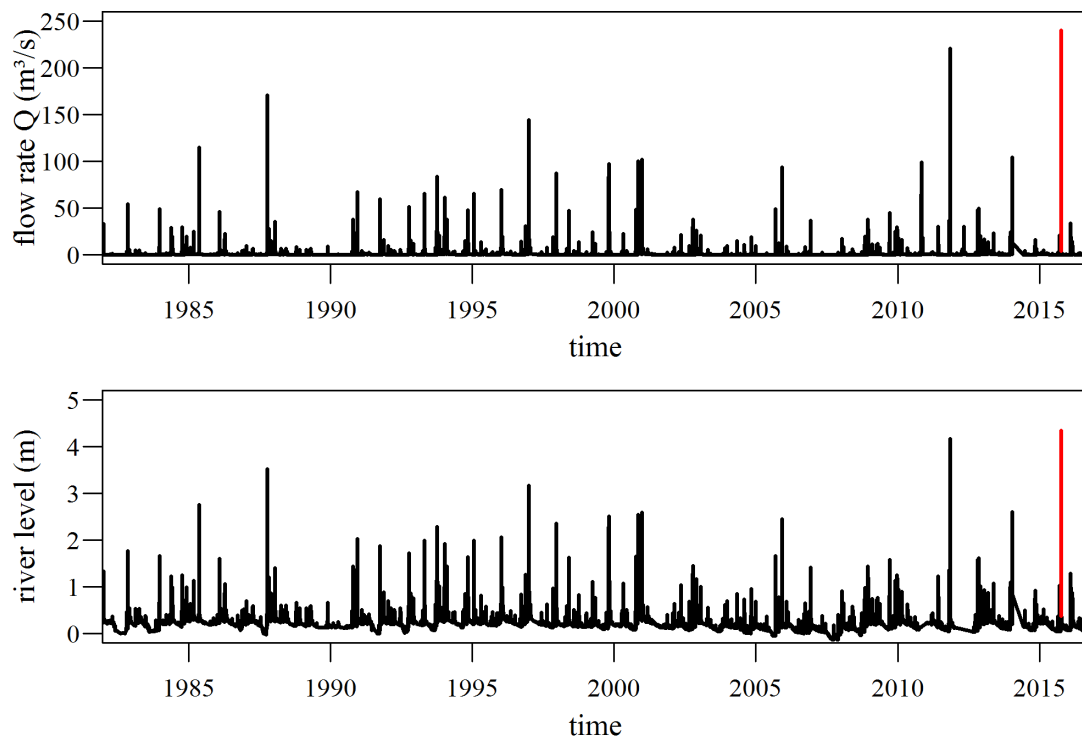
Figure 17 : Discharge and stage of the Brague hydrological station in black and in red the 2015 event as reconstructed (see later).

3.3.2 Oct. 2015 flood events data

During the October 2015 flood event, the station stopped measuring during the rising limb of the hydrograph (next figure).

The regional authority, assisted by a panel of experts, performed a comprehensive appraisal of the hazards and damages in the days following the event (Préfécture des Alpes-Maritimes 2016). Field measurements were performed to compute peak discharges based on topographical sections, flood levels and river bed roughness (Lebouc and Payrastre 2017). The peak discharge at the Biot station was estimated to reach 240 m³/s (envelope interval after error

propagation: 185-290 m³/s). A further study using the radar rainfall data and a hydrological model of the catchment were used to obtain hydrographs of the event (Lindénia 2016). The hydrograph which is displayed here correspond to the Lindénia's time series corrected proportionally by the peak value of Lebouc and Payrastre (2015).

Two complementary data suggest that this approach is reasonable:

- The discharge measurements of the Brague station until it stopped functioning are consistent with this hydrograph (see Figure).
- Cabinet Merlin (2016b) performed a numerical modelling of the hydrological station vicinity. The station had been by-passed during the event. Based on a thorough re-evaluation of the stage-discharge relationship of the station taking into account the pressure flows in the bridges and the maximum flood level, as well as the 50 m³/s by-passing flows, the total discharge was re-evaluated to 250 m³/s independently from the Lebouc and Payrastre (2015) data.
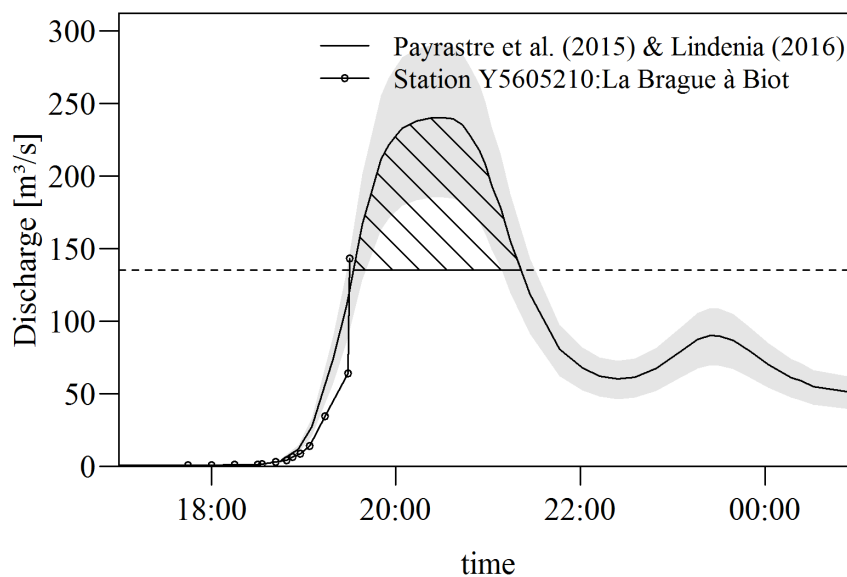
*Figure 18 : October2015 flood event hydrograph, measurement by the hydrological station until it stopped and hydrograph shape from **Lindénia (2016)** corrected proportionally using the peak discharge as reconstructed by **Lebouc and Payrastre (2017)**.*

The Figure 18 also displays the 135 m³/s threshold which is identified by Cabinet Merlin (2016c) to be the threshold value above which flooding occurs in Biot. The volume of the flood above this threshold, later called Flood Excess Volume (FEV) from the concept of Bokhove et al. (2018a), is estimated to be 488,000 m³ (see §4.2).

3.3.3 Discharges of selected return periods according to archives

Cabinet Merlin (2016c) provided discharge peak values for several return periods in sub-catchment of the Brague as provided in the Table 8 and
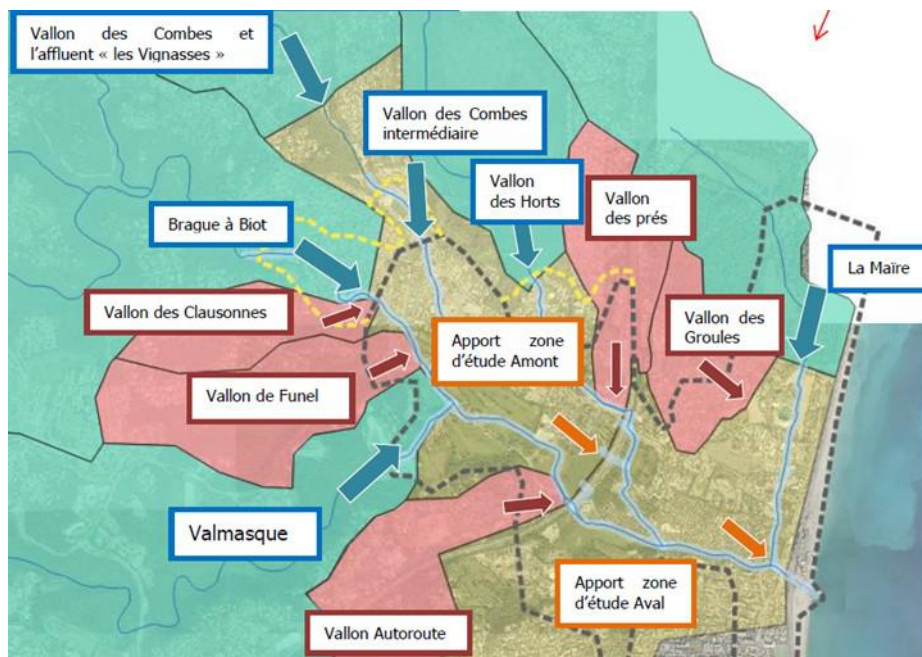
Figure 19, which provides the location of the points. They have been punctually reused at the calibration phase of the Iber model (see later).

Table 8 : Peak discharge values of the Brague sub-catchments.

Catchment name	Surface (km²)	Q$_{peak}$ T30yr (m³/s)	Q$_{peak}$ T100 yr (m³/s)
Brague à Biot	42.1	**135**	**225**
Vallon des Combes (Amont)	2.3	13.2	22
Vallon des Combes (intermédiaire)	0.7	4.3	7.2
Vallon des Horts (Amont)	1.4	8.9	14.8
Vallon des prés	0.56	4.3	7.1

Vallon des Groules	0.42	3.4	5.6
La Maïre	1.9	11.3	18.9
Vallon des Clausonnes	0.42	3.4	5.6
Vallon du Funel	0.83	5.8	9.7
Valmasque	14.6	57.9	96.4
Vallon Autoroute	0.78	5.6	9.3
Apport sur la zone d'étude amont	1.1	6.5	10.9
Apport sur la zone d'étude aval	2.5	14.1	23.5
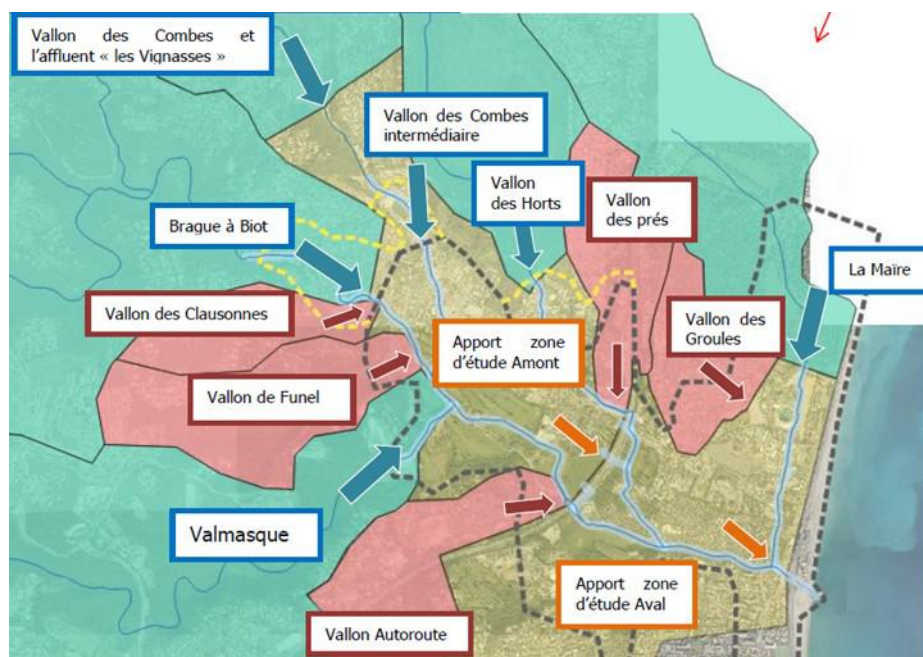
Figure 19 : Location of the Cabinet Merlin inlets and discharge calculation points **(Cabinet Merlin 2016c)**.

3.3.4   SHYREG modelling

The SHYREG model (Lavabre et al. 2003, Arnaud et al. 2014, 2015, 2017, Aubert et al. 2014) is a widely used approach in France. It enables generation of hydrographs for selected non-exceedance probabilities, i.e., return periods, based on a full chain of analysis involving a stochastic rainfall generator, a rainfall-discharge model, a spatial aggregation of run-off and an optimization to fit discharge measurement data (Figure 20).
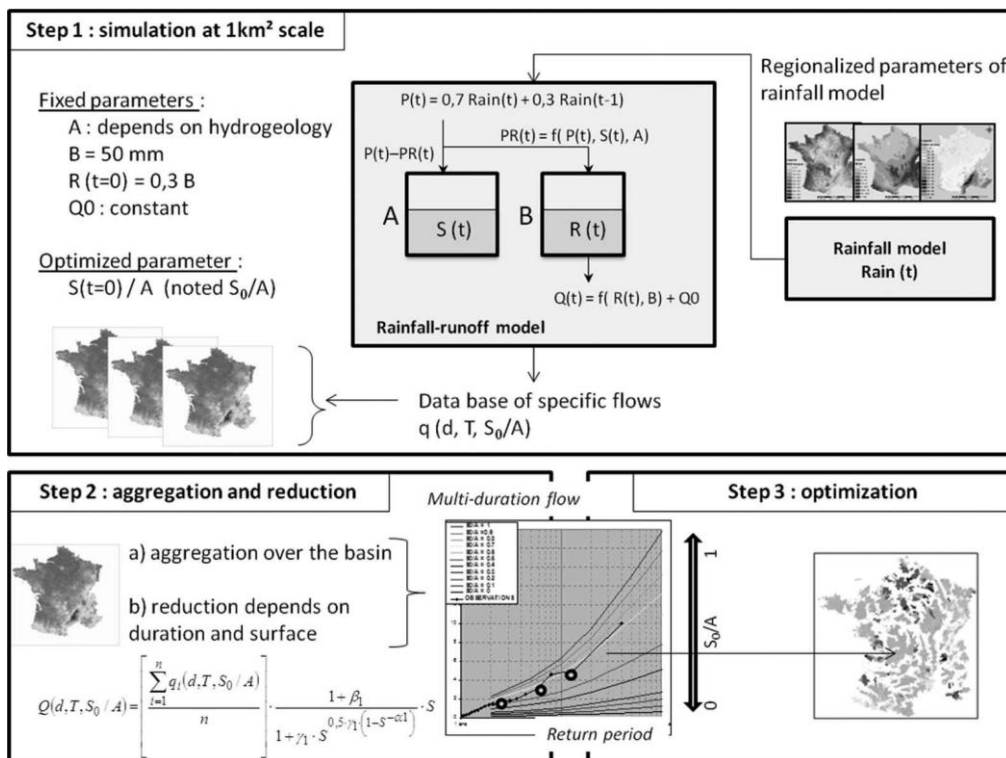
*Figure 20 : SHYREG method calibration principle **(Arnaud et al. 2015)**.*

The SHYREG method was used to generate hydrographs in several points of the Brague catchment. Each hydrograph has not been directly introduced in the model, as detailed in §3.3.6.

3.3.5   Consistency between measurements and old reports

Comparison between new hydrological analysis and older results are always interesting to perform. Since discharges were computed at slightly different locations, thus with different catchment sizes, it is often irrelevant to compare the peak discharges (see next Table). A good way to compare discharges is to compute Q_{ps} the pseudo-specific discharge $Q_{ps}=Q/A^{0.75}$ where A is the catchment area (km²).

Table 9 : Peak discharges according to archives (Cabinet Merlin 2016c) **and to SHYREG**

Catchment name	Archives			Shyreg		
	A (km²)	Q_{peak} T100 yr (m³/s)	$Q_{ps}=$ $Qp/A^{0.75}$	A (km²)	Q_{peak} T100 yr (m³/s)	$Q_{ps}=$ $Qp/A^{0.75}$
Brague à Biot	42.1	**225**	13.6	43.3	246	14.6
Vallon des Combes	*2.3*	*22*	11.8	*3.09*	*35.1*	15.1
Vallon des Horts	*1.4*	*14.8*	11.5	*2.58*	*30.3*	14.9
La Maïre	1.9	18.9	11.7	1.88	23.2	14.5
Valmasque	14.6	96.4	12.9	13.59	104	14.7

The data on surface areas (in grey) are quite different, while the comparison of pseudo-specific discharges is more relevant.

Q_{ps} values are quite comparable, although a bit higher according to SHYREG. It is worth stressing that if the peak value is higher, the duration of the peak is lower than e.g., the hydrograph reconstruction provided in §3.3.2. SHYREG's hydrographs are thus sharper than those from the archives.

3.3.6   Selection of discharge values to use in the model

The input points used in the modelling are located on the map below (Figure 21).
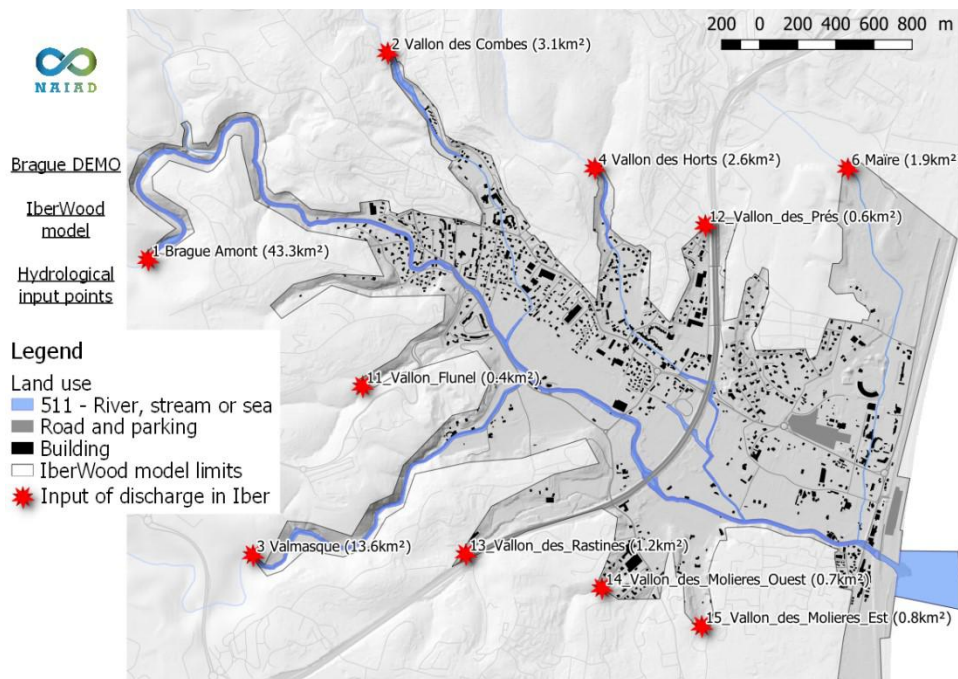
Figure 21 : Location of input points, equivalent catchment areas used for their computation.

The 10, 30, 100 and 300 years return period hydrographs for each of these points are provided in Appendix 1.

A   Issues related to the simultaneous use of multiple hydrographs

A reanalysis of the SHYREG hydrographs and, generally speaking, of any set of hydrographs computed for a given return period, was necessary because inserting hydrographs of a given return period *T* simultaneously is not the best way to model a return period T flood for the whole catchment. It is actually very unlikely, i.e. less probable (P=1-1/*T*)*,* that all tributaries experience a - return period T flood exactly at the same time. As a consequence, inserting all return period T floods hydrographs into SHYREG cumulate into a peak discharge much higher than the full catchment for the same return period T peak discharge. For instance, on the Brague, the sea outlet 100 yr Qp=332 m³/s for 68 km² of catchment, while the sum of 66 km² of its sub-catchment peak values is 465 m³/s, 140% of the relevant value. This fact could be summarized in the following equation, where A_i are the catchment areas:

$$Q_{peak}\left(\sum_i A_i\right) < \sum_i Q_{peak}(A_i)$$

Since this study aimed at modelling a return period *T* flood of the whole lowland Brague floodplain, we chose to introduce tributaries' hydrographs that will in conjunction trigger a return period T flood of the Brague at its outlet.

To our knowledge, no recommendations clearly state how to perform such correction. Several ways have been explored and are described hereafter.

B   Hydrology refereeing only to one station

In numerous cases, as for instance in the Slovenia NAIAD DEMO the Glinščica catchment, the only available discharge data come from one hydrological station from which the whole catchment hydrology is extrapolated (Pengal et al. 2018). In this case, if no distributed hydrological model considering land use and sub-catchment features are created, it is assumed that each sub-catchment supplies a water depending only on its size. A first simple method is to slightly correct each elementary hydrograph by a proportional coefficient. So, a correction coefficient α_i is defined so that:

$$Q_{peak}\left(\sum_i A_i\right) = \sum_i \alpha_i Q_{peak}(A_i)$$

Actually, hydrographs for each input point corresponding to a catchment size A_i could be introduced according to the following equation, e.g., with β =1:

$$Q_i(t) = Q_{outlet}(t) . \left(\frac{A_i}{A_{outlet}}\right)^{\beta}$$

In this way, the whole inserted hydrograph corresponds to the return period T flood of the whole catchment. To control how far these elementary hydrographs were from the return period T floods of the sub-catchments, the corresponding α_i were computed which provide the peak values in the next table:

$$\alpha_i = \frac{Q_{outlet}(t) \cdot \frac{A_i}{A_{outlet}}}{Q_{peak}(A_i)}$$

Table 10 : Equivalent correction coefficients between 100 yr return period peak discharge of sub-catchments and actually inserted values to model a 100 yr return period of the whole catchment.

Reference points	A_I (km²)	α_i
1_Brague_amont	43.35	86%
2_Vallon_Combes	3.09	43%
3_Valmasque	13.59	64%
4_Vallon_Horts	0.45	41%
6_Maire	0.57	39%
Brague outlet	68	100%

Using such a method resulted in higher α_i in the smaller sub-catchments compared to the whole catchment. This is a direct consequence of the fact that usually $Q_{flood} \propto A_i^{\beta}$ with $\beta \approx 0.75 < 1$. Coefficients α_i were computed also for the rising and falling limbs of the hydrographs. They were always higher than for the peak values as given in the table and higher than 100% on the hydrographs before 6h and after 16h, meaning that the smaller the sub-catchments, the higher their peak discharges and the lower their base flows, which is quite intuitive (higher and lower more than just by proportionality with the increase in catchment size).

We could have alternatively taken a β value of 0.75 as in Cabinet Merlin (2016c) but the cumulated discharge would have been higher than the peak outlet discharge as stated at the beginning of this section.

Finally, we conclude to some recommendations when analysing hydrographs or peak discharges for flood events between catchments only based on catchment sizes (Table 11).

Table 11 : Correction methods to hydrographs/peak discharge for various objective of the study.

Objective of the study	Correction of discharges
Computation of the hydrograph/peak discharge of same time return for a catchment *i* of different size, from the data of a catchment *X*.	$Q_i(t) = Q_X(t).\left(\dfrac{A_i}{A_X}\right)^{\beta \approx 0.75}$
Computation of the hydrographs of all sub-catchments *i=1, 2,… ,N* of catchment *X* to model an event of a given time return based on the hydrograph at the outlet of *X* for this time return.	$Q_i(t) = Q_X(t).\dfrac{A_i}{A_X}$

It regularly occurs that both objectives are required simultaneously. For instance, if one was to model the whole Brague ($\Sigma A_i = A_{Outlet} = 68$ km²) 100-yr return period flood based on the hydrological data of the Biot station ($A_{station} = 41$ km²), by introducing several sub-catchments *i* (A_i) hydrographs $Q_i(t)$, the first correction would be used to compute the whole catchment discharge and then the second correction would be used to compute each sub-catchment injections:

$$Q_i(t, A_i) = Q_{outlet}\left(t, \sum_i A_i\right).\frac{A_i}{\sum_i A_i} = Q_{station}(t).\left(\frac{\sum_i A_i}{A_{station}}\right)^{\beta \approx 0.75}.\frac{A_i}{\sum_i A_i}$$
$$= Q_{station}(t).\frac{A_i}{A_{station}^{\beta \approx 0.75}(\sum_i A_i)^{1-\beta \approx 0.75}}$$

C   Hydrology based on distributed models

As mentioned, §3.3.4, the SHYREG method takes into account the land use in its calibration and is discretized at a pixel size of 50*50 m in its present application. Using the correction method presented above would result in the loss of this spatial information. Since the method provides hydrographs for any point of the catchment, they were extracted just upstream of confluences and at the sea outlet.

Two proportionality corrections were eventually considered, the first only for the peak discharges, the second for every time step:

- Only based on peak discharges :
$$Q_i(t) = Q_{i,SHYREG}(t, A_i) * \frac{Q_{peak,SHYREG}(\sum_i A_i)}{\sum_i Q_{peak,SHYREG}(A_i)}$$

- Based on every time step:
$$Q_i(t) = Q_{i,SHYREG}(t, A_i) * \frac{Q_{i,SHYREG}(t,\sum_i A_i)}{\sum_i Q_{i,SHYREG}(t,A_i)}$$

D   Synthesis

The downstream part of the Brague lowlands constitutes a cumulated surface of 3.7 km² out of the 68 km² of the whole catchment. It is drained by small drainage ditches and the urban pluvial system. The scale of our analysis is too rough to detail these sub-catchments and it has been chosen to use the surface-based approach to compute the water supply of these 5% of the catchment. These small hydrographs are introduced in points 11 - 15 of
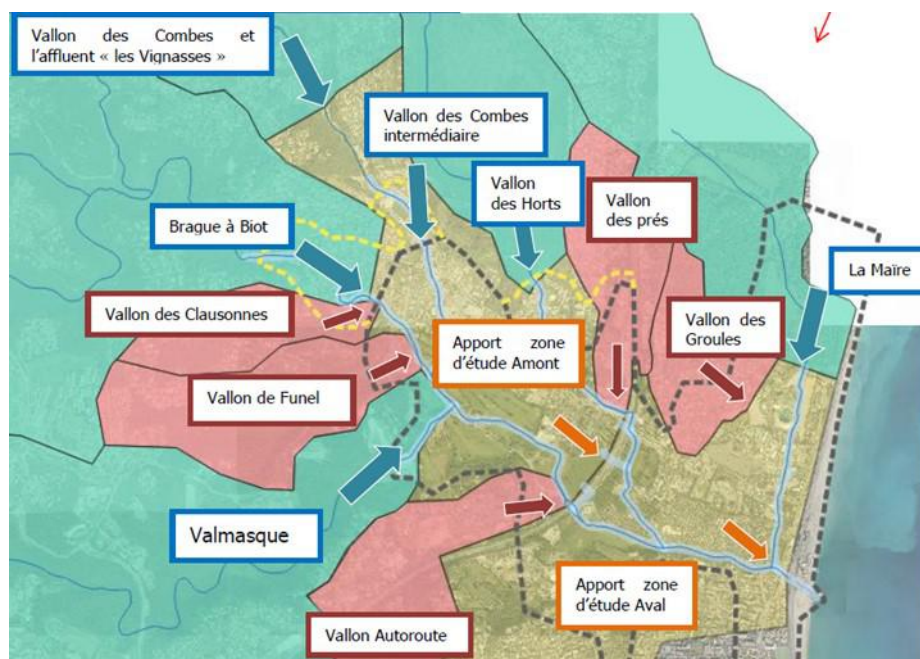
Figure 19.

Several correction methods were tested on the hydrographs coming from the complementary 95% of the catchment. Several features of the resulting cumulated hydrograph of the whole catchment were compared to the outlet hydrograph and are provided in a concise form in Table 12.

Table 12 : Input hydrograph correction methods and effects on discharge, total volume and ability to capture the spatial features of sub-catchments.

Correction method	Capture spatial features	$\dfrac{Q_{peak,SHYREG}(\sum_i A_i)}{\sum_i Q_{peak,SHYREG}(A_i)}$	$\dfrac{Q_{i,SHYREG}(t,\sum_i A_i)}{\sum_i Q_{i,SHYREG}(t,A_i)}$		$\dfrac{Volume(\sum_i A_i)}{\sum_i Volume(A_i)}$
			Mean	St. Dev.	
No correction method	YES	140%	113%	14%	108%
Surface-based	NO	100%	100%	0%	100%
Peak discharge-based	YES	100%	82%	10%	79%
Every time step-based	**YES**	**100%**	**102%***	**1%***	**102%***

*The difference with the outlet is related to the use of the surface-based method for the small lowland sub-catchments

As mentioned before, a direct use of the hydrographs without correction is not satisfying because it results in overestimation of discharges and volumes. The second method is naturally very good in predicting volumes and discharges, since all the inputs are simply proportional to the sub-catchment sizes. However, the spatial diversity of sub-catchments is lost.

The peak discharge-based method underestimates the volumes by applying too strong a reduction, while every time step-based method seems satisfactory on all points. The following α_i correction factors are computed at each time step of the hydrographs by the equation:

$$\alpha_i(t) = \frac{Q_{i,SHYREG}(t,\sum_i A_i)}{\sum_i Q_{i,SHYREG}(t,A_i)}$$

In order to illustrate this, the value for the 100 yr return period input hydrographs were computed in Table 13. Similar, but not exactly the same values were computed for other return period values.

Table 13 : Correction factor for 100 yr return period input hydrographs at each hydrograph time step.

Time [h]	0	4	6	6.67	7	7.33	7.67	**8**	8.7	9.3	10	10.7	12	16	24
α_i [-]	121%	103%	92%	88%	85%	82%	79%	**71%**	79%	82%	85%	88%	92%	103%	121%

The hydrographs used in this analysis all have their peak values at t=8 h. The difference between the α_i =71% at the peak for all catchments and the high range of variation for the surface-based method illustrated in

Table 10 (39%-86%) clearly demonstrates that the surface-based method was over- and under-correcting some catchments, while each hydrograph remains stable (although slightly lower) using the selected method.

4   Hydraulics

A wide range of modelling approaches exit in hydraulics, from simple ones to highly advanced ones. Several tools were tested and used on the Brague DEMO to accommodate the various objectives:

- *0D analysis*, i.e. a one transverse-profile scale, which enables very fast computation. It was used in a simplified and direct application of the Flood-Excess Volume (FEV) concept. This concept was developed by Bokhove et al. (2018a) to facilitate communication and preliminary analysis of flood issues and possible panel of protection measures.
- *1D analysis* enables:
    o   Flood hydrograph routing in hydraulic models and;
    o   Sediment and flood routing in hydro-sedimentary models.

    It was not implemented so far for the Brague catchment, because the flooding process in the floodplain has strong 2D components, for instance between the Brague River and its tributaries whose flows by-pass the confluence to directly supply the floodplain (Cabinet Merlin 2016c).
- *2D analysis* enables to map flow exchanges between floodplain and a complicated network of ditches and tributaries. These are depth-averaged models unable to capture complex 3D pattern as existing in meanders, but remain relatively reasonable in terms of computation power.
    o   The typical hydraulic models compute water flows exchanges, as e.g., Bladé et al. (2014). Advanced two-phase models exist with:
        ▪   Coupling with sediment transport and updating of the bed geometry using the Exner equation.
        ▪   Coupling the Eulerian flow description with a Lagrangian description of large wood pieces displacements, enabling to route large woods to assess large wood jamming hazards (Ruiz-Villanueva et al. 2013, 2014a, 2016a, 2016b).

    Cabinet Merlin (2016c) implemented a coupled 1D-2D modelling of the Brague in its floodplain. A 1D approach modelled the river network while a 2D approach modelled the floodplain with lateral sill equations governing the exchanges between the two modules.

Within the NAIAD project, a fully 2D modelling approach is applied to the Brague lowlands including the floodplain and the final reach of the Brague and Valmasque gorges using the IBER model (Bladé et al. 2014). The large wood transport will be computed using the IBERwood module in due time. In late 2018, at the time of writing of this report, the 2D "pure-water" model calibration is in progress; the data on actual wood transport during the 2015's event has been gathered but not yet modelled. We aim to complete it during 2019.

- *3D models* are now regularly used in scientific works (e.g., Gems et al. 2016) and increasingly used in engineering studies. Their construction and calibration are however still more technical than 1D & 2D models and the computation time remains a complementary obstacle whose weight is decreasing with time and increasing computation power.

- *Small scale models* are very complementary tools to numerical models. They were and still are particularly relevant in two (or more) phase problems, either water-wood or water-sediment (Couvert and Lefebvre 1994, Piton et al. 2018).

The following chapter mostly reviews the 0D and on-going 2D+wood approaches applied to the Brague catchment.

4.1 Existing reports

Following the Oct. 2015 disaster, a flood numerical model has been built, calibrated on the event and demonstrated that flooding may occur in Biot for any discharge higher than the 1:30-year return period event, i.e., Q>135 m^3/s (Cabinet Merlin 2016c).

The model extension is displayed in Figure 22.
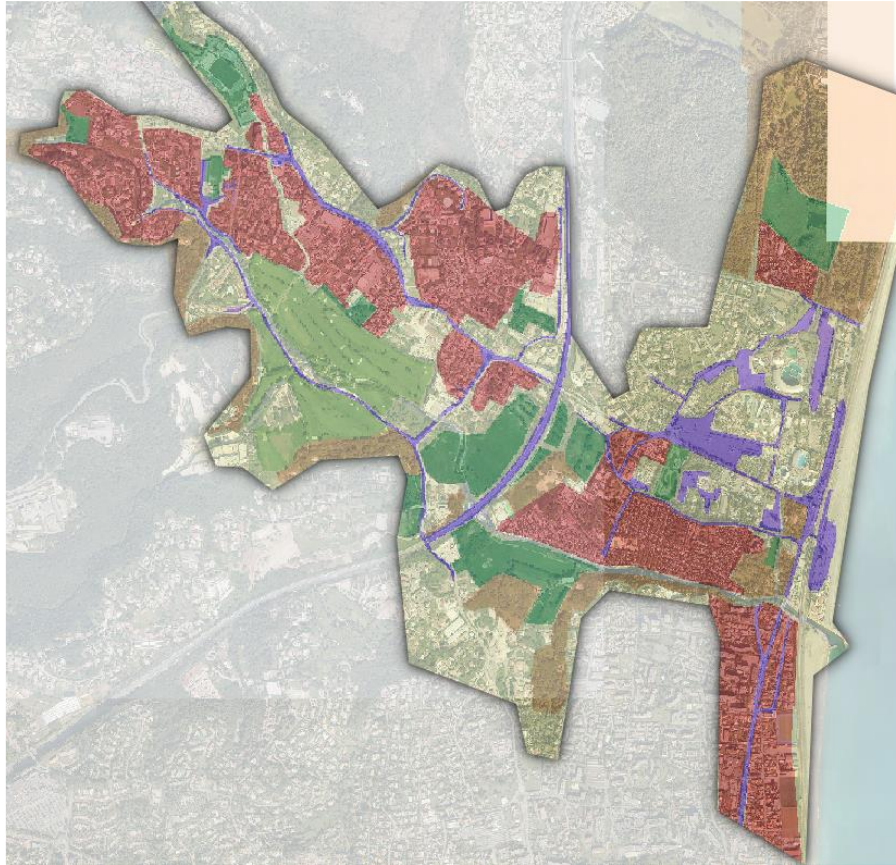
*Figure 22 : Brague lowland 1D-2D hydraulic model extension and Strickler roughness coefficients **(Cabinet Merlin 2016c)**.*

Flooded area extensions were mapped for the 1:30 year and 1:100-year return period events. It has been calibrated on the last two largest flood events (2011 and 2015) and accounting for large wood jams on hydraulic structure using an obstruction coefficient based on expert assessment.

Our study was built upon this engineering work performed directly following the Oct. 2015 disaster and uses the state-of-the-art techniques in engineering studies. Within NAIAD we aim to go one step further by using a fully 2D model accounting also for the large wood transport.

4.2   Simplified direct analysis: The Flood Excess Volume (FEV)

Discussions on protection measures with colleagues and stakeholders of various regions raised our awareness that people often have a very fuzzy idea of how much water was responsible for

a large flood event like the Oct. 2015 disaster and this lack of knowledge biases the discussions on relevant and irrelevant measures.

Based on the original idea of Bokhove et al. (2018a), a straightforward analysis was performed to quantify the flood-excess volume (FEV) for the Oct. 2015 event. This FEV *"approximately quantifies the volume of water one wishes to eliminate via flood-mitigation schemes"* (Bokhove et al. 2018b). The aim of this approach is <u>not to be precise</u> on hydraulics and protection measure effectiveness, but to be <u>very clear</u> about the amounts of excess water, thus accepting some simplifications. The following question motivates the study: what fraction of the excess water generating the flood is reduced, and at what cost, by particular mitigation measure? Such a quick-and-dirty approach should enable to dismiss measures obviously unable to achieve affordable flood protection and to focus only on promising ones that would be then further studied with advanced methods.

4.2.1 Principle

In essence, one can hypothesize that floods occur when water stage becomes higher than a certain water depth value, here called h_T [m]. h_T is typically related to the difference between the river bed and the height of the banks. All flows occurring below this value are not considered as "floods" within this framework, while all the water flowing over this value may overflow the bank and trigger flooding problems. Using water stage time series and a stage-discharge relationship, one can compute a discharge time series usually called a hydrograph and noted $Q(t)$. A certain threshold discharge Q_T is related to the threshold water depth h_T. The flood event can be assumed to last the time when $Q(t)>Q_T$, this period is called T_f. By computing the volume of the hydrograph above the value Q_T, i.e., $FEV = \int_{T_f}(Q(t) - Q_T)dt$, one can capture a first approximation of the water volume responsible for the flooding, hereafter called the flood-excess volume (FEV).

The number representing the water volume is sometimes hard to appraise as big, moderate or small. The "square lake representation" has been proposed as a conceptual object easier to imagine for non-experts. This FEV volume is thus represented by a lake, 2-m deep with a square shape. This lake could figure the size of the reservoir that one should built to store all the FEV. The lake side is a length that is hopefully more meaningful than a volume.

The analysis is then refined by splitting the square lake-FEV in a set of protection measures. The capacity of each measure to store, or deal with a volume by conveying it, is finally computed. The cost of each of these measures can be estimated. A very simple cost-effectiveness assessment is then performed by looking at the ratio between FEV assigned to a measure and the costs for implementation of this measure. The cost-effectiveness is then measured in terms of €/%-of-FEV.

The FEV concept is finally encapsulated in two graphical representations of the flood process:

- A three-panel graph displaying the stage-discharge relationship along with the discharge- (hydrograph) and water stage-time series highlighting the flood duration, peak discharge, water depth, threshold values and FEV (Figure 23a);
- A square lake representation (Figure 23b) explaining how big would be a 2 m-deep basin able to cope with this FEV. This lake can be split in parts, so that a panel of protection measures will cope with each part of the lake.
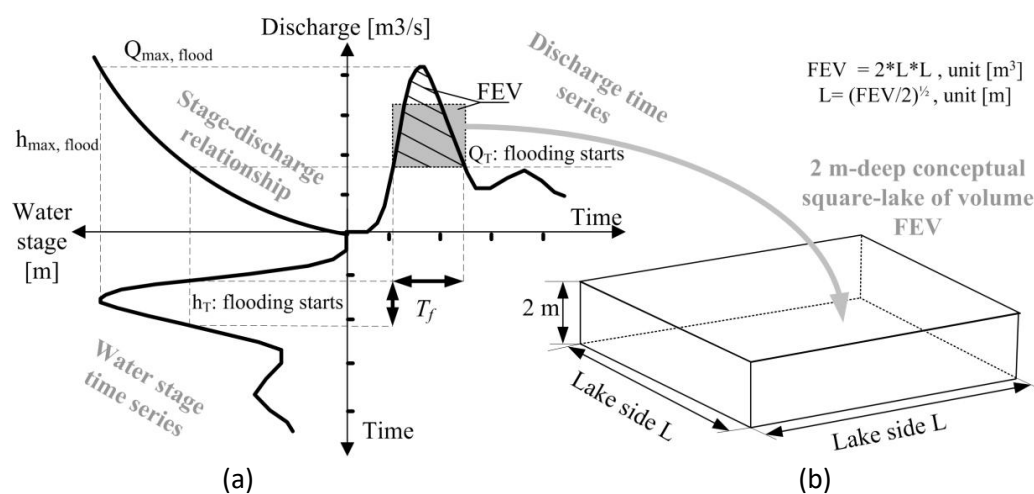
*Figure 23 : FEV concepts: (a) the three panel graph highlighting the FEV volume, i.e., the hydrograph volume over the bank overtopping discharge threshold and (b) the square lake representation of this FEV volume as a conceptual 2 m-deep lake to raise the awareness of the "size" of the flood excess volume, adapted from **Bokhove et al. (2018a)**.*

The FEV approach is thus a straightforward analysis of a given flood event at a given river section which tries to illustrate how much water is likely to overtop the banks and how a set of protection measures may be able to deal with it.

The most basic application of the FEV approach requires a known stage-discharge relationship and stage or discharge data. It is thus typically applied at a hydrological station. An application to the station "Brague à Biot [Plan Saint-Jean]" is presented hereafter focusing on the 1,200 m of river located upstream of the Valmasque and using the Oct. 2015 flood hydrograph as reconstructed in §3.3.2, p. 248.

4.2.2 Applications to the Brague River at the Biot hydrological station

The work developed in NAIAD is not advanced enough to clearly describe the protection measure panels that will be analysed in 2019. During the March 21st 2018 stakeholder workshop held in Nice at the IMREDD building, two trajectories were stressed as requiring wide implementation to the Brague: retention measures to store water in the headwaters and channelization to facilitate the flow route to the sea.

- Retention measures can be implemented in large basins relying on civil engineering or using their NBS equivalent according to the Natural Water Retention Measures approach: small retention ponds or optimized wetlands (NWRM: Strosser et al. 2015).
- River channelization can also be implemented by combination or not of embankments with dikes (grey solution) or large river corridors with wider beds. The latter measure, also called "giving room to the river" (hereafter "GRR"), is clearly an NBS, encapsulating several elementary green-blue measures as, according to the NWRM vocabulary:
  - N03 Floodplain restoration and management,
  - N04 Re-meandering,
  - N07 Reconnection of oxbow lakes and similar features,
  - N08 Riverbed material re-naturalisation,
  - N09 Removal of dams and other longitudinal barriers,
  - N10 Natural bank stabilization.

Two <u>absolutely theoretical</u> protection schemes have been studied hereafter with the hypothesis that a hybrid protection plan would both (1) give room to the river and (2) use retention measures. If they would be insufficient to accommodate the FEV, (3) flood walls could be prescribed to fully cope with the reference flood of Oct. 2015.

The two protection schemes were studied, assuming to give W_{GRR} = 5 m and 15 m to the river at z_{GRR} = 1.5 and 1 m, respectively (Figure 24). They were coupled with retention measures with cumulated retention capacities of 120,000 m^3 and 36,000 m^3, respectively. The first protection scheme, hereafter noted as "GRR-5m", thus more relied on large retention measures, while the second one, hereafter noted as "GRR-15m", relied more on the large river corridor.
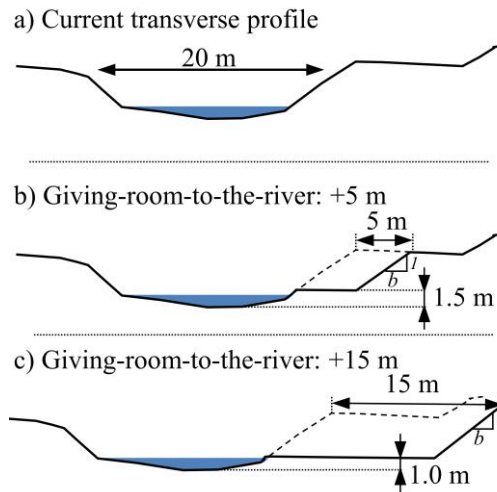
Figure 24 : Synthetic transversal profiles (a) current profile at the hydrological station (Lidar data), (b) profile with 5 m given to the river and, (c) profile with 15 m given to the river.

A Manning-Strickler equation, noted *Q(h),* was fitted on the stage-discharge relationship of the station for depths higher than 0.5 m using the actual geometry (Figure 24a), the longitudinal profile slope *S*=0.004 m/m, bank slope *b*=1.3 m/m and a Manning roughness of *n*=0.043. The Manning-Stickler equation and available geometry details were not suitable for smaller depths and lower flows with small depth/grain size ratio. The additional conveyance capacity related to the wider bed was computed using the compound channel theory (Te Chow 1959). The new river discharge capacity noted $Q_{GRR}(h)$ was thus computed using:

$$Q_{GRR}(h) = Q(h) + \frac{\sqrt{S}\big(W_{GRR}(h - z_{GRR})\big)^{\frac{5}{3}}}{n\big(W_{GRR} + (h - z_{GRR})\sqrt{1 + b^2}\big)^{\frac{2}{3}}}$$

A threshold water depth h_T=3.06 m corresponding in the current section to a threshold discharge for flooding of 135 m³/s was identified as described in Figure 18.

The following preliminary costs were used in this analysis: 120 €/m²-given to the river, 100 €/m³ of retention and 1,600 €/m of 1 m-high flood walls. If the flood walls must be higher or lower than 1 m, the cost is corrected proportionally to the square of the wall height as do hydraulic forces.

Water stages for both the current and the project bed profiles were computed as well as the FEV for both protection schemes (Figure 25 &

Figure 26).

Panel 1 displays the current (continuous line) and projected (dotted line) stage-discharge equations. The current threshold discharge Q_T of 135 m³/s reaches 150+ m³/s with a 5-m wider bed highlighting the higher conveyance capacity. Panel 2 displays the hydrograph whose FEV is computed for both values of Q_T and provided in panel 4.
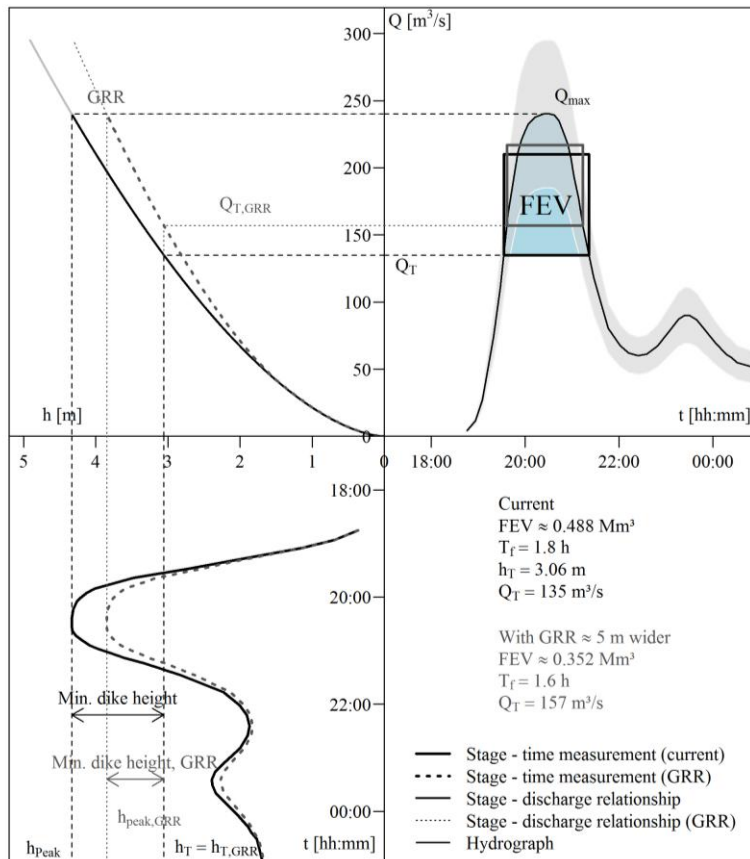
Figure 25 : FEV stage-discharge analysis for the GRR-5 m analysis.

Panel 3 displays a tilted stage time series for both the higher-current and lower-projected stages for the same discharges. Differences between the threshold water depth h_T and the depth peak value give an approximation of the dike height.
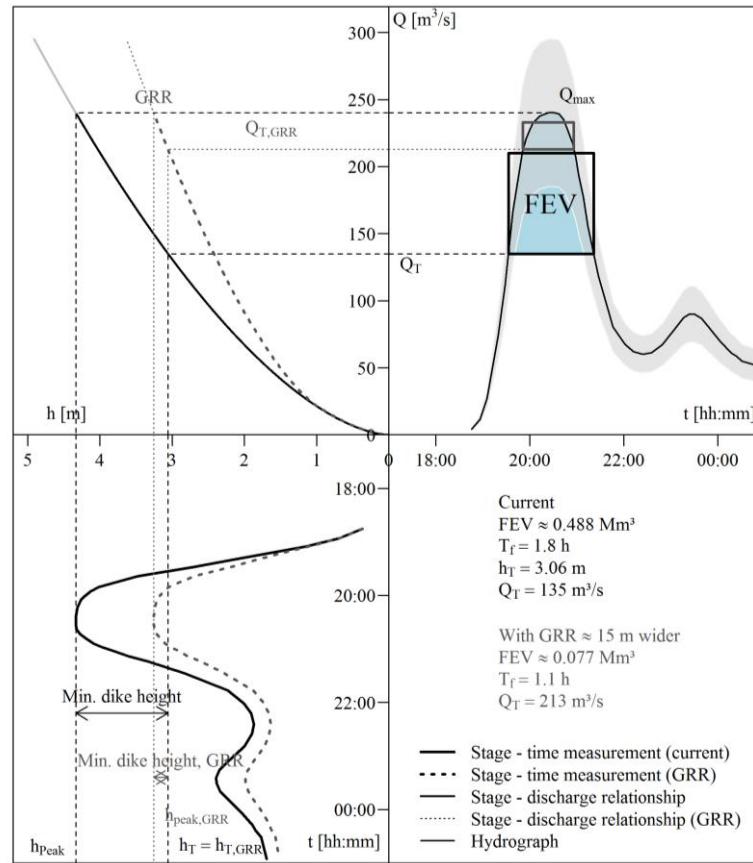
Figure 26: FEV stage-discharge analysis for the GRR-15 m analysis.

In the GRR-15 m scheme, the lowering of water at a given discharge is much more pronounced, (panel 1) resulting in much smaller FEV (panel 2, rectangle sizes) and thus eventual dikes (panel 3).

The full Oct. 2015 flood hydrograph generates a FEV of 0.488 Mm^3 which can be represented by a 2 m-deep square lake with 494 m-long sides in

Figure 27 and

Figure 28 for both protection schemes. In addition to the retention volume provided before and
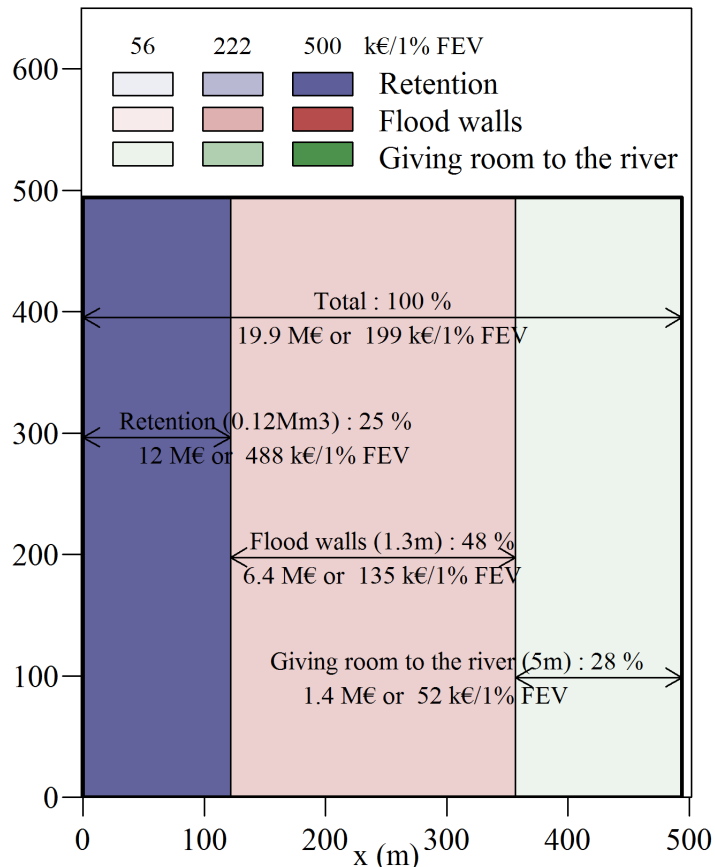
the GRR effectiveness computed above, the remaining FEV is assumed to be dealt with via flood walls. A 0.5 m freeboard has been added to the maximum flood height for security reasons.

Figure 27 : FEV square lake cost-effectiveness for the GRR-5 m analysis.

According to the Figure 25, giving 5 m to the river reduces the FEV by 28% to 0.352 Mm^3. Further, 0.12 Mm^3 of water will be dealt with by other retention measures and the remaining excess volume will be secured by addition of 1.3 m-high flood walls. The full protection scheme is evaluated to nearly 20 M€.

Giving 15 m to the river would decrease the costs by half, although one must stress that land acquisition costs have not been evaluated and could weight a lot in this area.
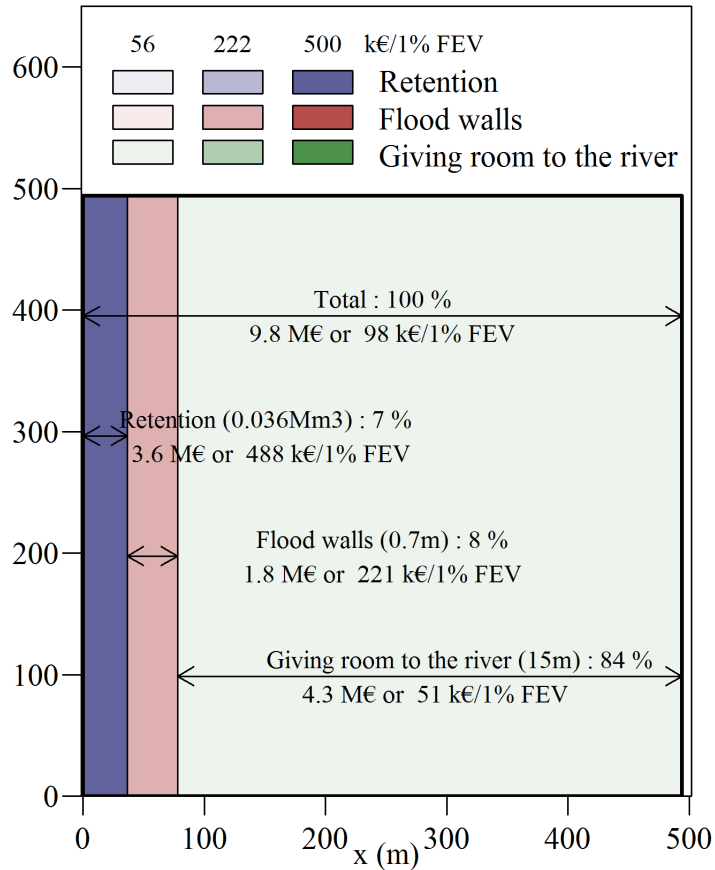
Figure 28 : FEV square lake cost-effectiveness for the GRR-15 m analysis.

It remains obvious that the ratio investment costs/effectiveness is strongly unbalanced toward GRR, which is usually ten times more cost-effective than the grey retention measures.

4.2.3   Limitations of the FEV approach

We are perfectly aware that the FEV approach cannot be trusted as an expert engineering study. Such studies, however, take time and cost money, while the FEV approach is on the contrary, a toy-model for popularization aiming at exploring rapidly a wide range of ideas rather than an actual advanced risk mitigation modelling approach. The following section stresses some of the method limitations.

A   Hydrology and hydraulics

0D approach limitation

Being a 0D analysis, the FEV approach strongly simplifies 1D and 2D processes. A river natural bed section is usually not perfectly homogeneous in geometry and roughness justifying, at least, the use of 1D model. The FEV approach considers only one stage-discharge relationship in the analysis thus ignoring parts of backwater effects. The change related to a widening operation as used in our example may for instance be curtailed by a bridge further downstream. The FEV approach user must consequently pay attention to take into account a relevant stage – discharge relationship and protection measure strategies in accordance with this hypothesis, in our example the bridge widening should for instance be automatically included to the bed widening operation.

Retention measures and routing

Not only changes in the local hydraulics such as bed widening and flood walls, but also upstream retention measures are considered in the approach, eventually spread on the entire catchment. The flood hydrograph analysed locally in the method is actually the result of rainfall – runoff processes spatially distributed over the entire catchment and reaching the section simultaneously after being routed from the point where the rain actually fell. This spatial distribution, the time required for the routing and the usual water self-flushing of retention measures during the recession limb of the flood are ignored in the analysis.

In the discussion section of Bokhove et al. (2018b), an attempt to overcome the spatial distribution challenge and issues related to the spreading of retention measures is proposed. However, rainfall data were lacking to assign relevant probabilities to each of the rainfall spatial distribution scenarios.

The FEV approach should also be used at several sections of the river and the cost-effectiveness considers the costs at the catchment scale: while the local investment in flood walls is often the more cost-efficient, it only protects the asset behind the walls. Conversely, investing in a retention measure will protect the whole downstream catchment.

Available storage capacity

Another issue stressed by Bokhove et al. (2018b) is the hypothesis that the retention capacities are available when the floods reach the threshold discharge above which water must be stored. If most of the retention basin is already filled by water when the flood peak reaches it, the actual stored volume can only be the surface of the basin multiplied by the variation in water depth and not the actual full basin volume.

An interesting example of this issue can be found in a paper related to the effect of a beaver colony in UK on hydrology and pollutant transfers (Puttock et al. 2017). The authors installed hydrological and pollutant monitoring stations upstream and downstream of a beaver colony and performed GIS and geomorphic analysis of the 13 ponds created by beaver dams. The maximum volume of water stored in the lakes themselves is about 1,000 m^3 on a surface of 2,000 m². Even for the big flood event of 12/12/2014 reported in the Figure 3 of the paper, the pond levels hardly changed for more than 10 cm (Figure 2 of the paper). The water volume buffering capacity of the lakes is thus a maximum 2,000*0.10 = 200 m^3, and clearly not 1,000 m^3. It highlights this available storage capacity issue which is the consequence of the beaver willingness to maintain their ponds filled by water.

Additionally, failures of beaver dams during big events are neglected but could also aggravate the flood peaks. Our conclusion on this point is thus that rather than providing flood buffering capacities during extreme events, beavers seem much better at storing water to feed the river during drought. Their effect on sediment buffering is also already widely acknowledged (Wohl 2006) and the additional pollutant trapping demonstrated by Puttock et al. (2017) is another really interesting co-benefit but clearly flood mitigation is not a very good argument.

B   Effectiveness

In its current version, the FEV approach focuses only on one given flood hydrograph, while it is increasingly recommended to look at several scenarios in hazard and protection measure effectiveness studies (Mazzorana et al. 2012).

The French official requirement on flood risk prevention plans is to consider the 100 years return period flood event as the reference event for urban planning, except if a stronger event is known sufficiently in detail. In such a case, the strongest known event is used as reference event. In the Brague catchment case, the Oct. 2015 flood was stronger than the 100 years return period flood and has therefore been used as the new reference event for risk mapping (Préfécture des Alpes-Maritimes 2017). Consequently, focusing on designing solutions to cope specifically with this event makes sense.

It would be possible to look at several hydrographs in the FEV approach, although the method would probably lose in its communication power given by its simplicity. Uncertainty propagation is another challenge. The uncertainties on the hydrograph of the Oct. 2015 flood in Biot are displayed as a grey belt in Figure 25 and

Figure 26. The FEV computed for those extreme hydrographs that are envelopes of minimum and maximums peak discharges are 194,000 m^3 and 815,000 m^3. The uncertainty on the FEV volume is thus relatively high, being at most in the range ± 60%.

C   Costs

The cost-effectiveness analysis is really preliminary in the application presented here. More in-depth analysis should be performed to reinforce the method conclusions. Land acquisition for each measure may have a big impact on the cost balance in the Mediterranean French coast. Maintenance costs were considered in Bokhove et al. (2018b) for the UK sites but not for the Brague site. Finally, co-benefits of each of the measures such as the landscape preservation or environmental quality of a river corridor crossing an urban valley as the Brague were not yet considered and could also impact the decision between measures relying on civil engineering or NBSs.

4.3   Advanced modelling: IBERwood 2D model

4.3.1   Software and theoretical framework

The IBER software is a widely used numerical model in engineering and research. The original model presentation can be found in Bladé et al. (2014). Applications to erosion and flood protection measure effectiveness can be found in Castillo et al. (2014) and Garrote et al. (2016).

According to Ruiz-Villanueva et al. (2014a), *"The hydrodynamic module solves depth-averaged shallow water equations (2D-SWE or two-dimensional Saint Venant equations). The turbulence module allows turbulent stresses to be included in the hydrodynamic computations, and includes different turbulence models based on the Bousineq turbulent viscosity approximation (a parabolic model, a mixing length model, and a k–ε model). The sediment transport module solves the Exner sediment conservation equation together with the bedload and the suspended load transport equations to predict the evolution of the riverbed. In 'Iber', the hydrodynamics, turbulence and sediment transport are solved using the finite volume method (FVM) with a high resolution (second order and non-oscillatory) extension of Roe's upwind scheme, a time explicit scheme, on non-structured meshes."*[1]

The main interest of the IBER software in the particular context of the Brague DEMO site is the recent development of a module by Ruiz-Villanueva et al. (2014a) able to compute large wood piece transport. This module enables to compute the transport of multiple wood elements, assuming logs as cylinders or two cylinder one for the main stem, the other for the root wad, of different sizes at short timescales coupling a discrete element Lagrangian model to the Eulerian approach of the hydrodynamics module of IBER.

---

[1] Since the publication of this description, modules were added to model dam breaching, wind friction, water quality and hydrology, see http://iberaula.es/ for new updatdes.

Validated against experimental tests (Figure 29), it has already be used to explore the process of large wood transport in several pioneering papers (Ruiz-Villanueva et al. 2013, 2014b, 2016a, 2016b, 2016c, 2017) and is hereafter referred to as IBERwood software.
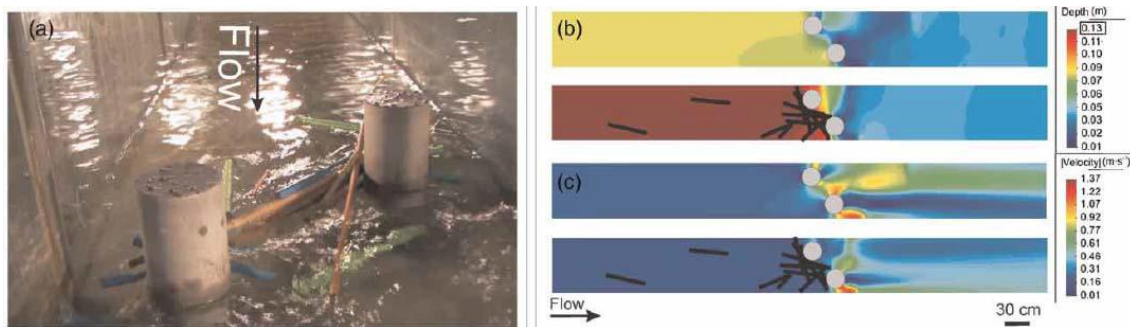
*Figure 29 : Experimental and numerical results for a flume equipped with two large piles. (a) Flume geometry 4; (b) water depth; (c) velocity field with and without large wood (black lines), taken from by **Ruiz-Villanueva et al. (2014a)**.*

Direct contacts with Prof. Ernest BLADE (Univ. Politèc. Catalunya, ESP) and Dr. Virginia RUIZ-VILLANUEVA (Univ. Genève, CHE) facilitated the model use. We gratefully acknowledge their help and wise advices.

4.3.2   Geometry

4.3.2.1   Ground soil

A model geometry limit is always a balance between calculation time and sufficient size to prevent boundary condition uncertainties to influence the area of interest as well as mesh precision to capture the required process details.

In order to test the model capability to compute the transport of large woods from the gorges to the floodplain, the model was extended in the upstream gorge of the Brague on 2.5 km and of the Valmasque on 1.5 km. These distances were chosen according to the availability of topography data (Lidar, pixel 1x1 m). The lowland were modelled on the area known as being concerned by flood hazard following the Oct. 2015's event according to the Préfécture des Alpes-Maritimes (2017) new flood risk map. A small part of the sea was also included to the model as the downstream boundary condition. Its bathymetry was extracted from https://webapp.navionics.com data.

The full model extension is mapped with elevation data of the lidar in Figure 30.
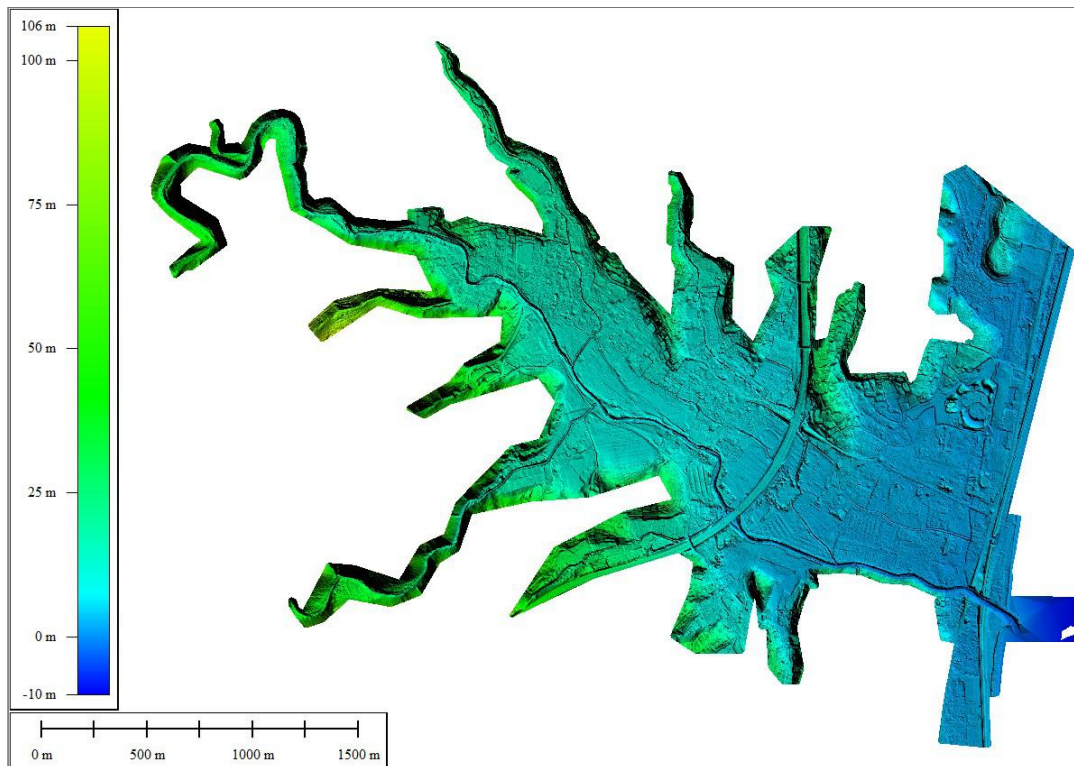
Figure 30 : IBERwood model extension and elevation data from the lidar and bathymetry.

The laser signal used in normal lidar acquisition does not pass through the water surface. In addition, its resolution at 1x1 m was not enough to capture the rectangular concrete channels of the Vallon des Combes and Vallon des Horts tributaries. River bed descriptions are consequently satisfying in the lidar data only providing that no water was flowing or remaining in the bed and that the river bed was large compare to the resolution.

As a consequence, it has been necessary to reconstruct manually on a 3D software a full bathymetry of all the Brague bed and of the bed, top banks and close vicinity of the Vallon des Combes and Vallon des Horts tributaries from a large number of terrestrial topographical dataset provided by the Brague basin agency (SIAQUEBA). Two holes in the highway embankment and the sea bathymetry were included in this correction to the lidar dataset (Figure 31). A raster with a higher resolution (0.25x0.25 m) was generated from these 3D polylines and was systematically used to correct the model mesh after its creation with lidar.
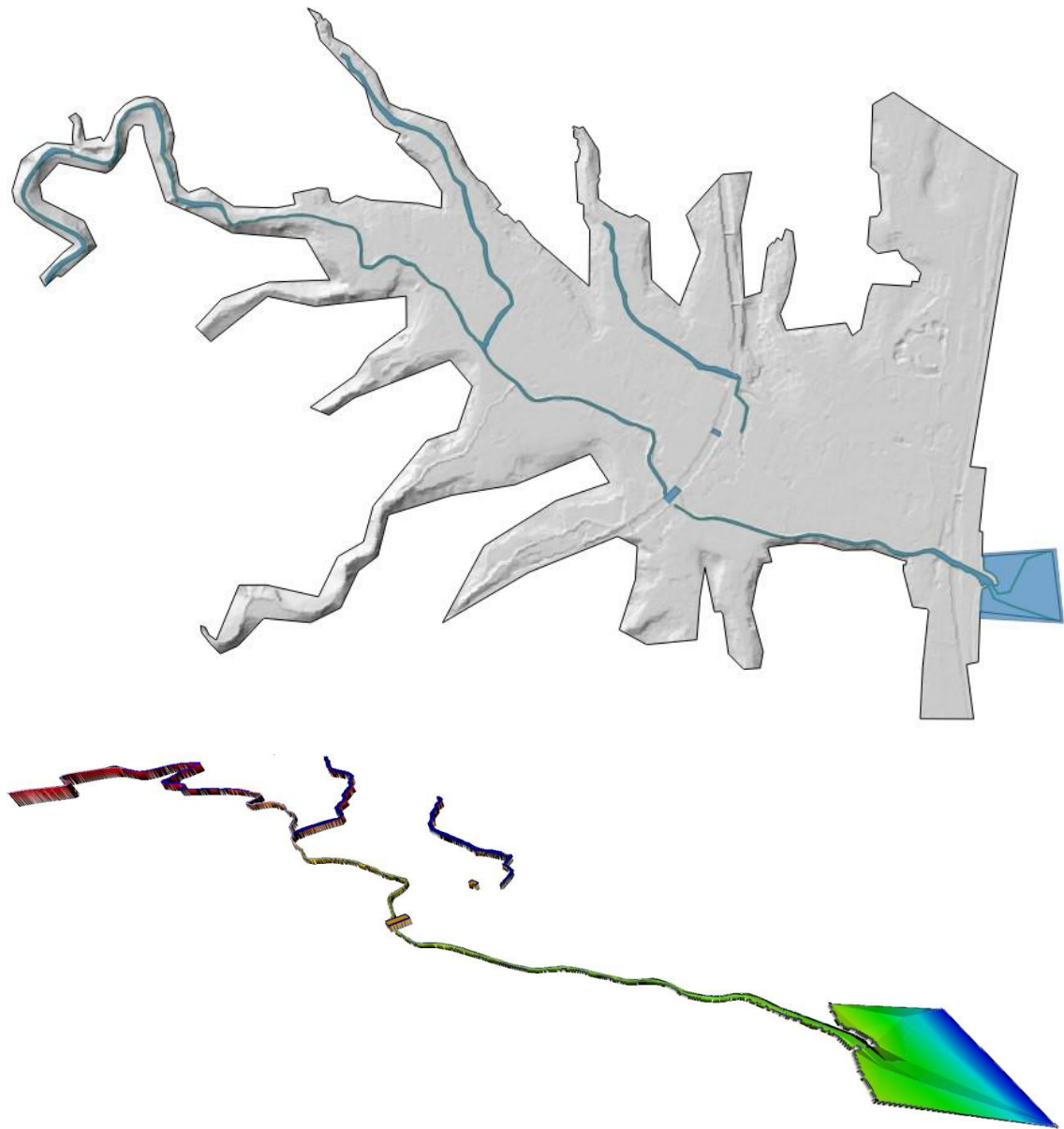
Figure 31 : IBERwood model limits and location of corrections to the lidar dataset using terrestrial existing topographical data (upper panel) and 3D view of the bathymetry digital elevation model

4.3.2.2   Bridges and culverts

Bridges and culverts are numerous on the Brague and its tributaries. The SIAQUEBA topographical dataset was sufficient to describe most of them. Some field visit enabled to control the existing one and measure the few missing small structures. The transversal structures are localized on Figure 32.
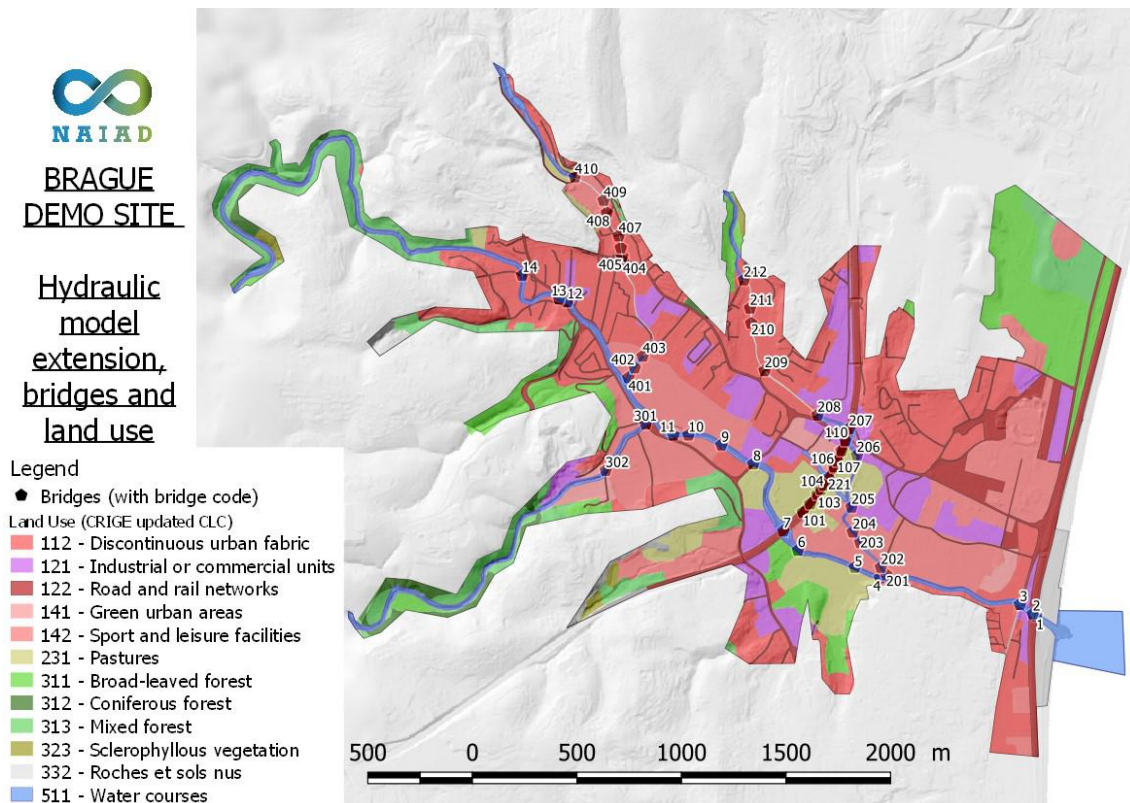
Figure 32 : Bridge and culvert locations and land use in the model extension

4.3.3   Calibration and validation

The model calibration is in progress at the time of writing of this report (Nov. 2018). It is performed in three phases:

1. Computation with increasing discharges to identify step by step the location of overflowing, i.e., bankfull discharge values for each reach. This phase enabled to calibrate the river bed capacity by checking the consistency between the model results and historical data and previous models results.
2. Major flooding with the Oct. 2015's flood event hydrographs to adjust the floodplain calibration by comparing model results with flood level measured after the event.

3. Moderate flooding with the November 2011's flood event hydrographs to check the model calibration (validation phase) using the same method.

4.3.3.1   Bed capacity calibration

4.3.3.1.1   Threshold discharge

A cross control of discharges at the Biot stations and archive references to flooding enabled to define the threshold discharge above which we are sure that flooding occurs to be 120-140 m3/s (Table below).

Table 14 : Cross comparison between peak discharges and archive references to flooding

Date (DD/MM/AAAA)	Official NAT CAT: arrêté CATNAT	Peak discharge at Biot station [m3/s]	Flooding of Brague surrounding	Flooding of tributaries surrounding	No reference of flooding	Extrapolated costs per community Brague catchment*
03/10/2015	**X**	**143** (240)	**X**	**X**		**€ 198,002,201**
06/11/2011	X	221	X	X		€ 34,669,998
11/10/1987	X	171	X	X		No data
25/12/1996	X	144	X	X		No data
13/05/1985		115			X	No data
17/01/2014		104			X	No data
25/12/2000	X	102		X		No data
06/11/2000	X	99.8		X		€ 2,664,535
01/11/2010	X	98.8				No data
24/10/1999	X	97.1			X	€ 5,972,248
02/12/2005		93.6		X		€ 215,576
20/12/1997		87.4			X	No data
06/10/1993	X	83.4		X		No data
23/10/1999	X	82.9		X		€ 3,341,094
19/12/1997		75			X	No data
06/09/2005	X	No data				€ 7,975,153
11/01/1996	X	70				€ 1,227,478

*Extrapolated costs per Brague catchment community (CCR, CERES, Athena Database)
**The Oct. 2015 peak discharge has not been measured due to the flooding of the station. It has been estimated to 240 m3/s by Lebouc and Payrastre (2017).

These data also highlight that the Brague main-stem has not systematically the same hydrological response than its tributaries: several mentions to major flooding of the Vallon des Combes, Valmasque and Vallon des Hortes during a none major, although high discharge of the

Brague triggered damages along the tributaries or downstream the confluences in Antibes and close from the highway.

4.3.3.2   Floodplain calibration and validation data

A   Hydrographs

The hydrographs in each inputs points were digitalized in Cabinet Merlin (2016c) appendix for both the 2015's and the 2011's floods events.
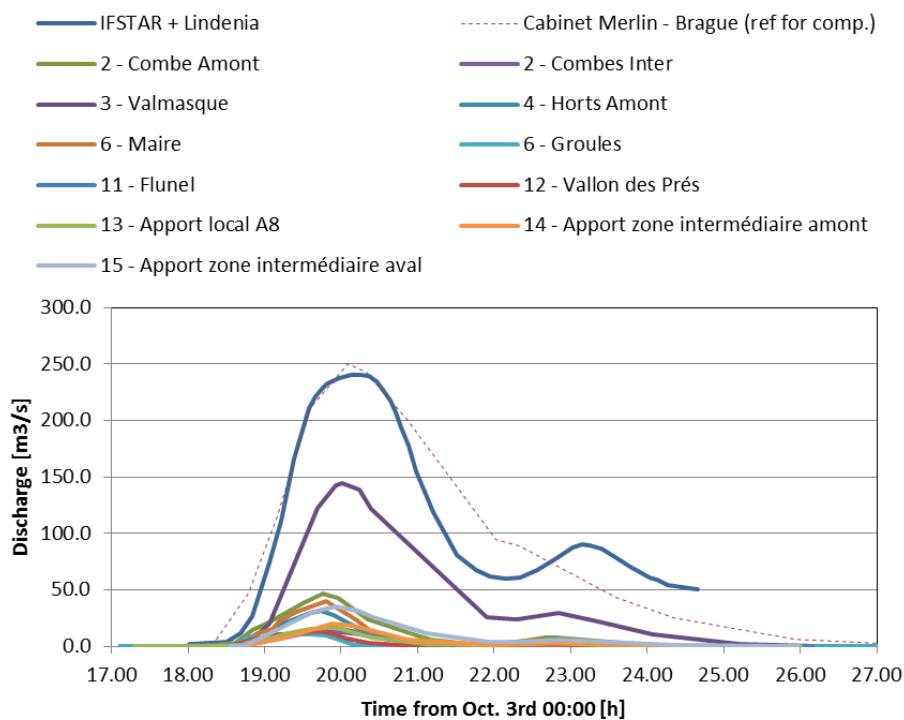
Figure 33 : Hydrographs used for the 2015's flood event.

The Brague mainstem hydrograph used by Cabinet Merlin (2016c) was extracted for comparison but the hydrograph presented in §3.3.2 is used.
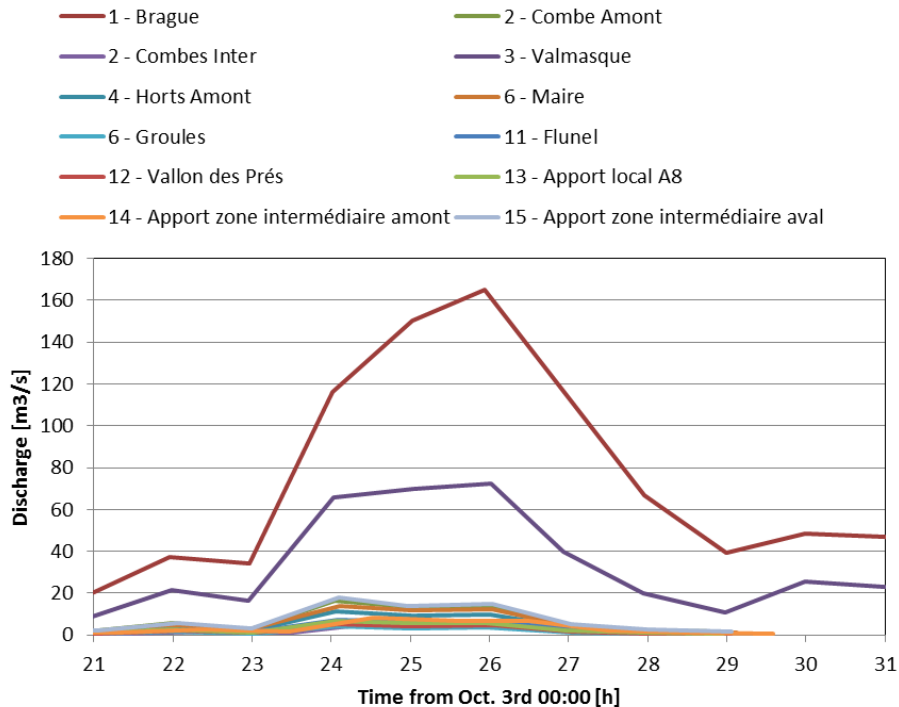
Figure 34 : Hydrographs used for the 2011's flood event.

B   Land uses

The Corine Land Cover database has been reanalysed regionally by the CRIGE GIS centre[2]. Slight corrections and simplifications were performed using the IGN BD carto database to map land uses of the Brague lowlands as displayed in Figure 32.

Currently, the idea is to assign one Manning roughness coefficient to each land use. In addition, our model includes all building from the IGN BD topo database as holes in the model mesh. Flows through building are consequently neglected which is a conservative hypothesis regarding flood levels.

C   Flood levels

A flood mark inventory was performed Immediately after the Oct. 2015's flood within the in-depth analysis organized by the Préfécture des Alpes-Maritimes (2016). Nearly 400

---

[2] Downloadable here : http://www.crige-paca.org/# and online portail here : http://lizmap.crige-paca.org/lm/index.php/

georeferenced points with the flood mark elevation can be downloaded on the French national flood mark data base[3] (Figure 35).

Sources: https://www.reperesdecrues.developpement-durable.gouv.fr for flood mark dataset, IGN BD topo and carto, Flood risk map from Porté à Connaissance (Préfécture des Alpes Maritimes, 2017)
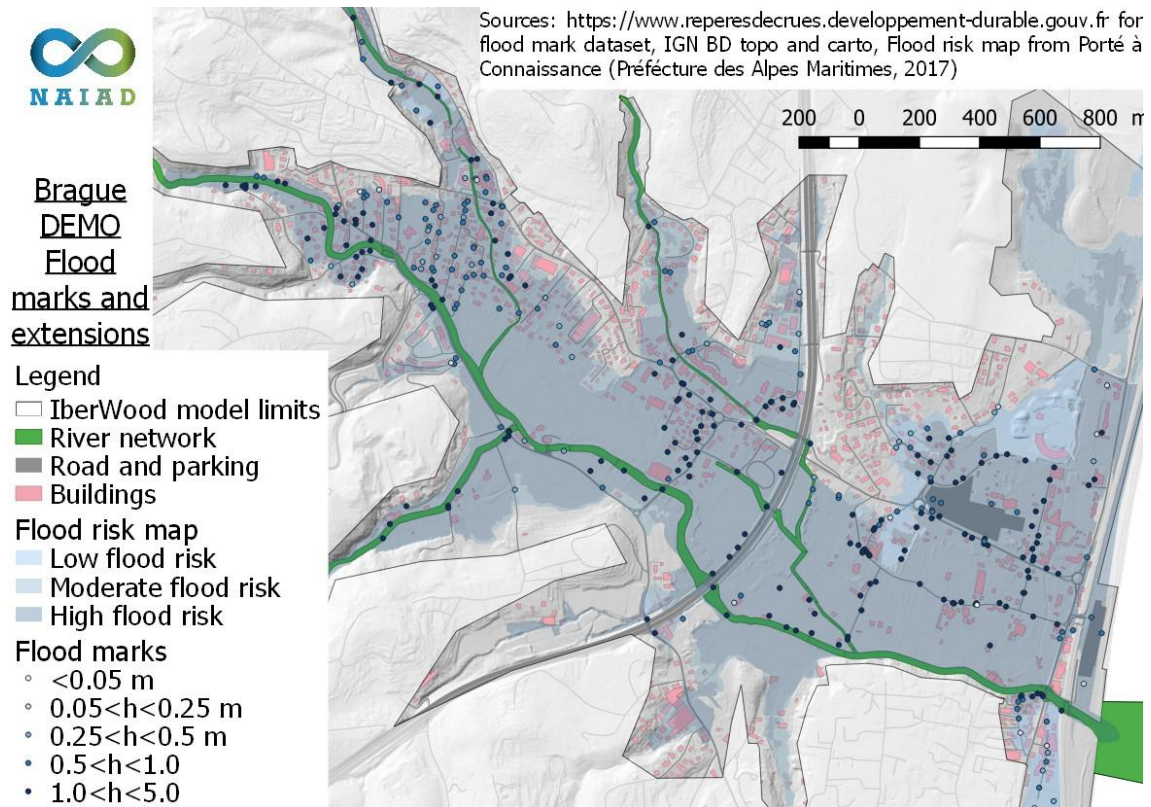
Figure 35 : Flood marks and flood extension used for the model calibration.

The flood level computed with the hydrographs provided in Figure 33 will be compared to these data to optimize the IBERwood model calibration as done by Cabinet Merlin (2016c). A second set of flood mark are available for the 2011's event and will be used in the validation phase.

4.3.3.3   Large wood transport calibration data

As mentioned before, the Brague case study is particularly interesting from a scientific point of view because of the magnitude of large wood recruitments, transport and depositions that occurred during the Oct. 2015's flood event.

The torrent control service of the national forest office performed an inventory of the large wood jams in the day immediately following the event (RTM06 2016a, 2016b). The locations and

---

[3] Open access data: https://www.reperesdecrues.developpement-durable.gouv.fr

volumes of large wood jams reported in their inventory were provided in the NAIAD Deliverable 6.1 (Pengal et al. 2017).

In order to get more elements for the calibration of the IBERwood model or any other method for the analysis of large wood-related process, the national geographic survey (IGN) and the Alpes-Maritimes torrent control service (ONF-RTM 06) were subcontracted within the NAIAD project to:

- Perform an inventory of the areas eroded during the flood and trees located in these areas (Guitet 2018);
- Update the original inventory or large wood jams with complementary pictures (RTM06 2018).

A   Inventory of source areas and recruited trees

A manual analysis of differences between the orthorectified aerial pictures of 2014[4] and 2017[5] was performed to digitalize polygons of eroded areas for a total of 93 334 m² (Figure 36).

---

[4] 20 cm resolution, ORTHO-HR® taken between 04/23/2014 et 07/08/2014
[5] 20 cm resolution, ORTHO-HR® taken between 06/13/2017 et 07/06/2017
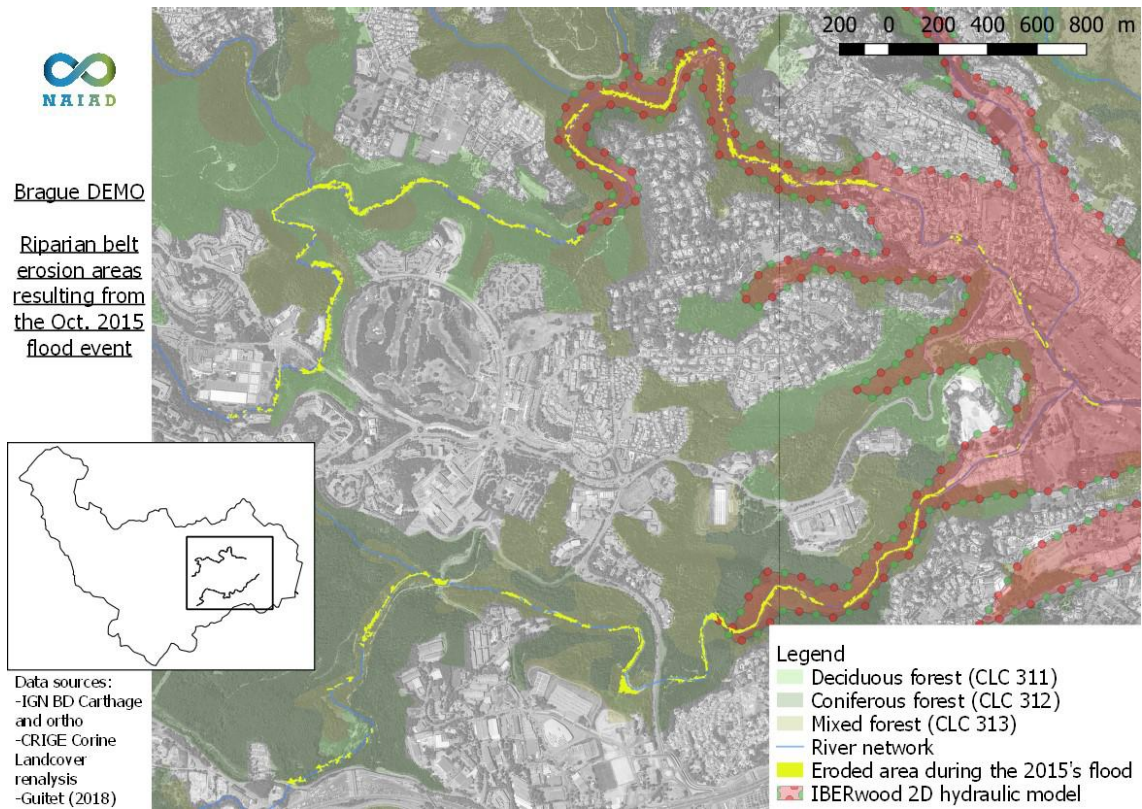
Figure 36 : Erosion areas observed between 2017 and 2014 as mapped by **Guitet (2018)**.

These erosion areas were used to compute bed widening due to the flood (see below). Within these polygons, the crowns the 2,945 trees present in 2014 and which disappeared before 2017 due to the flood were digitalized as ellipses (Figure 37). The surfaces of these ellipses were an interesting proxy of the tree sizes (Guitet 2018). An example of the digitalization is provided in Figure 38.
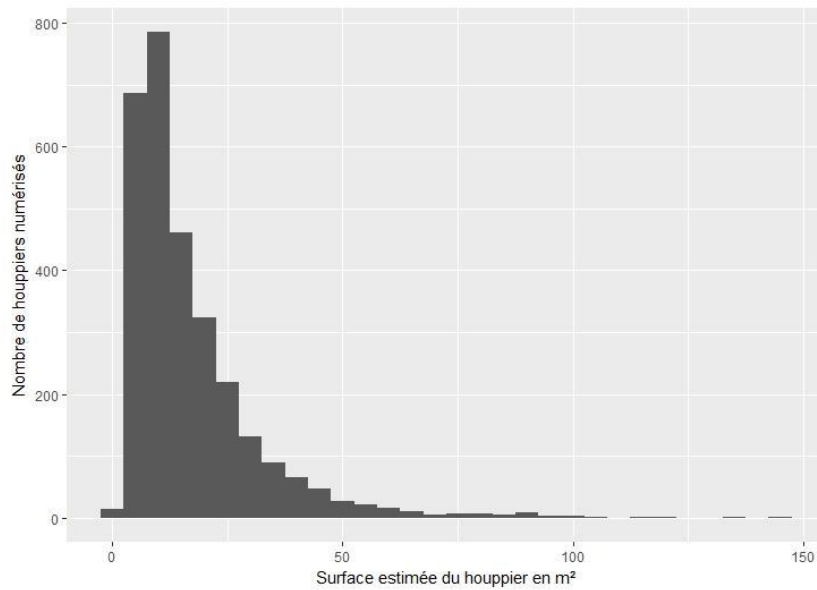
*Figure 37 : Tree crown surfaces VS numbers of trees of the 2,945 trees digitalized **(Guitet 2018)**.*
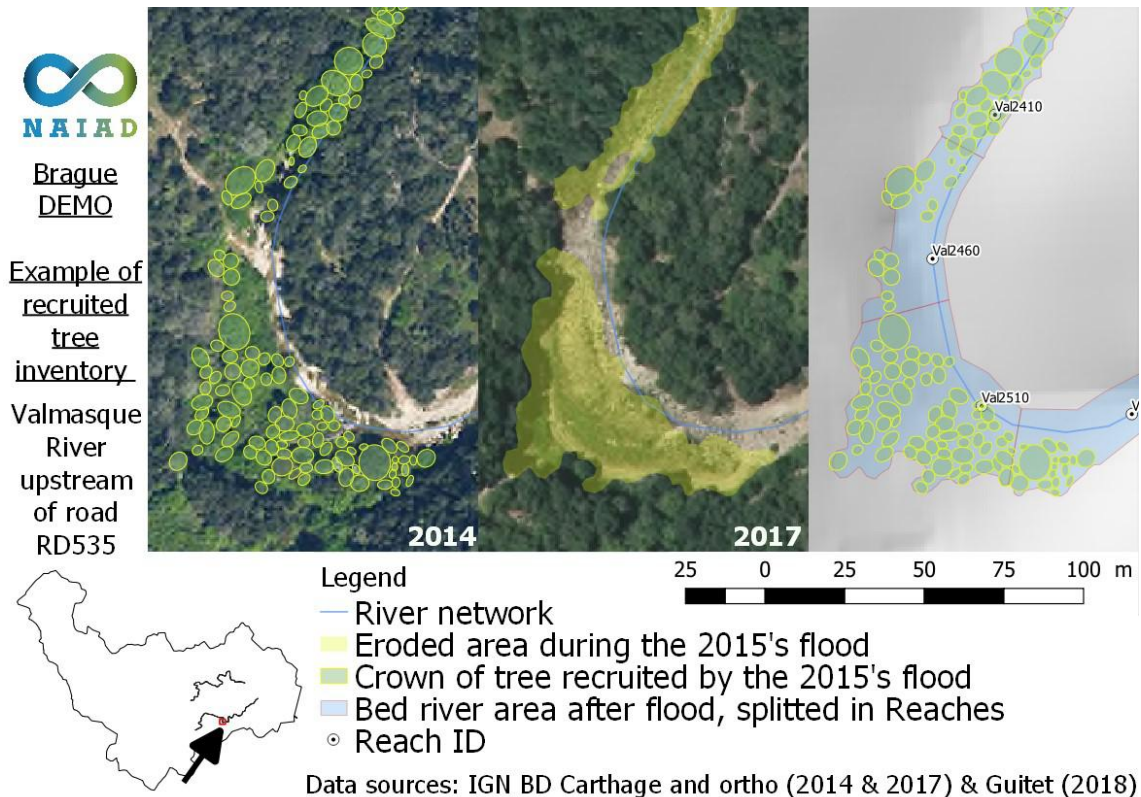
Figure 38 : Example of the recruited tree inventory: the Valmasque reach upstream of the road RD535, 2014 picture with yellow ellipses on existing trees, 2017 picture with light yellow polygon on eroded area and synthesis map of river bed area after the event, reach ID codes (see later)) and trees recruited.

B   Estimation of large wood volume from crown areas

A field campaign was organized to locate a sample of 138 trees, measure their tree and trunk heights and diameters and specify their species. The crown surface of this sample was also digitalized on the aerial pictures. The trees features were used to determine the large wood volume of each tree with two different equations:

- The IFN equation aimed at quantifying the "strong wood" volume, i.e., volume of particularly thick branches and stems;
- The EMERGE equation aimed at quantifying the wood volume of a tree, giving a bigger volume than the IFN Equation, thus capturing also small branch volumes.

The equations are not provided here; they are complicated and very specific, one would refer to the dataset which will be made open access and to the joined report of Guitet (2018) for further

details. Based on discussion with its author and cross controls with large wood jam pictures, it has been assumed that the IFN equation was more representative of the type of logs triggering large wood jams and is hereafter use to compute the trees' large wood volumes and sizes to be introduced in IBERwood.

Using crown tree surfaces on the one hand and the tree volume on the other hand, proportional equations were fit on the whole sample (Figure 39). The same approach was used with the two more frequent species and the remaining sample. Using power equations did not improve the statistical significance of the equations.
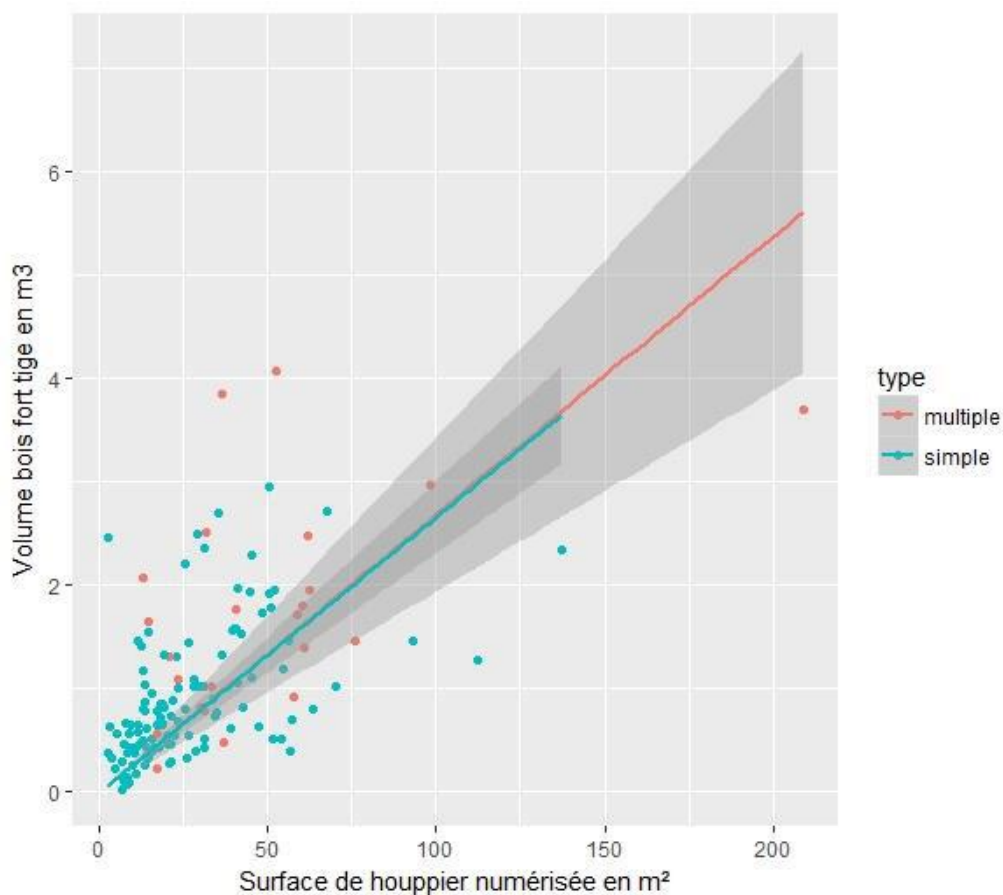
*Figure 39 : Tree crown surface VS large wood volumes and proportional fits **(Guitet 2018)***.

For the computation of a single tree large wood volume $V_{Large\ wood}$ [m³] only knowing the tree crown surface $S_{tree\ crown}$ [m²] and eventually the specie, it is thus proposed to use an equation:

$$V_{Large\ wood} = \beta . S_{tree\ crown}$$

With β coefficients as provided in

Table 15 : Proportionality coefficient between tree crown surfaces and tree large wood volumes

Sample (*Latin name*)	β
Whole dataset	0.026708
Alder (*Alnus)*	0.032783
Ash (*Fraxinus*)	0.02480
"Other": whole sample except *Alnus* and *Fraxinus*	0.028876

A cumulated volume of 1 450 m^3 ± 150 m^3 of recruited large wood volume was computed using the 2,945 ellipses digitalized on the whole erosion areas mapped in Figure 36 using this equation, resulting in an average large wood surface density of 144 m^3/ha. The EMERGE equation with also specified coefficients provided a cumulated volume of 1 650 m^3 ± 300 m^3, i.e., 187 m^3/ha on average.

C   Estimation of log sizes based on large wood volume

The IBERwood software is able to route large woods under the form of cylinders with given diameter, length and density, eventually comprising second shorter and wider cylinders figuring root wads. Each of these parameters should be estimated based on literature data or the crown sizes.

Wood density

We could not afford within NAIAD a field campaign of wood density measurements; it had thus been decided to rely on literature data. Guitet (2018) provided a table of wood density of living and dead trees coming from the literature (Table 16), stressing that the variability within a population is very high. As first approximation, a random value taken in a uniform distribution in the range 0.7-1 would be acceptable.

Table 16 : Wood density for species and living or dead dry trees

Species (*Latin name*)	Dry wood density (12% water content)	Living wood density
Alder (*Alnus*)	0.42	0.95
Ash (*Fraxinus*)	0.56	0.90
White Oak (*Quercus pubescens*)	0.65	1
Holm Oak (*Quercus ilex*)	0.73	1
Hornbeam (*Carpinus*)	0.66	No data
Maple (*Acer campestre*)	0.51-0.56	0.95
Elm (*Ulmus glabra*)	0.52	1.05
Lime (*Tilia*)	0.43	0.7

Log length and diameter

The large wood volume of a tree varies with its total height, trunk height, trunk diameter and specie that influence its shape. Simple linear multivariate regressions constrained by conditions, e.g., total height higher than trunk height, were fit by Guitet (2018) on the 138 trees' sample. Using a probabilistic approach, he computed a large sample of possible tree features, i.e., values of *specie-diameter-total height-trunk height*, each of them being related to one large wood volume value through the multivariate linear regressions.

To estimate the features of each digitalized tree, he proposed to randomly pick the features in this probabilistic sample knowing its volume by the crown surface regression.

In addition, among the 138 measured trees, 17% were multi-stems trees, i.e., with several trunks. The sample was not large enough to provide a precise estimation of the probability for a given crown to be a multi-stem tree. Guitet (2018) recommended to consider 80% of crowns as mono-stem trees and 20% as multi-stem trees. For the latter group, he proposed an algorithm to compute the features of each stem such that their cumulated volume is the total crown surface-based volume. See Guitet (2018) for details.

In essence, one can estimate log sizes for each digitalized crown although the approach is necessarily probabilistic, since the trees were recruited and disappeared during the post-flood cleaning operation: we will never know the actual features of each of these trees.

Such a dataset is unique to our knowledge and will be useful for testing the capability of tools as IBERwood to compute large wood transport. The next section aims at analysing the erosion area features.

D   Bed widening analysis

Estimating the large wood supply from a given catchment and under a given flood is a key step of protection scheme design and remains very complicated (Piton and Recking 2016). In rivers where the main large wood sources are banks and alluvial terraces as the Brague, a possible way to compute the large wood production is to estimate the erosion surface and to multiply this surface by the large wood surface density (m^3/ha). The latter may be measured and computed based on field survey. The first requires estimating the bank and alluvial terrace erosion potential, a complicated step lacking references and recommendation in the literature. A back analysis of the erosion surface distribution and bed widening on our well know Brague case study was thus interesting to perform.

The three rivers were massive erosion occurred as mapped in Figure 36 were split in 50 m-long reaches for a total of 214 reaches as exemplified in Figure 38:
- 79 reaches for the Brague,
- 31 for the Bouillide and

- 104 for the Valmasque.

The river bed precise surface had been mapped in the lower part of the Brague using terrestrial topographical data on a length of 1.8 km during the bathymetry construction (see §4.3.2). In this well-known area, the Brague width was 10.8 m on average for a catchment area of 37.3-41.8 km². Upstream of this reach and on the Valmasque River, canopy covering most of the river in the *pre*-flood stage (aerial picture 2014), the initial bed could not be digitalized and had to be indirectly mapped.

The IGN BD Carthage database was used to define the river axis. According to the well-known fact that river bed widths W [m] are proportional to catchment areas A [km²] to a power coefficient of ≈0.4 (Parker et al. 2007, Piégay et al. 2009, Bertrand and Liébault 2018):

$$W = \gamma A^{0.4}$$

We used the lower Brague to compute the proportionality coefficient γ=2.4-2.5. This equation was used to map the Bouillide and Valmasque River bed surfaces as strips surrounding the river axis, with width depending on the reach catchment area. These strips were merged to the bathymetry-based bed surface of the lower Brague to form the *pre*-flood bed surface.

These polygons were merged with the erosion surfaces mapped by Guitet (2018) and displayed in Figure 36 to map the *post*-flood bed surface as displayed in Figure 38. For each reach, several parameters considered as possible drivers of erosion or bed widening susceptibility were computed:

- Catchment areas were preliminary computed to estimate the strip width.
- *Pre*- and *post*-flood widths were computed by reach areas divided by their length.
- Slopes were computed based on the lidar data with linear fit on homogeneous lengths.
- Maximum flood discharge were extracted from Lebouc and Payrastre (2017).
- Width ratio $W*$ were defined as the ratio between *post*- and *pre*-flood widths.

The range of variation of each parameter is reported in Table 17.

Table 17 : River reaches parameter ranges

River name	Cumulated length [km]	Catchment area [km²]	Bed slope [%]	Peak discharge [m³/s]	W_0 *pre*-flood [m]	W_1 *post*-flood [m]	$W* = W_1/W_2$
Brague	3.95	37.8-41.8	0.7-1.7	210-240	6.4-20.1	8.9-42	1-4.0
Bouillide	1.55	12.2-13.1	2.0	115	6.7-7.1	6.9-35.5	1-5.1
Valmasque	5.2	7.2-13.4	0.9-3.2	75-133	5.4-7.2	5.6-45.7	1-7.0

Figure 40 displays a multi-panel scatter plot and the correlations between the various parameters of this 214 reaches' sample.

Figure 40 calls for the following remarks:
- Catchment sizes have two modes: 7-13 km² for the two tributaries and about 40 km² for the main stem, and show:
  o Significant correlation**[6] with peak discharges: larger catchments drain naturally higher amount of water as discussed in §3.3;
  o Significant correlation** with *pre*-flood width, partially an artefact of our width construction method discussed above;
  o Partial correlation with *post*-flood width** and partial inverse correlation with width ratio*, W_0 increase more with catchment size than W_1 or with slope**, because bigger catchments usually feed milder reaches.
- Slopes are generally close from 1.5%, although the lower reaches are usually milder than 1%. Poor correlations* with other parameters are detected.

---

[6] (absence of) correlations with p-value < 0.05 and < 0.01 are respectively noted with "*" or "**".
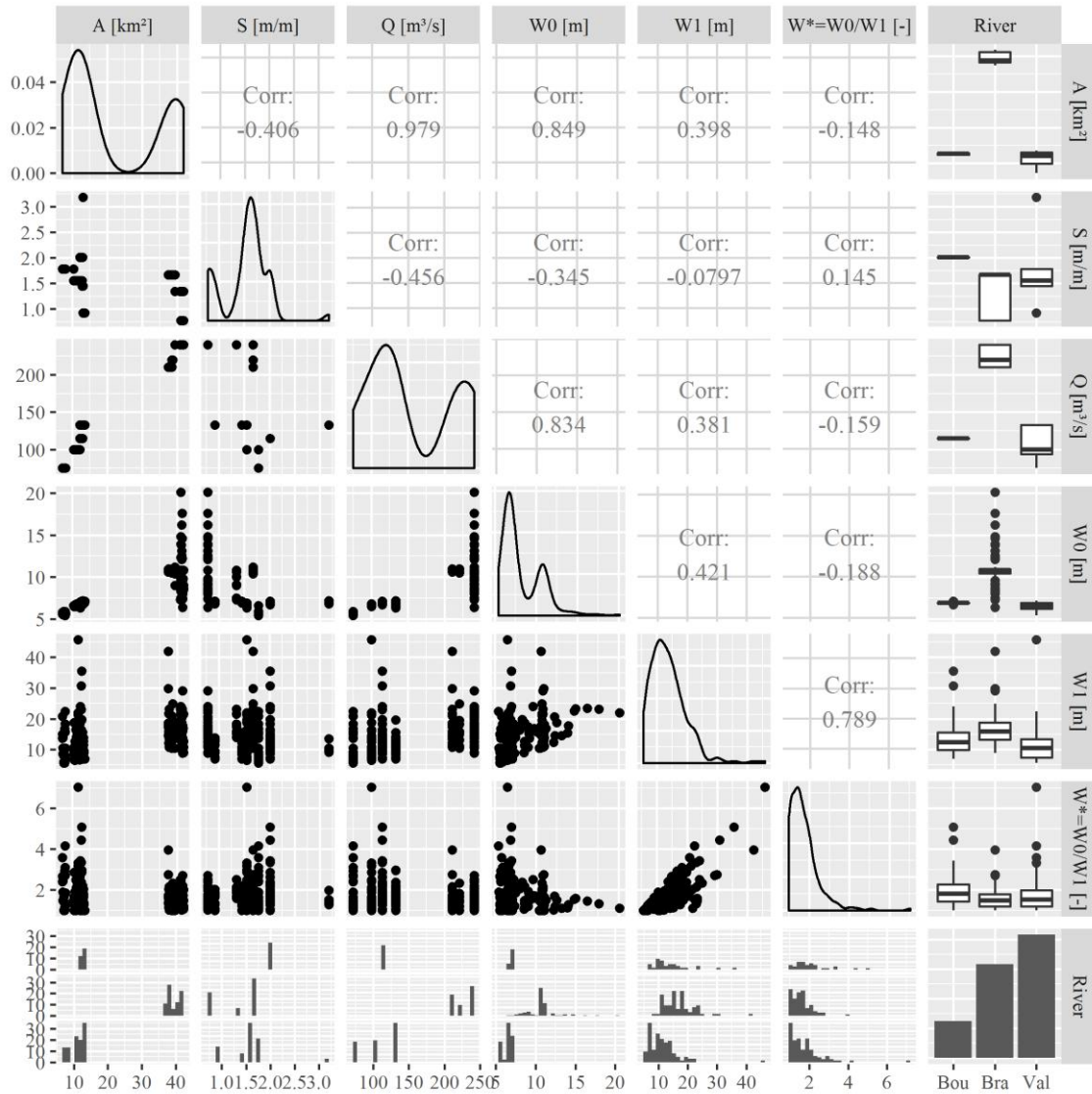
*Figure 40 : Correlation between main possible drivers of bed widening : Catchment size, slope, peak discharge, pre- and post-flood widths (plot using GGally R package of **Schloerke et al. 2018**).*

- Peak discharges have two modes similarly to catchment sizes and show;
  - Significant correlation** with *pre*-flood widths, likely a result of the correlation with catchment size.

- o Partial correlations with *post*-flood width**, the scattering remaining very high although higher discharges seem to induce higher *post*-flood widths and width ratio* as mentioned before about catchment size. The peak discharges are thus a driver but not sufficient to compute accurately the width increases.
- *Pre*-flood widths are bimodal with the same pattern than catchment sizes and their correlations with *post*-flood width** and width ratio** may be artefacts of their mapping and computation methods.
- *Post*-flood widths are no longer bimodal: the river bed widened with variable magnitude, the width ratio was 1.7 ± 0.76 (mean ± standard deviation), its 90%, 95% and 99% quantiles were respectively only of 2.5, 3.0 and 4.4, but a few extreme values went up to 7.

Eventual correlations between width ratio and unit discharge (Q/W_0), steam power (ρgQS), unit stream power ($\rho gQS/W_0$), Shields parameters and velocities using a Manning equation to compute flow depths were explored and gave disappointing results without significant correlations (p-value >0.05).

Overall the occurrence of bed widening remains a partially stochastic process, obviously related to the occurrence of an extreme flood event but with only very partial correlation to peak discharges and other flow describing parameters.

Two possible ways could be explored in further works with dataset comprising several case studies:

- Using an average value of the width increase on a reach length to be selected based on a criterion still to be defined.
- Using a probabilistic approach by applying an average probability density function of width ratio, also on a reach length to be selected based on a criterion still to be defined.

E   Inventory of deposition areas

The officers who performed the first large wood jam survey (RTM06 2016a), came back to the main large wood jams for which additional data were obtained within NAIAD under the form of pictures. They updated the dataset compare to the mapping provided in D6.1 of NAIAD (RTM06 2018). This new version is mapped in Figure 41 and will be made openly accessible in accordance with H2020 European project rules.

The cumulated large wood volume reaches 8 619 m^3 including voids.

The void ratio is consequently of 80%-83% if using a solid fraction based only on the large wood production volumes inventoried by Guitet (2018).

Once the flood levels both in the river bed and in the flood plain will be reasonably reproduced by the IBER model, we will try to introduce large wood pieces based on the Guitet's (2018) inventory and will test the capability of the IBERwood software to reproduce the jams' locations, particularly at bridges. Jams on other trees strong enough to resist the flood as e.g., all along the upstream gorges, are suspected not to be reproduced by our model due to its accuracy. Large remaining trees' locations and sizes are not included in the mesh which is rougher.
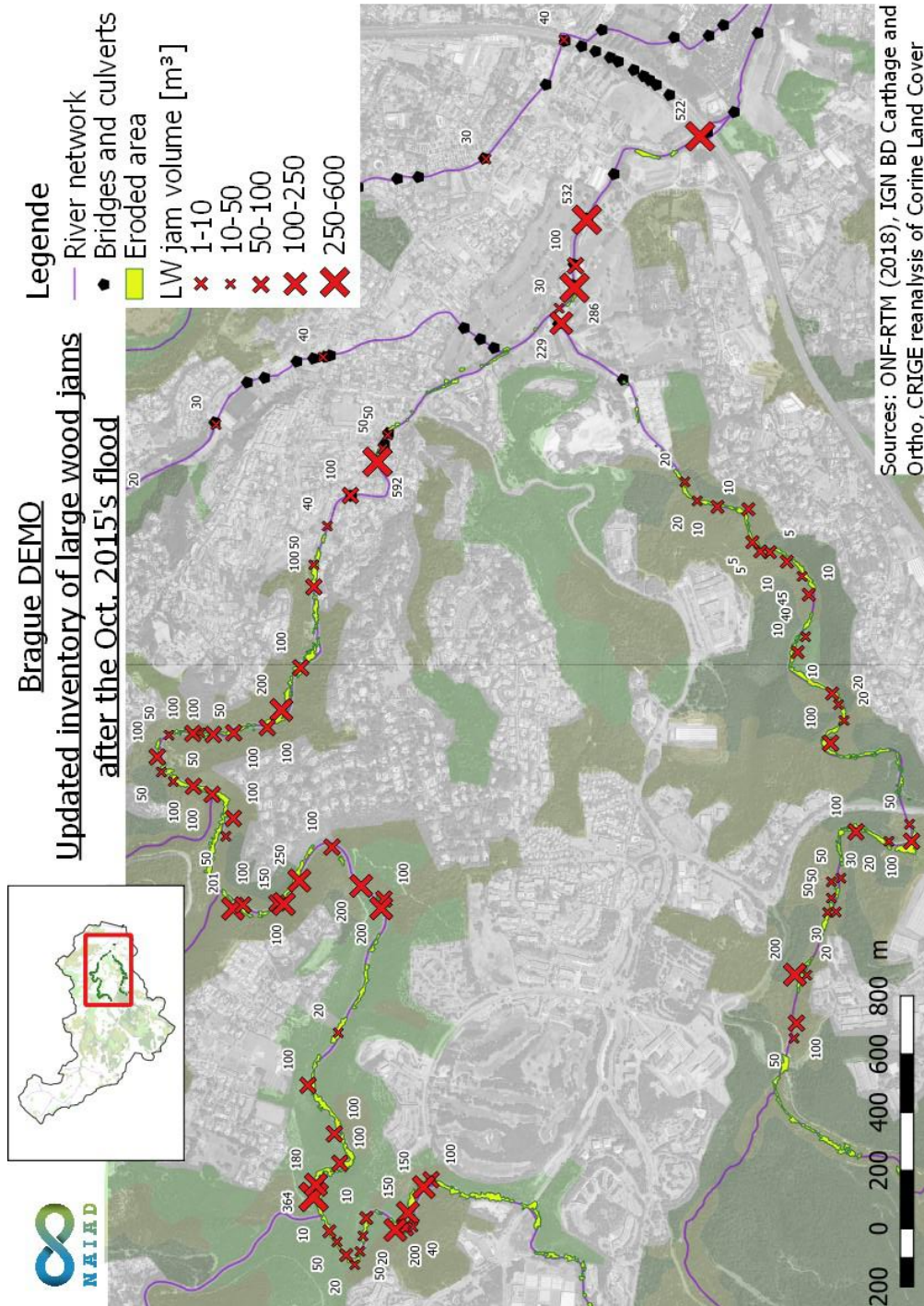
Figure 41 : Updated inventory of large wood jams occurring during the Oct. 2015 flood.

5   Exposition to flood and runoff risks results

This chapter synthesizes and analysis of the CCR claim database aiming at better knowing the exposition of assets to flood (and runoff) risks. Vulnerability and damage estimations will be part of Deliverable 6.3 and are thus beyond the scope of this report.

5.1   CCR flood claim database

CCR has a historical claims database created under the framework of bilateral contracts with its ceding companies. At each contract renewing, ceding companies have to transmit these data under confidentiality conditions (Moncoulon et al. 2014, Naulin et al. 2016). As CCR reinsures a large proportion of French insurance policies, historical claims associated with historic flood event managed under the NatCat system, offer a global vision of the French exposure to flood risks. This database describes the usage of the asset (residential or professional), the nature (house, building or apartment) and its occupation (owner, tenant and co-ownership). Most of the historical claims are georeferenced at the address level (buildings), some of them are localized at street level or at the community centre (Table 18).

Table 18 : CCR historical flood claims geocoding quality for the Brague catchment

Geocoding quality	Rate
Address	59%
Street centre	16%
Town centre	25%
Fail	0%

Regarding these data collection, some cautions have to be taken such as that this database could not be publicly shared due to personal requirement reasons (data contains private information).

5.2   Exposition to flood and surface runoff from the 2015 event CCR

A first analysis consisted in distinguishing the claims related to flood hazard and those related to runoff hazard (also called pluvial flooding).

Only 40% of the 2015 damages are located inside flood hazard areas. We thus estimate that about 60% of the damages (in value) are due to runoff in the DEMO (Figure 42). Based on this information, it seems very important to explain these damages through runoff modelling, thus CCR has focused its efforts on modelling runoff hazard on the October-2015 event.
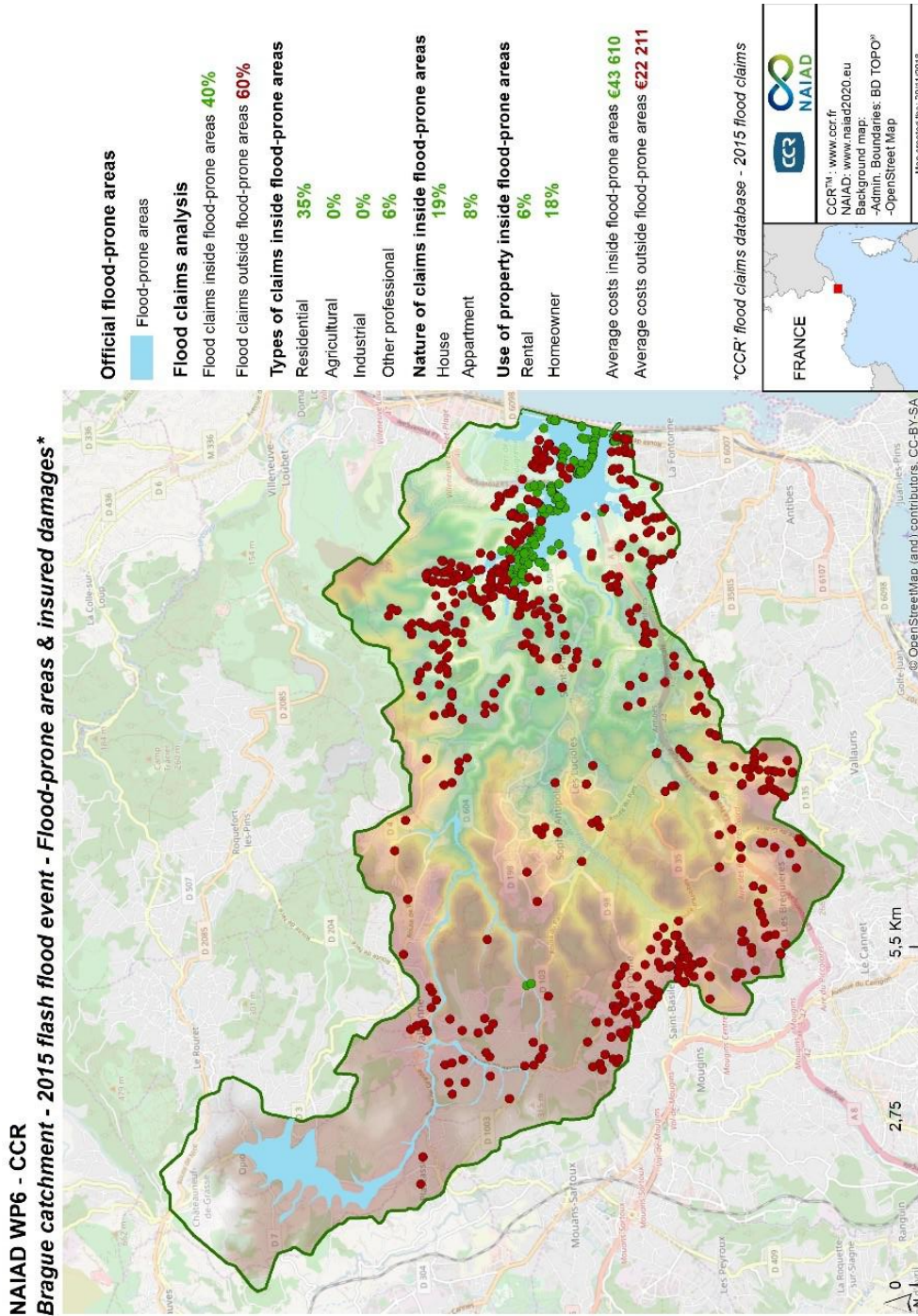
Figure 42: Location and types of claims for the 2015 event.

First of all, the analysis of, the damage profile for the selected 2015 event in the Brague catchment highlight that residential areas are the most damaged type inside flood-prone areas (35%), notably individual houses (19%) and homeowners (18%). The average costs inside flood-prone areas are higher (€43 610) than the average costs outside (€ 22 211). Globally, average residential flood claims are lower (€33 370) than professional ones (€101 560). Based on the database portfolio, for the 2015 event, residential claims represent 81% of the total number of flood claims – with houses the most impacted 55% -, and professional claims represent 17% of the total. Policyholders located in dense discontinuous urban areas are highly exposed to floods, and thus, a great majority of 2015-flood claims are located in these areas.

An analysis on detailed land use cover (Figure 43, right panel) allows more precise information on relation land-use/claims than the large Corine Land Cover (Figure 43, left panel).
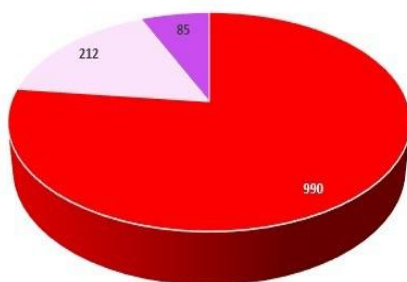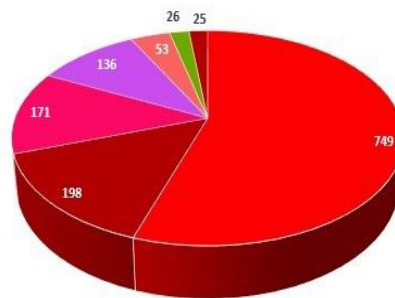
Figure 43 : Flood claims related to land-use cover in the Brague catchment.

All the Brague catchment areas are not exposed to the same degree of risk due to their different degree of hazards, exposure and vulnerability (Figure 44). The downstream areas are the most exposed and impacted. The aggregated 2015 flood claims at the IRIS scale demonstrate that the Biot Village, North part of Antibes and Vallauris village are the most exposed areas. This is notably due to the high degree of impervious areas, e.g., the highway, continuous and discontinuous urban areas increasing hazards, and concentration of population increasing vulnerability.

A finest aggregation at mesh 250m precisely target the most damaged areas such as Antibes near the sea and at the confluence of the Vallon des Combes/Brague and Vallon des Hordes/Brague (Figure 45).

Table 19 illustrates the analysis of the claims' ratio[7] per type of land-use[8]. For continuous urban areas, the main typology of risk is "collective building" with the problem of floor levels. For these reasons, the claim ratio is only 1%. But when focusing on ground level risks (most commercial and individual houses), the claim ratio increases significantly to 3% and 9%. In discontinuous urban areas, individual houses accounting for the great number of claims in 2015 (493). This represents a claims ratio of 18%.

Table 19 : Analysis of the 2015-flood event at the Brague scale

Land-use	Number of claims	Number of properties	Claims ratio (%)	Average costs (€)	Damage weight per land-use (%)
Continuous urban areas	25	985	3	8,783	1
Commercial	*8*	*284*	*3*		
Individual houses	*12*	*135*	*9*		
Discontinuous urban areas	749	7883	10	25,565	42
Commercial buildings	*83*	*609*	*14*		
Individual houses	*493*	*2778*	*18*		
Agricultural areas	9	220	4	25,811	1
Industrial areas	334	2418	14	52,900	19
Whole Brague catchment	*1410*	*13619*	*10*	*33,290*	*100%*

Source: Caisse Centrale de Réassurance, insurance database.

---

[7] The claim ratio is the number of claims divided by the number of property, number for the 2014 portfolio. Claims ratio for individual houses is the number of individual houses claims divided by the number of residential property. The same for commercial buildings.

[8] Adapted-land use cover CRIGE PACA.
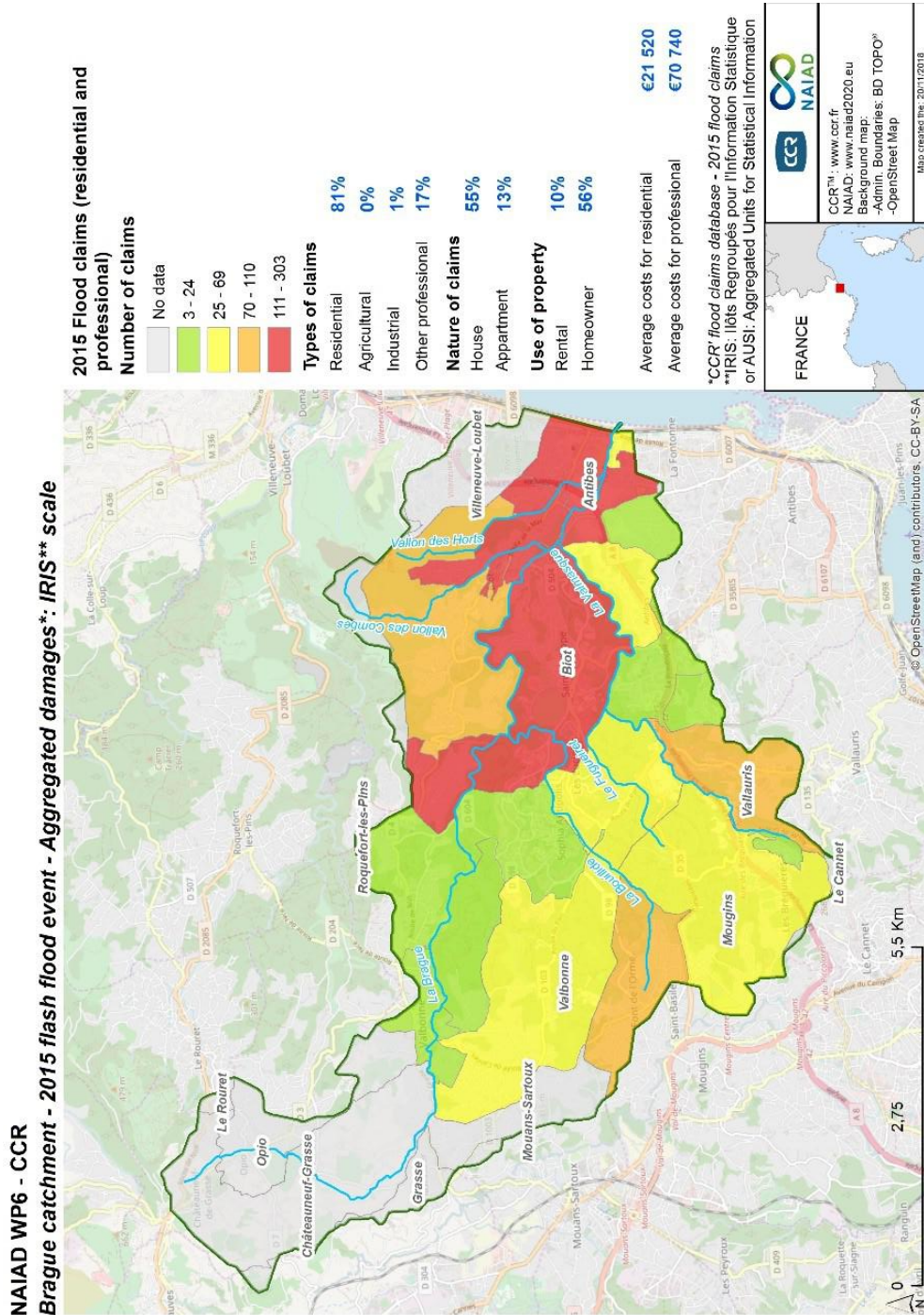
Figure 44: Flood claims localization at the IRIS scale.
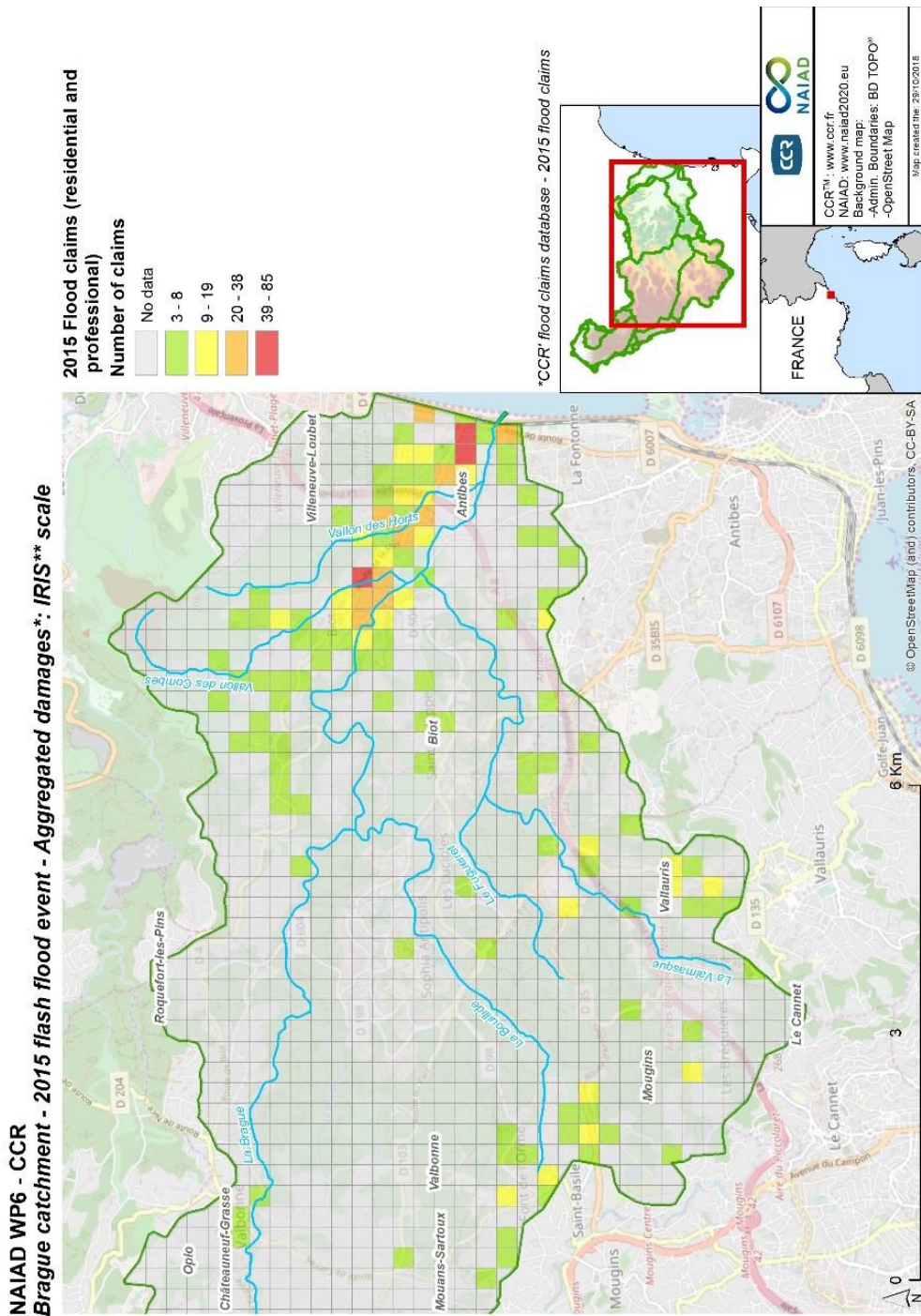
Figure 45 : Flood claims localization at a 250m x 250m scale.

5.3   Runoff model results

5.3.1   Land use data

Based on the 60% of 2015-flood claims located outside the flood-prone areas, the runoff model has a real significance for understanding damages in the catchment. The table below highlights the number of claims located inside each hazard map results. In other words, it helps to understand the accuracy of each map results compared to the number of claims located inside.

To model floods, CCR normally uses Corine Land Cover input data. These data are available for the all French territory and are not local-based assessment. That's why a comparison between the Corine Land Cover and the adapted-land use cover CRIGE-PACA has been done.

The adapted land use cover of the Brague catchment has been integrated within the CCR runoff model in order to get better precision on the runoff coefficient. The inventory of the land use realised since 1999 by the CRIGE, detailed the land use of the PACA area based on detailed legend in 30 parts (3 parts for the coarser). The land use cover is regularly updated (every 7-10 years) based on interpreted satellite imagery and aerial photographs, this allows in depth analysis (1/5000 digitalization scale) of evolution in the regional land use: urban sprawl, land use changes, mutations of rural areas etc. Coefficient of runoff of the CCR models have been assigned for each land use type based on the coefficient values of the Manning-Strickler formula. The Manning formula enables to compute the mean velocity and flow of water on a free surface. These coefficients intervene in the runoff modelling taking into account the roughness of the different land use cover.

5.3.2   Comparing land use cover data used for the Brague catchment

The mapping and graphics below (Figure 46 & Figure 47) highlight a comparison of two land use cover database and related runoff coefficients used to model hazard on the Brague catchment.

 The maps on the right, the coefficients are represented into three classes of runoff sensitivity (low, moderate, high). This simple classification highlights spatial sensitivity to runoff between the large scale Corine Land Cover and the adapted-CRIGE-PACA land cover. On the CRIGE-PACA land cover the urban, commercials and roads areas (in red) are largely highlighted than sparse inhabitants and opened areas (in orange) and of the natural, rural and agricultural areas (in yellow). On the contrary, runoff coefficient for Corine Land Cover to runoff are less precise and diffused. The difference between dense and sparse areas is less clear than the coefficients map for CRIGE-PACA.

The runoff model was run at the catchment scale and based on the 2015 rainfall data, which allow accurately precise information.
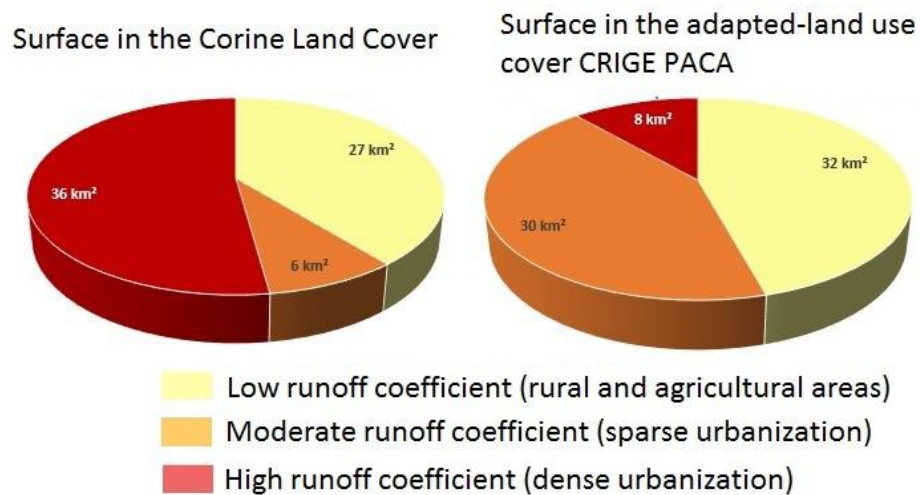
Figure 46 : Comparison of runoff coefficient between the two land-use data.
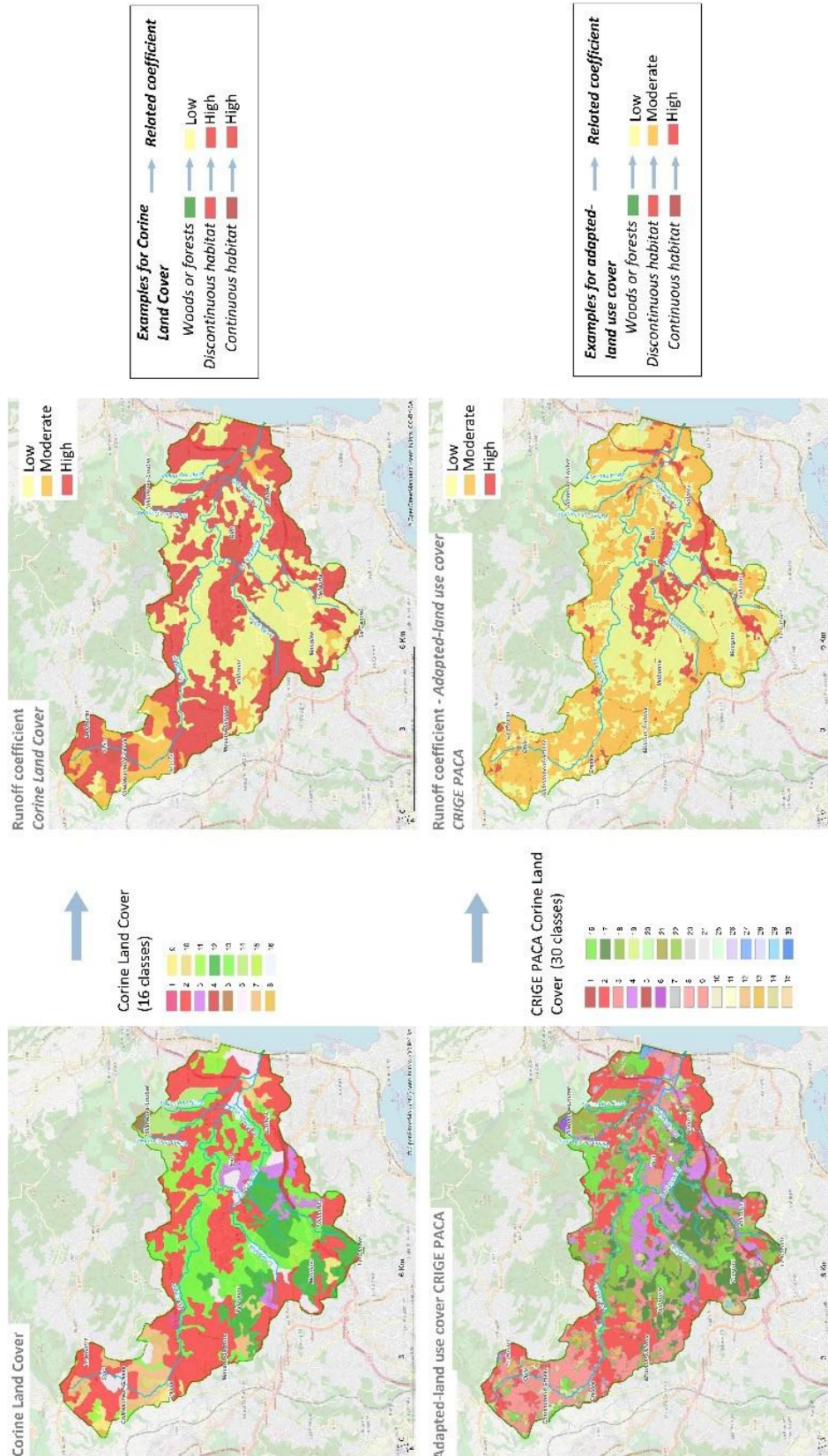
Figure 47 : Comparison of land-cover data and related runoff coefficient (Official Corine Land Cover 2012 and adapted-land cover CRIGE PACA).

5.3.3   Runoff hazard for the October 2015 event based on the two land use data

The October 2015 thunderstorm was modelled on the two land use data. The Figure 48 demonstrates that runoff is more important on the most impervious areas. The two maps show a runoff hazard on the red and orange areas (high to medium runoff coefficient). The integration of the CRIGE PACA adapted- Corine Land Cover within the CCR model generates changes on spatialization of runoff according to land-use. We observed less diffuse runoff areas with the CRIGE PACA detailed land-cover, it generates more precise hazard location (Figure 48).
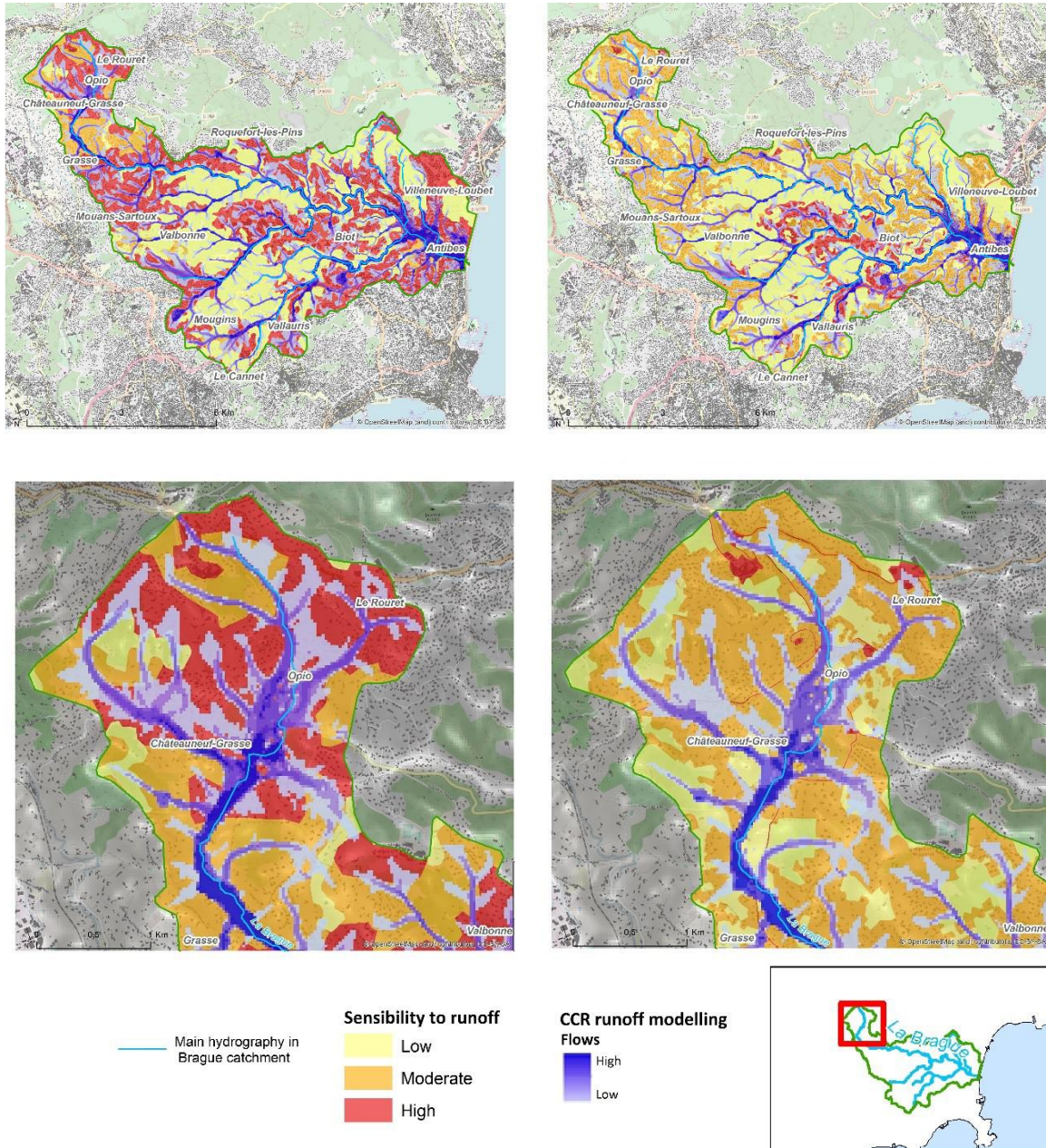
Figure 48: Comparing runoff hazard during the October 2015 event from the Corine Land Cover (left panels) and the CRIGE PACA data (right panels).

Thus, with the official Corine Land Cover, the runoff hazard area in the urban areas is 17 km² and of 5.3 km² with the Corine Land Cover adjusted by CRIGE PACA (Figure 49). The runoff coefficient related to impervious land use types influences areas' exposure to runoff. The results are based on a detailed land-cover, it justifies the significant part of precise information and will participate to assess the role of nature-based solutions on runoff hazards. Further analysis will be done on damages related to runoff (NAIAD Deliverable 6.3).
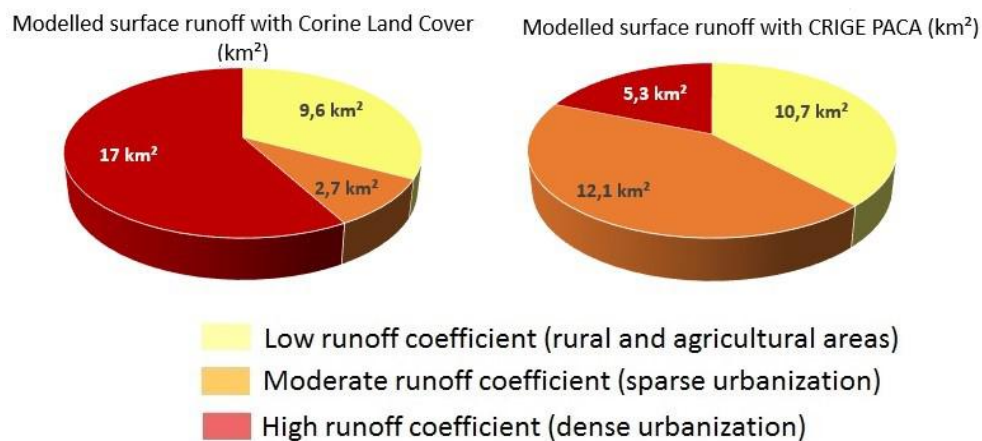
Figure 49 : Distribution of modelled surface runoff based on the two land-use cover.

The CCR runoff model helps to better understand the risk exposure of numerous areas damaged during flood events but not captured within the flood process (Moncoulon et al. 2014). Thus, Figure 50 demonstrates that the runoff modelling result for the 2015 event has a very similar hazard extension than the reality of the event according to the map provided by Préfécture des Alpes-Maritimes (2017). In depth comparison of the CCR results and the actual height will be done later.
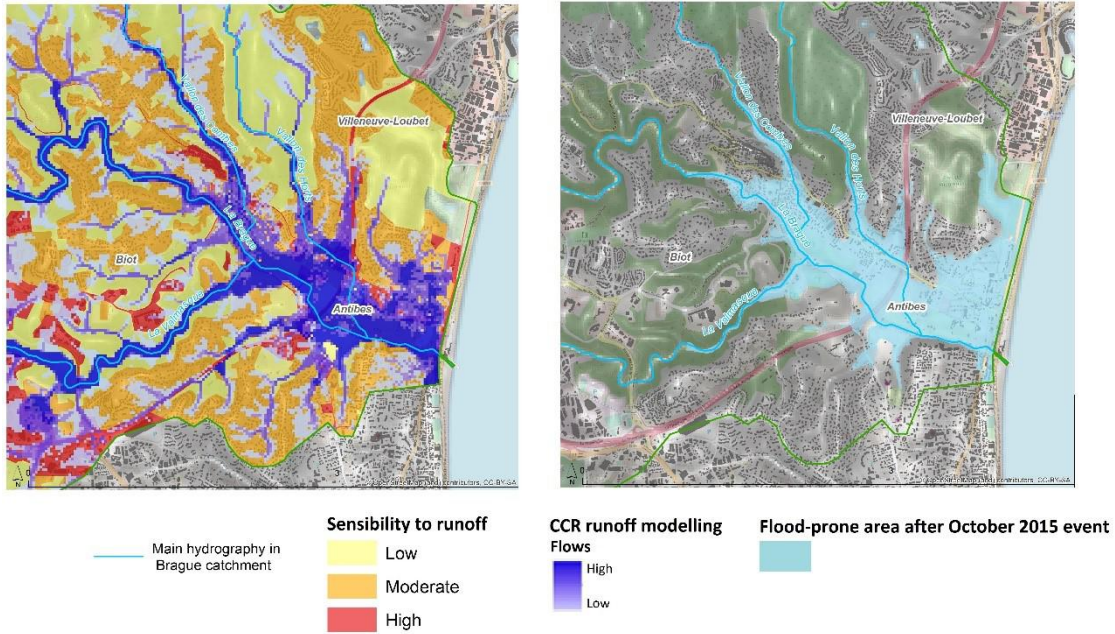
Figure 50 : Comparison of the CCR runoff model results on 2015-event and the real flooded areas.

Moreover, the runoff map is overlaid with the adapted-Corine Land Cover which detailed roads e.g., highway A8 and main/secondary roads D4/D135, and also all watercourses on the watershed (Figure 51). This demonstrates that the model is consistent and robust to compute the real extension of the flooding and of the most impervious areas.
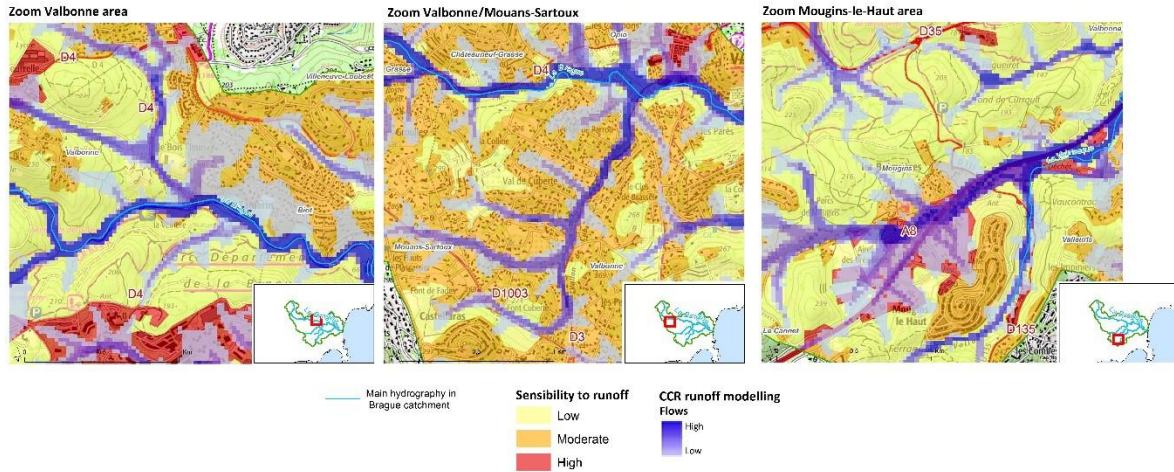
Figure 51 : CCR runoff modelling result according to the adapted-land Cover CRIGE PACA.

5.3.4 Location of claim in or out of runoff concentration areas

By using a not detailed Corine Land Cover, we capture more claims, i.e., 1024 claims in the runoff hazard area, than with a detailed land-cover, i.e., 952 claimed in the runoff hazard area (Figure 51). This is likely an issue related to the excessively high precision of the flow modelling compared to the relatively coarse claim spatial location. This will have to be compared with the percentage of false alarms which are not yet available.

Table 20 : Comparison of mapping results with the actual 2015-flood number of claims (1410)

Flood-prone areas* ''Porter à Connaissance''	CCR runoff modelling CORINE LAND COVER 2012	CCR Runoff modelling CRIGE PACA Land use database
571 / 1410	1024 / 1410	952 / 1410
40%	72.6%	67.5%

Source: Caisse Centrale de Réassurance, insurance database.

In essence, 0D simplified analysis enables to capture local hazards and excess of water depth, e.g., within the Flood Excess Volume approach. Runoff modelling are able to spatially capture widespread hazards everywhere in the catchment but are unable to accurately model bridge pressure flow or large wood jam impacts. Accurate 2D models as IBERwood enable in depth analysis but require time consuming and heavy workforces to refine the hazard modelling.

6 Integrated flood protection schemes

Two analysis scales are presented in this chapter: the first section provide a new analysis on the flash flood regulation service of Mediterranean forests at catchment scales, the second focus on the Brague lowlands and detail the flood mitigation strategies tailored to our DEMO catchments main flood risk hotspot.

6.1 Highlighting forest influence on hydrology through post-wildfire hydrological changes: an exploratory study of the France southern region

6.1.1 Introduction

As one of the main agents regularly affecting the physical characteristics of catchments in Mediterranean regions, wildfires are assumed to have a strong impact on hydrology. Though, the numerous studies tackling this issue led to widespread conclusions depending on fire and catchment characteristics. In addition, despite being highly prone to both forest fire and flash flooding risks, the region of south eastern France has received surprisingly small interest regarding this subject so far. In order to have a clearer insight on how the hydrological modelling of the Brague catchment DEMO site should be adjusted under different wildfire scenarios, it was deemed necessary to conduct our own cases study on a set of French Mediterranean catchments.

6.1.2 Literature review

The noteworthy conclusions of several studies related to wildfire impact on hydrology are summarized below:

- There is a strong variability in the assumed impact of forest fires on hydrology. Regarding annual water yields, some studies reported increase up to 200 % (Hallema et al. 2018) while other notice no significant change (Aronica et al. 2002). As for peak flow, conclusions range from no increase (Owens et al. 2013) to around 100% increase (Seibert and McDonnell 2010).
- The effect of forest fires is short lasting and may only be noticeable on the first year after the fire (Saxe et al. 2018).
- There is no clear evidence that any of the fire characteristics have more control on catchments hydrological response (Bart and Hope 2010).
- All studies point out the potentially heavy uncertainties linked to modelling approach.

6.1.3 Methodological framework

In order to compare the watershed hydrological response before and after the fire, other changes such as climate variability must be filtered out. The simplest way to do so was by calibrating a hydrological model on the pre-fire period only. The difference between observed and simulated runoff on the post fire period was then assumed to be mainly representative of fire effects on hydrology (Figure below).
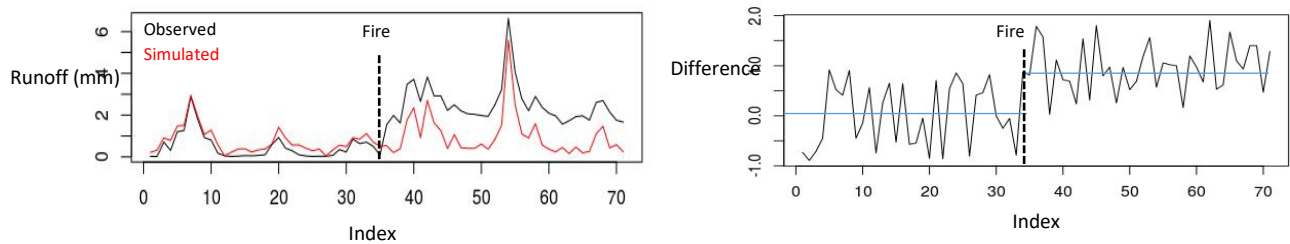
Figure 52 : Illustration of the method with hypothetical data. Observed and pre-fire calibrated simulated flow (left panel) and relative difference between observed and simulated (right panel).

The method validity largely depends on the calibration efficiency. The pre-fire period must thus be long enough to capture the watershed hydrological specificities. Following recommendations from the literature, the pre and post fire periods' lengths were set to 5 years. For each catchment, significant "isolated" forest fires for which no other significant event occurred in the pre and post fire period were then selected. Significant fires were defined as those that burned more than 5 % of the catchment's area. As single fires in this region were usually restricted to small area, all the fires occurring during each summer were aggregated and considered it a single event. After this treatment, we ended up with a sample of 22 forest fires located in 17 different catchments. Catchments' location is shown on Figure 53 and the main characteristics of catchment-fire pairs are presented in Table 21. The sample offers a good representativeness with catchment areas ranging from 5,4 km² to 367 km² and burned area ratio ranging from 6,7 % to 63 %.

Table 21 : Main characteristics of the 22 fire-catchment pairs

Catchment ID	Catchment area (km²)	Number of fires	Burned area ratio	First fire date	Last fire date
Y4022010.1	295.86	3	6.91	10/07/1979	29/07/1979
Y4022010.2	295.86	2	15.0	01/08/1989	28/08/1989
Y4225610.1	71.28	2	21.0	24/07/2004	24/07/2004
Y4305610.1	8.07	1	27.9	30/04/1982	30/04/1982
Y4617610.1	5.41	2	63.5	26/03/1989	21/08/1990
Y5215020.1	228.3	1	20.3	10/08/1979	10/08/1979

Y5305030.1	99.33	1	27.8	15/12/1973	15/12/1973
Y5325010.1	73.06	2	21.4	27/06/1982	28/09/1983
Y5424010.1	65.84	1	33.3	31/08/2003	31/08/2003
Y5435010.1	42.62	4	50.8	24/05/1989	21/09/1990
Y5444010.1	198.97	1	6.70	10/08/1979	10/08/1979
Y5444010.2	198.97	4	16.6	24/05/1989	21/09/1990
Y5444010.3	198.97	1	11.0	31/08/2003	31/08/2003
Y5505410.1	47.26	1	40.6	25/08/1987	25/08/1987
Y5505410.2	47.26	1	8.9	25/07/2003	25/07/2003
Y7114020.1	367.23	2	6.9	25/08/2003	29/08/2003
Y7315010.1	52.33	3	18.4	31/07/1989	02/08/1989
Y7315010.2	52.33	1	8.56	20/08/1999	20/08/1999
Y7505010.1	69.71	1	11.6	12/08/1994	12/08/1994
Y8324020.1	201.34	2	12.3	15/07/2003	08/08/2003
Y9025010.1	147.47	1	13.2	24/08/2000	24/08/2000
Y9414020.1	115.21	1	22.9	24/08/2000	24/08/2000
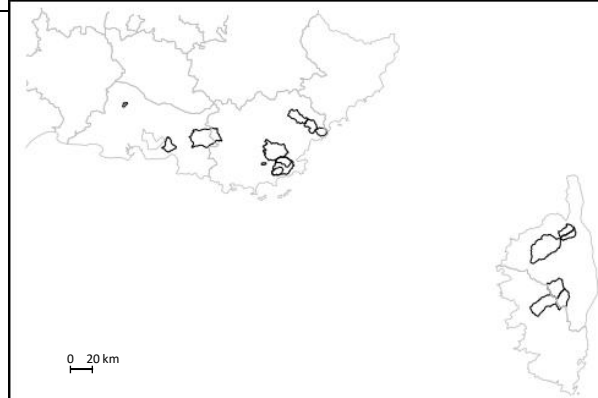
Figure 53 : Location of the 17 catchments used for the study.

To investigate the impact of fire on different flow conditions, three flow characteristics were analysed, namely mean monthly flow, and monthly 5% and 95% quantiles, which represent the flow exceeded 95% (respectively 5%) of the time. Four different tests for step change were run on the time series of relative difference between observed and simulated flow for each flow characteristic. The regressions between observed and simulated flow characteristics were also analysed.

6.1.4   Results

The first results were in agreement with the literature review and showed that there was no clear evidence to support the existence of a systematic, quantifiable impact of forest fire on

catchment hydrology. Moreover, when a significant change related to a forest fire was detected, there was no apparent link between the direction and magnitude of the change and the characteristics of the catchment or the fire. A detailed analysis of the results showed that:

- Calibration efficiency was variable, with almost a third of the results deemed unsatisfactory as shown on Figure 54 (NSE below 0.7 on the calibration period).
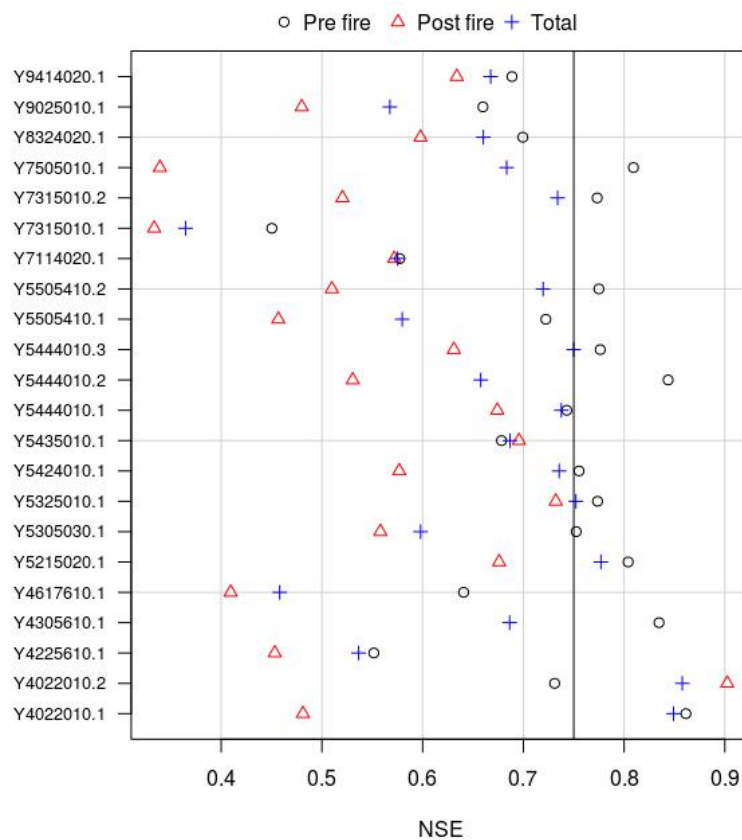
Figure 54 : Nash Sutcliffe Efficiency computed with daily simulated and observed flow on the pre-fire, post fire and total period for the 22 fire-catchment pairs. Black vertical line indicates NSE = 0.75.

- Tests for step change often detected multiple significant breakpoints in addition to the "true" one. This could mean that there were several other disturbances that had a significant impact, or that the seasonal variability of the difference between observed and simulated flow was large enough to create detectable breakpoints.
- Tests setting the "true" fire date as input were not always significant as shown on Figure 55. It would tend to support the conclusion that, in the strict framework of our cases study, forest fires did not always impact hydrology. However, it could also mean that these impacts were either too small to be detected or that it is compensated by another disturbance.
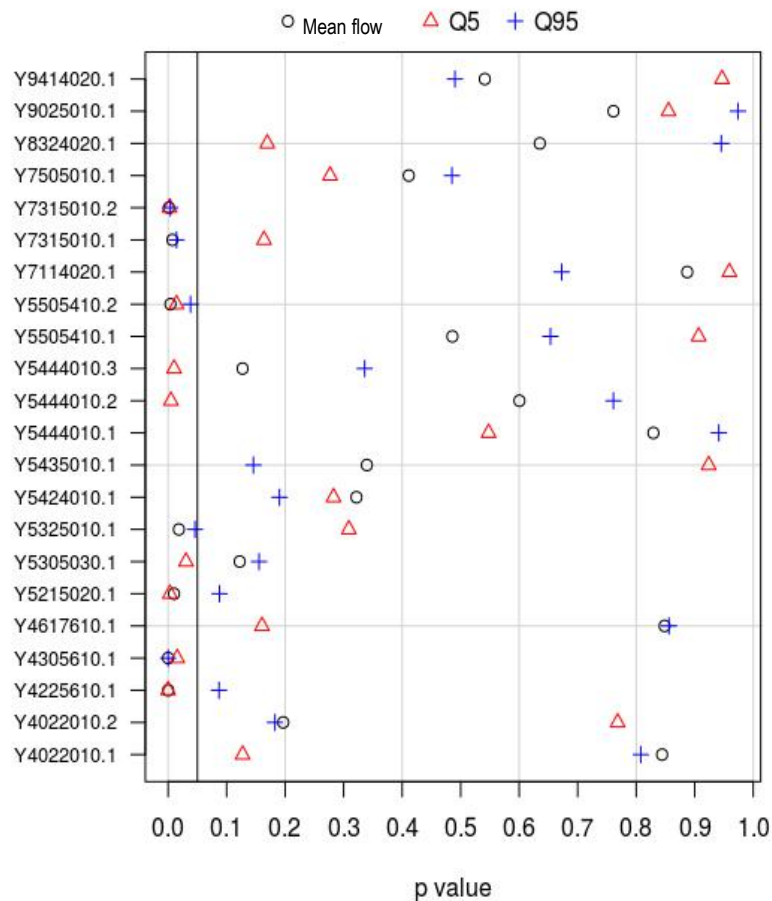
Figure 55 : p value of the Mann Whitney test with assumed breakpoint at the fire date for the three flow characteristics. Black vertical line indicates 5% significance level.

- Comparison of pre and post fire regressions between observed and simulated flow lack significance due to the violation of several statistical assumptions.

The results were thus not sufficient to start working on potential modifications of the hydrological model parametrization. These findings were however important and will serve as guidelines for future work year 2019, in which we intend to particularly focus on:

- the calibration procedure and the uncertainties related to it
- the use of a finer (hourly) time scale to investigate the specific impact of forest fire on peak flows right after the fire occurred

6.2 Lowlands' flood protection strategies: Three options

After careful analysis of the local technical literature, numerous discussions with stakeholders during bilateral exchanges, the two stakeholder workshops (March 21st, 2018 and December 20th, 2018) and three focus groups (June 2018), the NAIAD partners working on the Brague DEMO came up on an analysis of three comprehensive flood protection strategies for the Brague lowlands:

- An ambitious strategy in term of protection objective relying mostly on NBSs, namely giving-room-to-the-river which encapsulates[9], as explained in §4.2, floodplain restoration and management, re-meandering, reconnection of oxbow lakes and similar features, riverbed material re-naturalisation, removal of dams and other longitudinal barriers and natural bank stabilization.
- A strategy of lesser ambition, also relying on NBSs as giving-room-to-the-river, though less room, but possibly feasible on a shorter term due to its smaller real estate impact.
- An ambitious strategy in term of protection objective relying on civil engineering solutions, namely retention basins.

The Flood-Excess-Volume analysis performed in §4.2 explored the flow confinement required to contain the Oct. 2015 event and resulted in a flow depth at least 1.3 m above the current threshold for flooding. Flood walls must be designed with suitable freeboard (Hunzinger 2014), embankments enabling a full protection against this event should thus be nearly 2 m high which seems irrelevant in the urban context of the Brague lowlands. Even if mixing retention basins of relatively large size, i.e., ten time bigger than currently: 120,000 m^3, bed widening equivalent to the short-term NBS strategy (+5 m), flood walls should still be more than 1 m-high including

---

[9] For the sake of consistency with other European project and DEMO sites, the NBSs are hereafter, whenever possible, designated using the Natural Water Retention Measure (NWRM) framework and vocabulary (Strosser et al. 2015).

freeboard as done in §4.2. Several roads, house access and other structures located along the rivers are not consistent with such flood wall height. The option to implement flood walls along the whole river network is thus considered irrelevant and not further studied.

6.2.1   Ambitious NBS strategy

The preliminary exploration of a giving-room-to-the-river plan provided in §4.2 proved that a 15 m increase of the already 20 m-wide river does not seem sufficient for the Biot municipality protection.

Widening the Brague river had yet been proposed in past engineering works as recalled in Cabinet Merlin (2016a), it is still envisioned but not to the extent of the hereafter studied strategy.

A higher ambition seems appropriate to this case study for several reasons:

- Several houses which experienced severe flooding in multiple occurrences in the last decades were eligible to expropriation by the Fond Barnier[10] in the upper part of the lowland area, with willingness by several owners to leave their goods;
- The area surroundings the Brague lower part were until the Oct. 2015's flood mostly occupied by camp sites, subsequently partially closed by the local authority.
- The intermediate reach is the less densely urbanized section and is mostly occupied by leisure activities, i.e., golfs and equestrian activities, thus constituting an eventually more flexible constraint than housing or economic activity as camp sites.

These reasons create a window of opportunity to re-think the Brague River corridor on the long term, i.e., after acquisition or expropriation of the houses and real estates located in the corridor.

This window of opportunity has been perceived by the local stakeholders. The CASA, the agency grouping the local municipalities, asked a consulting team to work on the question. Two options were proposed which inspired the NAIAD ambitious based on the AE-RMC's recommendations (2016) and intermediate NBS strategies (Folléa-Gautier et al. 2017, 2018).

The AE-RMC's guidelines (2016) for the definition of river integrated corridor recommends a corridor three time wider than the bankfull width. In the Brague case this corresponds to a 60 m width, part of this could become the river bed, the remaining width encompassing the forest

---

[10] Public fund, fed by a 12% tax on building and car insurance policies dedicated to fund protection investments and expropriation of houses in excessively high risk areas (see NAIAD Deliverable 3.2). The Biot municipality published a webpage on the state of progress of the Fond Barnier acquisitions: http://www.biot.fr/fonds-barnier-subvention-lacquisition-de-10-maisons/

and wetland riparian belt. The whole seems more consistent with a comprehensive flood protections scheme relying on an appropriate river corridor although being very wide in the constrained context of the Brague lowlands.

Discussions are also in progress with the Conservatoire du Littoral[11], a structure acquiring and protecting coastal natural areas, already managing 2,000+ km², to organize a consistent natural site in the sector surrounding the highway A8.

The following ambitions and constraints were taken into account to define the works belonging to the ambitious NBS strategy for the Brague DEMO.

- Pedestrian and cycle paths, usable for equestrian activities whenever possible, would be organized along both banks from the upstream gorges for later connection with the natural parks and the Valbonne activity zone of Sophia Antipolis, down to the sea outlet.
- Large wood trapping facilities would be built on the Brague and its lowlands tributaries, i.e., the Vallon des Combes, Vallon des Horts and Valmasque. The main stem and the latter would be equipped with two facilities, one located near the gorge outlets, dedicated to trap trunks and very large wood pieces; the other located a bit downstream, wider but with lower heights and dedicated to trap medium and large wood pieces that the first facilities would not have trapped. These facilities are likely to be racks made of piles embedded deeply in the river bed and protected on the banks to prevent outflanking.
- The river bed would be widened in the Brague upper section which implies to remove a number of houses, swimming pools, garden walls and diverse works flooded in Oct. 2015 and before. At this preliminary stage of study, the full real estate is considered to be included in the project although some assets located sufficiently far from the river bed could eventually finally be maintained if relevant. This will be studied in a later stage.
- Bank reshaping would be necessary along these areas and would be protected against erosion by light bioengineering bank protection techniques (Evette et al. 2009, Genialp 2012).
- Heavier bank protection bioengineering techniques would be implemented in bends with close proximity of assets or in confluences. In scour-prone area, the bank protection could eventually by hydride with riprap embedded below the river bed to protect the structure from scouring (Posi et al. 2018).
- Houses of the 'Brague neighbourhood', located in a river meander, severely flooded in multiple occasions, would be removed to increase the river capacity, build a large wood

---

[11] See the website http://m.conservatoire-du-littoral.fr/

trapping rake and create wetlands. Some of them have already been acquired by the Fond Barnier and be removed in 2018.

Figure 56 : Removing houses located in the Brague high flood risk area has yet started (source: Nice-Matin, © Frantz Bouton, https://nouveau.pressedd.fr, published on Oct. 3rd, 2018).

- The old and new bridges of Biot have not a sufficient hydraulic capacity and locally increase the water depth (Cabinet Merlin 2016c). They should be removed (old bridge) or reconstruct longer (new bridge).
- The road, garden and houses located on the left bank downstream should eventually be removed to widen the bed. Some of them could eventually be maintained with an appropriate rethinking of their access and vulnerability reduction depending on the flood level after works.
- The Brague River would be widened on the Golf area and its wood riparian belt recreated.
- The Valmasque confluence must be profoundly reworked:
  - The houses located on the right bank would be removed.
  - A by-pass channel would be created toward the Brague with a short-cut having a sharper angle than the current perpendicular confluence configuration to ease the tributary flowing during simultaneous floods.
  - This by-pass channel would cross the road with a bridge or culvert of large dimension.
- The Bregnev Bridge would be dismantled and reconstructed with a doubled capacity and without central pile prone to create wood jams.

- The industrial site located on the left bank, actually in the path of the flows coming from the golf would be removed to ease the bridge and river widening.
- An additional large wood trap with a lateral configuration would be implemented in the meander upstream of the highway A8 culverts with a design similar to the one described by Schmocker and Weitbrecht (2013). It would secure the toppling trees downstream of the other traps and eventual logs that would pass them.
- Wetland restoration would be performed by a reconnection and stream restoration in the wet pastures located on the left bank upstream of the highway embankment.
- The river bed would be widened on two banks in this section.
- The houses and economic activities located on the right bank upstream of the highway would be removed also to decrease the vulnerability and install agriculture activities.
- The highway culverts are a bottleneck section which is very complicated to replace due to geotechnical and technical constrained. It is not envisioned in the current project although the ministry in charge of transportation recently decided to focus on the question.
- The areas located downstream of the highways would enable an ambitious river corridor since the campsite located on the left bank are closed.
  - The river bed could be widened more than twofold.
  - Part of the terrain could be used for economic activities in the framework allowed by the flood risk prevention plan (PPRi) whose updating is in progress. Only activities resilient to flood would likely be allowed.
  - Part of the terrains would be also reconnected with the river bed and restore as wetlands with stream re-naturalisation.
    - Terrains that have natural features at the moment would simply be reconnected and a stream re-meandering operation would be organized to feed these areas with more water and better natural connectivity.
    - Old campsite or inhabited areas would have deeper restoration operation: light building, road and networks would be removed, the surface soils would be replaced and enhanced and a full restoration operation would be performed.
  - A buffer strip between the wetlands and the economic activity could be organized with urban agricultural activities.
- Finally, the last three bridges before the sea are not envisioned to be changed but small embankments would be built on the right bank to protect the asset located in Antibes close from the shore.

The work locations are synthetized in Figure 57 and Figure 58.

Figure 57 : General view of the Brague lowlands and location of works in the ambitious Nature-based solution strategy.
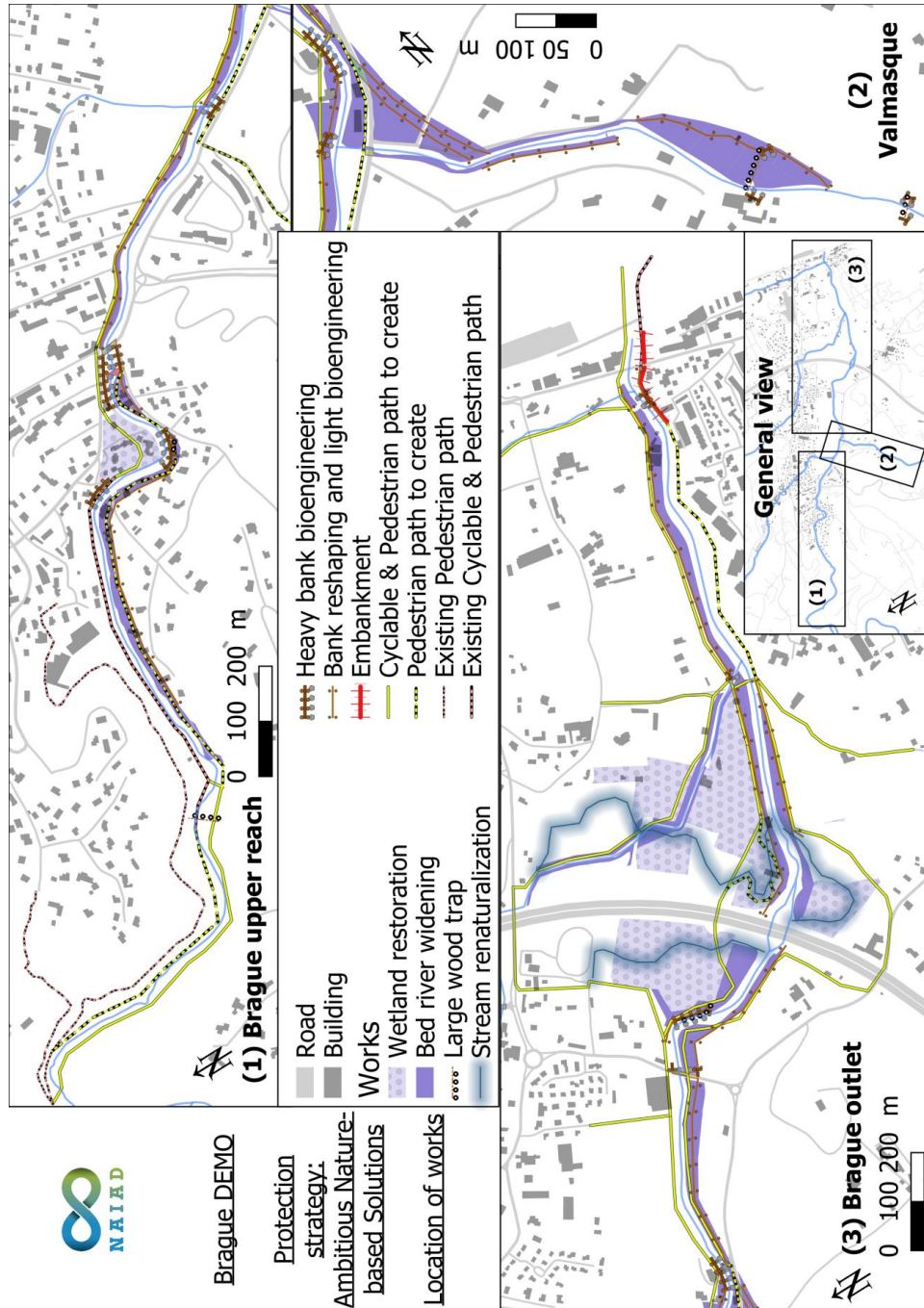
Figure 58 : Detail in the work locations in the ambitious Nature-based solution strategy for flood protection of the Brague lowlands.

Areas were real estate acquisitions likely to be necessary for the full strategy implementation are mapped in Figure 59.
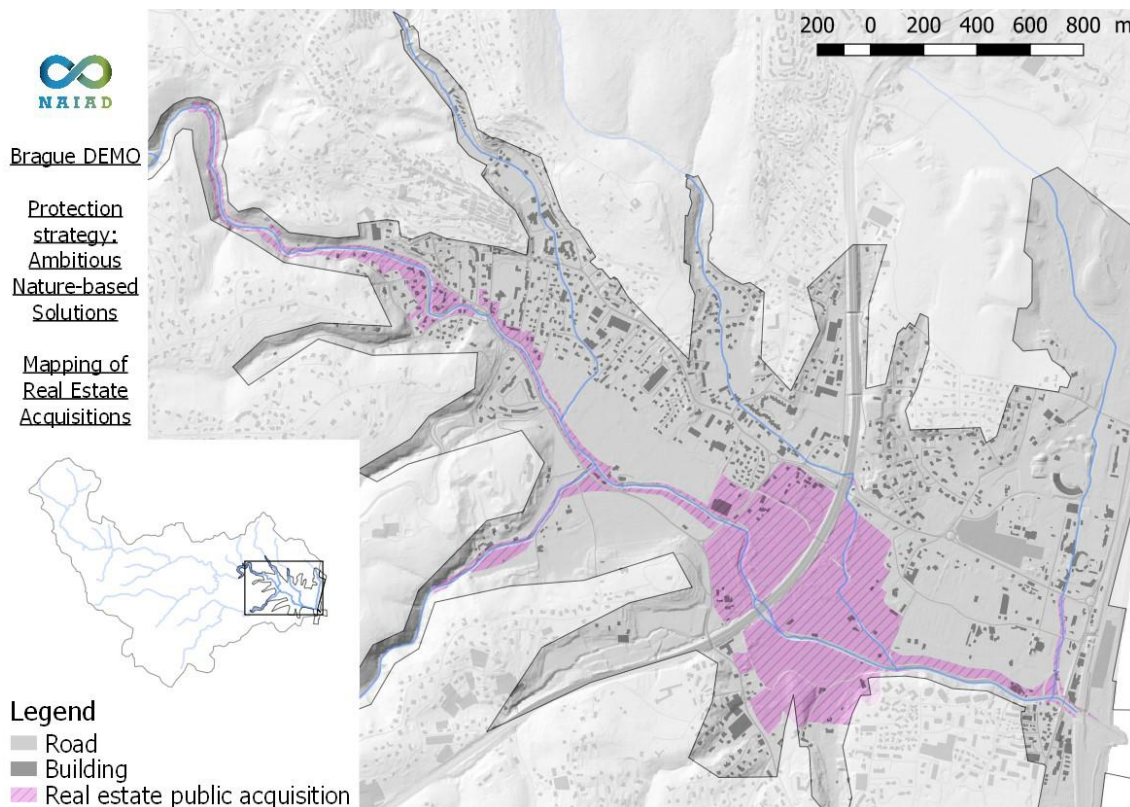
Figure 59 : Real estate acquisition in the ambitious Nature-based solution strategy for flood protection of the Brague lowlands.

The locations of works, extension of areas and other features of the project could be subject to changes while the modelling progress or other elements are brought to our knowledge during discussion with stakeholders.

The investment, real estate and maintenance costs will be assessed in the next phase of the project to be presented in NAIAD Deliverable 6.3 (submission date: May 2019).

Other natural water retention measures will likely be implemented upstream in the catchment. The former Brague basin agency organized an inventory of the eventually suitable sites (Lindénia 2012). The optimization of some of them will likely be implemented in the medium term. A hypothesis of a certain number of retention ponds or wetland restoration for a certain

cumulated area will be proposed in the next phases of NAIAD. It will be integrated in the scenarios of changes within a time window of several decades that should cover:

- Changes in hydrology and wildfire hazards due to climate changes;
- Changes in hydrology related to urban sprawling as well as natural water retention measures.

6.2.2   Intermediate NBS strategy

Real estate and houses acquisitions will take time while stakeholders, particularly inhabitants, are asking for actions and works to begin. A short-term protection plan is consequently under study by the local authorities, helped by consulting companies. A public land acquisition procedure is in progress to start this operation.

Accesses to the river banks to ease maintenance operation and eventually start giving-room-to-the-river are the priorities. Building one large wood traps per river stem is another key step.

However, out of the houses yet benefiting from a Fond Barnier acquisition, it has been decided to keep the buildings located in the potential river corridor out of the areas involved in this short-term protection plan. Discussions for direct acquisitions of the building will be launched by the authorities but it has been considered counter-productive to start the discussions with an expropriation procedure.

The corridor proposed in the ambitious NBS strategy presented in the previous section was reworked to avoid existing buildings in an as-consistent-as-possible way.

Areas where real estate acquisitions are likely to be necessary for the full strategy implementation are mapped in Figure 60.
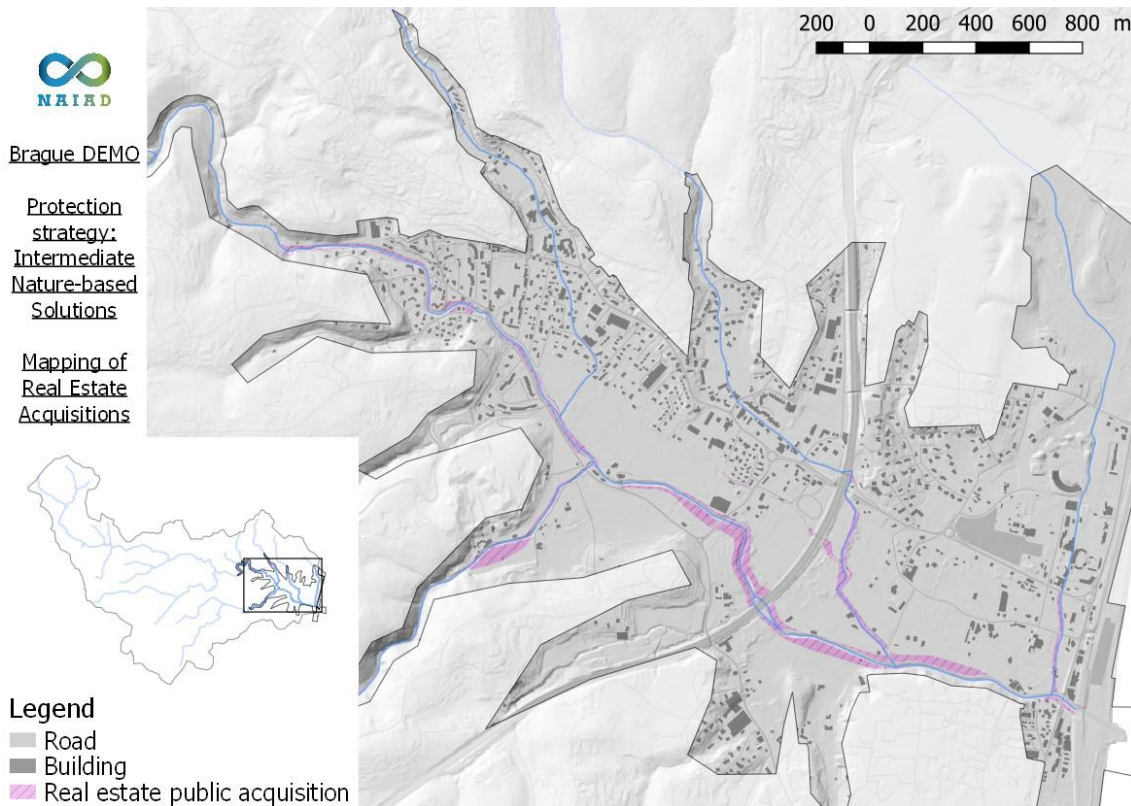
Figure 60 : Real estate acquisition in the intermediate Nature-based solution strategy for flood protection of the Brague lowlands.

The locations of works belonging to the Intermediate Nature-based solution strategy are synthetized in Figure 61 and Figure 62. Similarly, to the ambitious NBS strategy, the locations of works, extension of areas and other features of the project could be subject to changes while the modelling progress or other elements are brought to our knowledge during discussion with stakeholders.
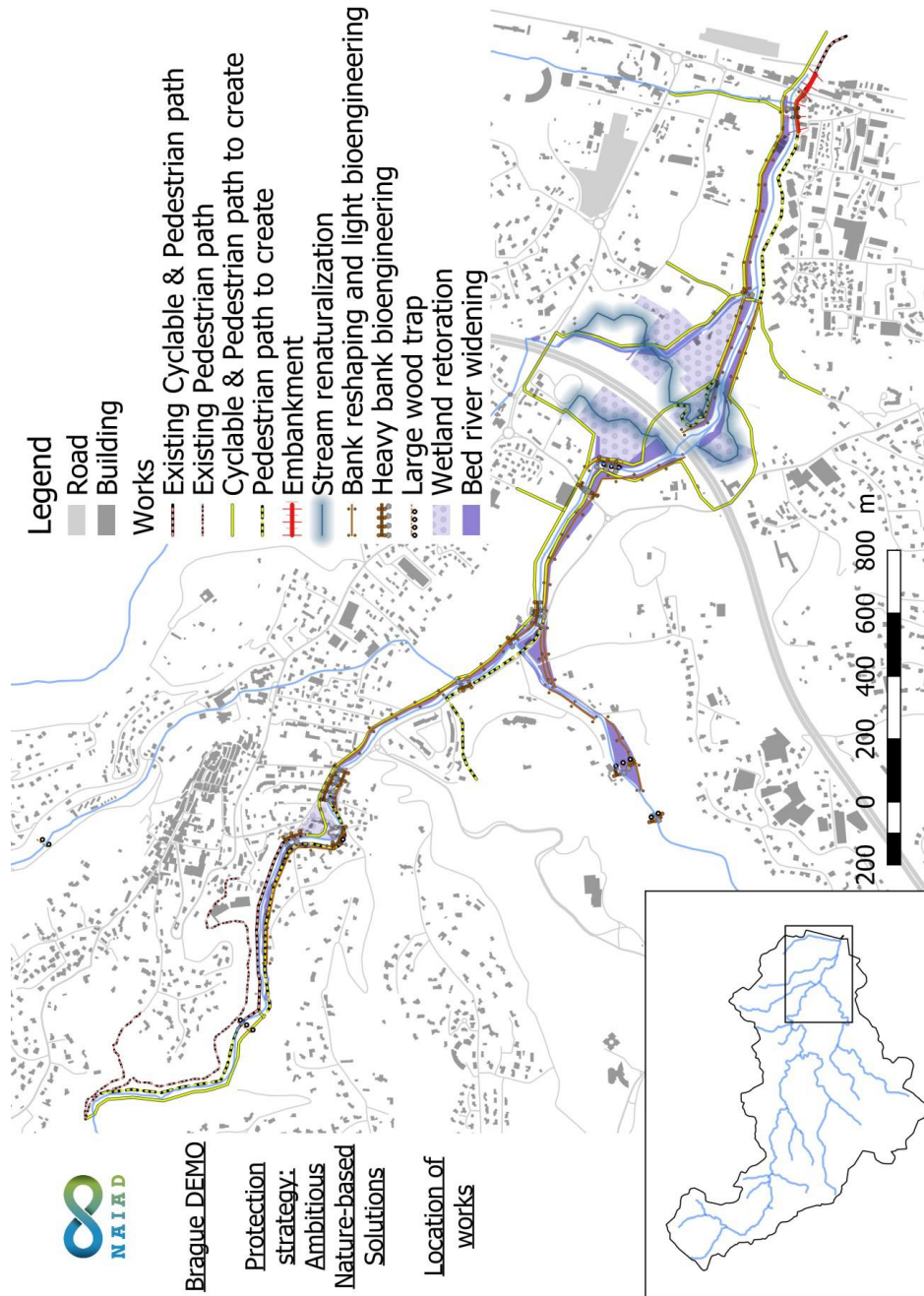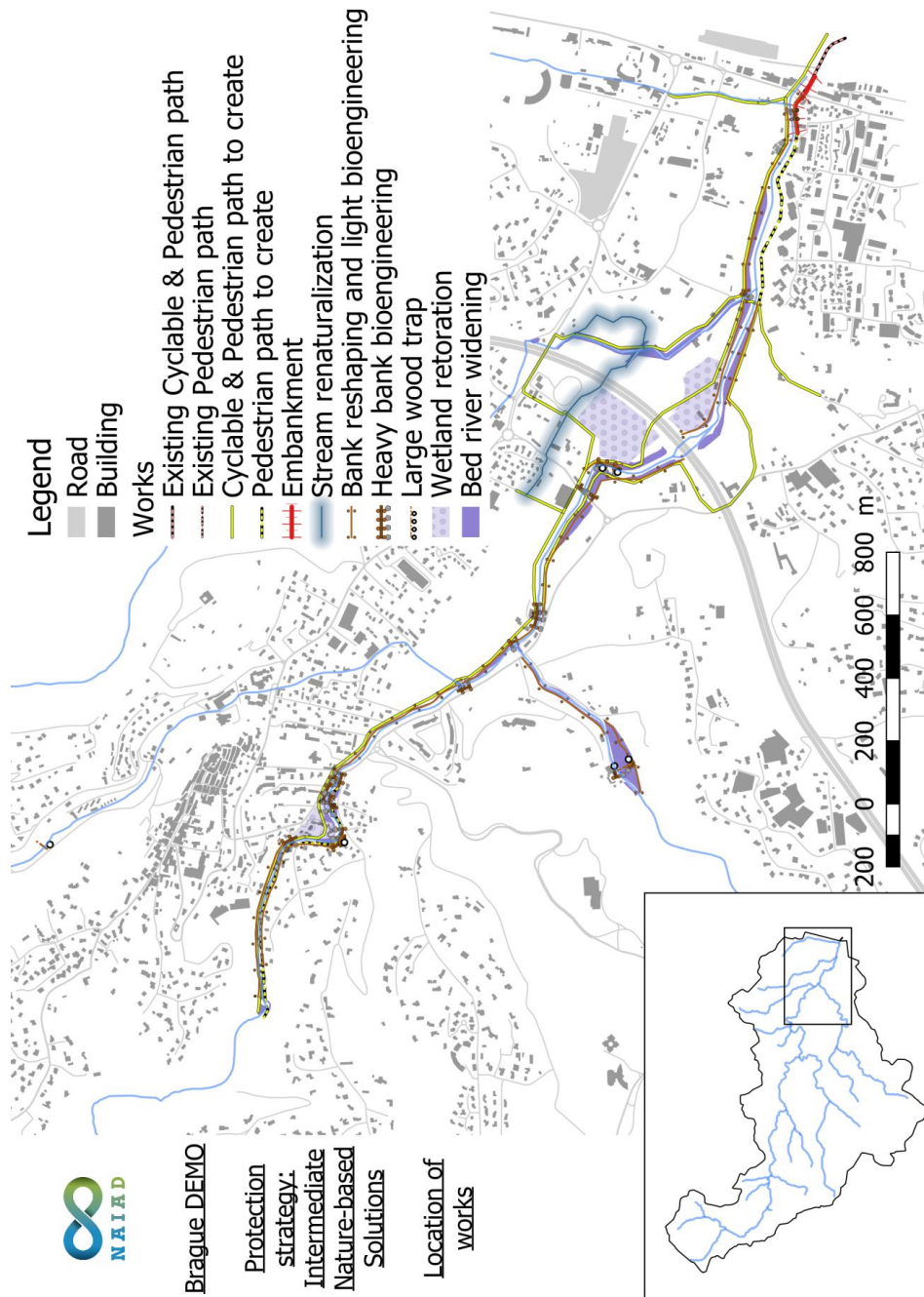
*Figure 61 : General view of the Brague lowlands and location of works in the intermediate Nature-based solution strategy.*
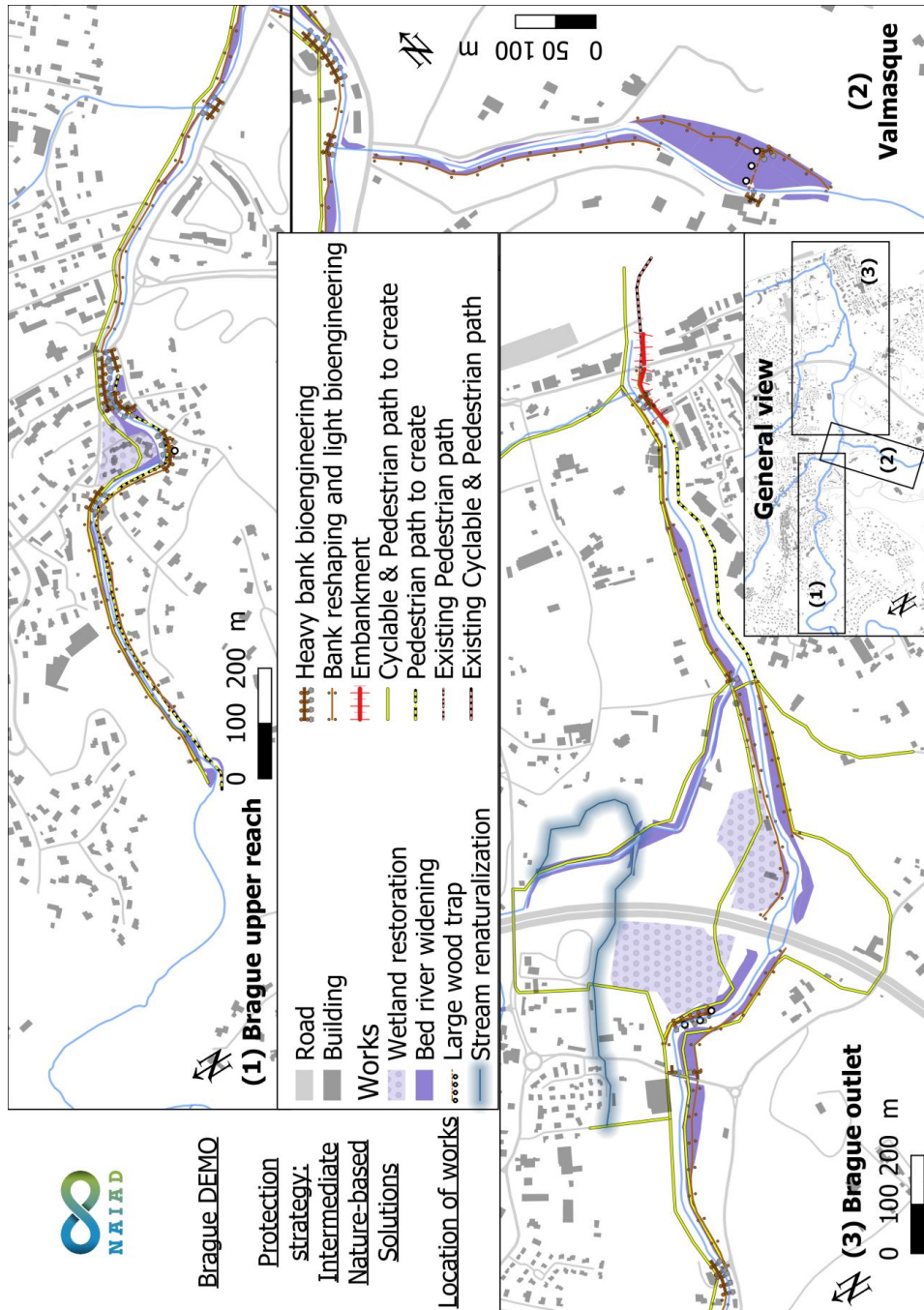
Figure 62 : Detail in the work locations in the intermediate Nature-based solution strategy for flood protection of the Brague lowlands.

The investment, real estate and maintenance costs will be assessed in the next phase of the project to be presented in NAIAD Deliverable 6.3 (submission date: May 2019).

6.2.3   Large retention basin strategy

So far, a few retention basins have been implemented in the Brague catchment:

- 12,000 m^3 of retention on the Vallon des Horts tributary in Biot,
- 10,700 m^3 of retention on the Maure Val Martin basin in Valbonne, 7.15-m high dam.

However, the FEV analysis performed §4.2 demonstrated that such volumes should be increase by one to two orders of magnitude to reach a satisfying protection level: for instance the Brague main stem upstream of Biot has a 41 km² catchment and a FEV of at least 488,000±311,000 m^3 to protect the area against a flood similar to the Oct. 2015 disaster with an outflow discharge of 135 m^3/s; this volume reaches 739,000±355,000 m^3 if using an outflow discharge of 100 m^3/s, i.e., close from the 10 years return period discharge. The full catchment being 68 km², a cumulated retention volume higher than 1,000,000 m^3 should be sought as a first approximation to refine it later. Locations of sites for dam implementation where sought according to the following criteria:

- The intercepted catchment must be as large as possible;
- The dam axis should be set:
    - at a reasonable distance of existing houses, typically more than 50 m;
    - in a valley as narrow as possible to diminish the structure costs;
- Its upstream valley should on the contrary be as wide and flat as possible to maximize its storage capacity;
- The maximum level underlined studied, but not necessarily retained for the maximum water level in the reservoir during safety check flood, typically the 10,000 years return period event, should not flood existing houses upstream, but flooding of roads is acceptable.

Figure 63 displays the locations and maximal extension of the reservoir respecting these constraints.
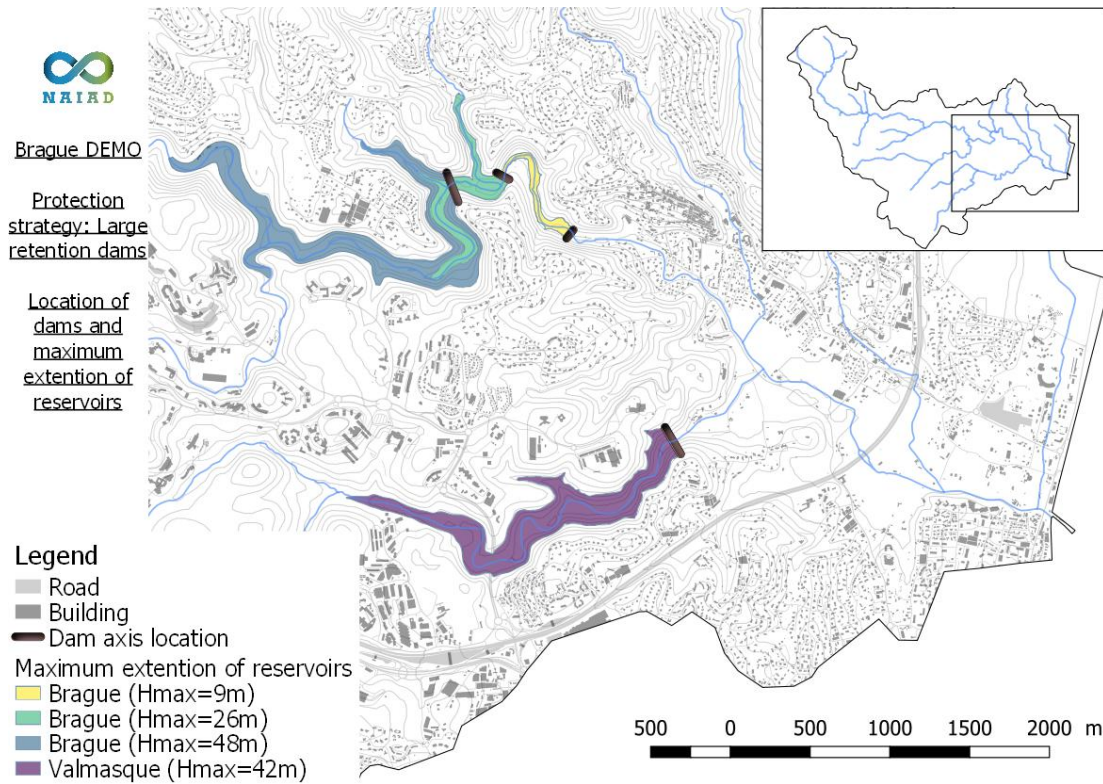
Figure 63 : Location of dams and extension of maximum reservoir areas for each location.

A 3D analysis has been performed to compute the volume potentially contained within these areas depending of the water level. Elevation data came from LIDAR data as well as the IGN BD Alti databases with 5x5m and 25x25m pixel sizes.

The areas coloured in Figure 63 will obviously not be fully flooded: it would require dams forty-meter-high that would have retention capacities higher than 5 Mm^3 for the two biggest on the Brague and Valmasque. In the next steps, a panel of structures will be selected with retention volumes consistent with catchment areas and their costs will be computed. Figure 64 displays the volumes of retention against the elevation of the water surface and the dam height.
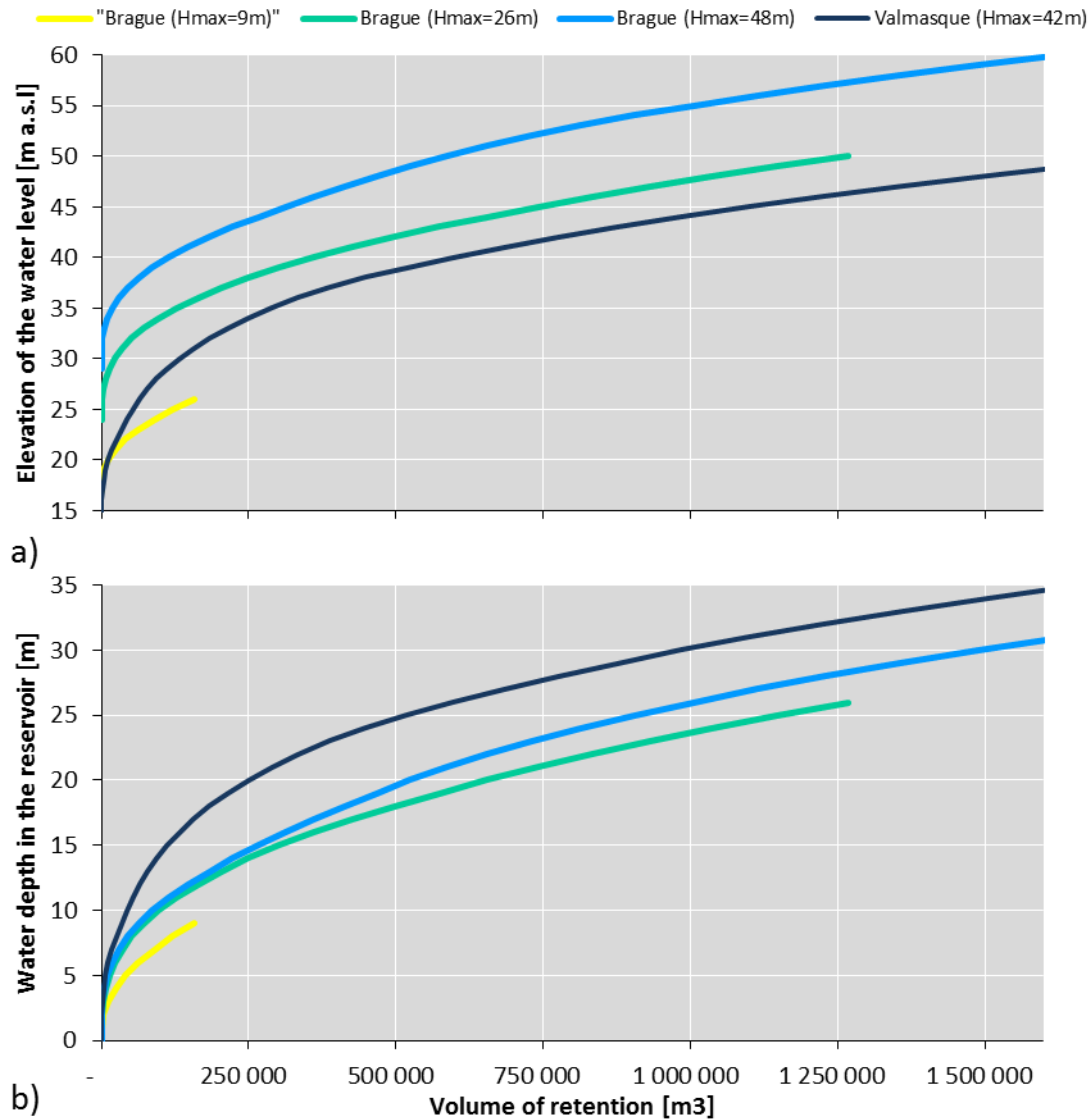
Figure 64 : Retention volume VS (a) water surface elevation and (b) dam height for the four dams' locations.

From Figure 64b, one can see that a reservoir filled by 10 m of water has typically a capacity of only a few hundreds of thousands of cubic meters and that storage of 0.5 Mm^3 is usually reached for water depths in the range 18-25 m.

Large retention basins with high dams must additionally be designed according to safety rules of dam reservoirs, i.e., with a spillway able to transfer the 1000 years return period event in

France for flood retention dams (CFBR 2013) and up to a 10,000 years return period event may would be chosen, e.g., for dam reservoir storing water all the year or in case of numerous assets threaten by dam failure.

According to the Shyreg analysis of the Brague station[12], the 1000 years return period peak discharge is 393 m³/s. Such a discharge flowing over a 30 m large spillway would induce a 4.15 m elevation in the reservoir; value to which the freeboard must be added. At this preliminary stage, we consider that a 5 m height must be added to the spillway level to compute the full dam height.

Computations were performed to define which water depth should be stored to achieve outflow discharge close from 10 years return period events. Cabinet Merlin (2016c) demonstrated that if damages are likely to start for discharges higher than about the 30 years return period peak discharge in Biot, flooding appear for return periods lower than 30 years further downstream. The 10 years return period is thus selected as relevant as first approximation.

In synthesis a possible scenario that should be refined in the later stage of the project is presented in Table 22.

Table 22 : Synthesis table for a possible Large Retention Structure strategy

River	Water depth under spillway level	Total dam height	Culverts Width*Height	Retention volume under spillway level	Event similar to Oct. 2015[13]	
					Upstream discharge	Downstream discharge
Units	[m]	[m]	[m]	[Mm³]	[m³/s]	[m³/s]
Brague	24.5	~30	2.9*2	0.878	240	100
Valmasque	25.5	~30	2.15*1	0.557	145	40
Vallon des Combes	Unknown	Unknown	Unknown	0.012	Unknown	Unknown
Vallon des Horts	Unknown	Unknown	Unknown	0.010	Unknown	Unknown

---

[12] Form: "Y5605210" – "La Brague a Biot [Plan Saint–Jean]", downloaded on https://shyreg.irstea.fr/
[13]

6.2.4   Modelling of protection measures

6.2.4.1   Adaptations of the hydrology model for NBS modelling

6.2.4.1.1   Widespread changes in the catchment

In the same line to what is described in §6.1 on wildfire effect on hydrology, eventual other deep changes in the hydrological regime of the catchment could be studied and included in the hydrological boundary conditions through changes in the model calibration or more likely through proportional changes in discharge quantiles. It will be performed during the last year of NAIAD project and presented in next deliverables.

6.2.4.1.2   Large retention basins

For the special case of structures having a major hydrological effect on a restrained location located close upstream of the 2D model extension, a dynamic computation of in-flow/storage/out-flow based on basic hydraulic rules as orifice and weir hydraulic formula and the site-specific curve of elevation-basin volume can been performed. It requires a basic design of the barrier closing the basin, thus fixing:

- Its height,
- Its orifice type and size,
- Its spillway level and width.

Computations have been performed for the hydrographs related to the Oct. 2015 disaster as provided in Figure 33 for the Brague and Valmasque catchments and with the design parameters provided in Table 22. Their synthetic time series are provided in Figure 65 and Figure 66 where one can observe that reservoir water levels nearly reach the spillway levels and that outflow discharges are durably reduced to maximum values of about 100 m^3/s and 40 m^3/s, respectively.
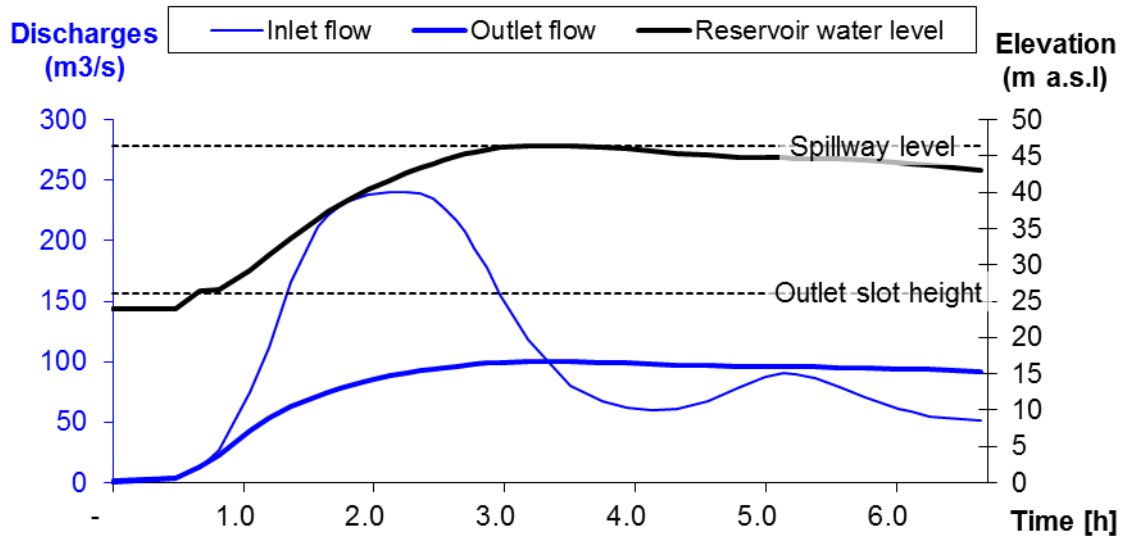
Figure 65 : Time evolution of inflow and outflow discharges for the Brague dam.
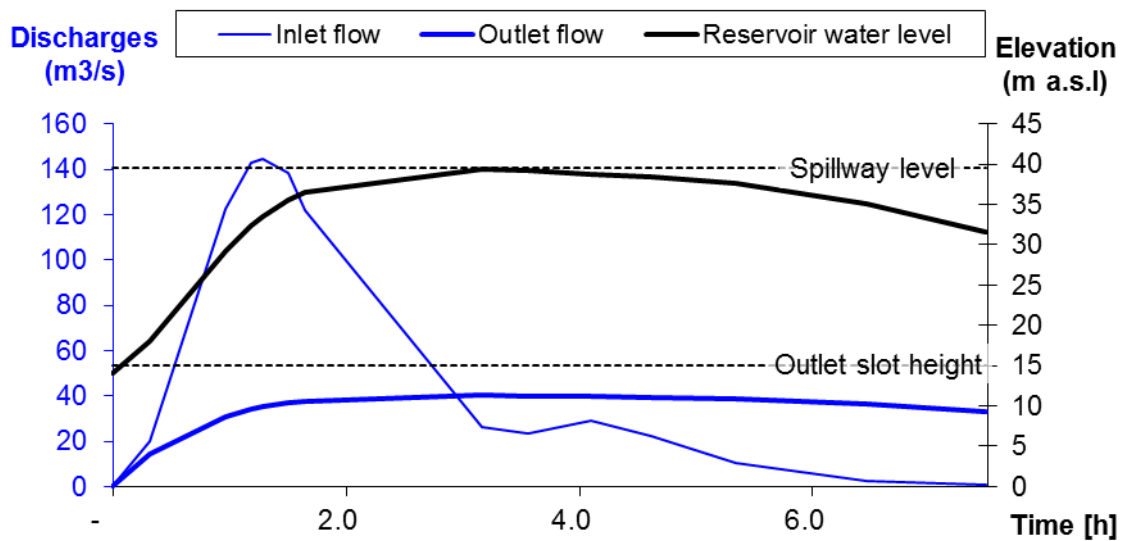

Figure 66 : Time evolution of inflow and outflow discharges for the Valmasque dam.

Such computations should be extended to hydrographs of various return period and the computed out-flow can be introduced as boundary conditions to the model.

6.2.4.2   Adaptations of the hydraulic model for NBS modelling

The giving-room-to-the-river scenarios mostly rely on changes in the river geometry and vegetation type. Both of them are included in the 2D model through the digital elevation model and the roughness coefficients.

In the same line than the 3D analysis that has been performed to reconstruct the bathymetry (see §4.3.2), the widened bed, wider bridges and changes in the river section will be reconstructed in 3D. The land use GIS database will also be changed to take into account the new vegetation types on the modified areas.

6.2.4.3   Adaptations of the CCR runoff model for NBS modelling

In the next step (D6.3), the land use scenarios and NBS strategies developed by IRSTEA will be expressed within the infiltration/runoff inputs for the CCR runoff model. By changing the land use cover data, related runoff coefficients and/or integrating water retention basin within the Digital Terrain Modelling, it is possible to model NBS effect on runoff hazard and thus, to assess the avoided damages after the implementation of such protective measures.

7   Conclusions

This report is the Brague DEMO site contribution to NAIAD Deliverable 6.2 entitled '*From hazards to risk: models for the DEMOs'.*

It first addressed wildfire hazards within the catchment in order to appraise the vulnerability of the flood protection ecosystem services to their local main natural threat. Using a multi-criteria method aggregating hydro-meteo and forest indicators, we demonstrate that forest wildfire hazards are high on average years and extremely high on the whole catchment on dry and hot years. A temporal increasing trend to higher wildfire-prone days has additionally been detected. Firefighters' data demonstrated that indeed wildfire events are common in the catchment but annual burnt areas remain low thanks to the existing high effort in fighting each starting wildfire. The firefighter's capacities are however limited and too spread on the territory to stop all starting fires during particularly dry and hots years for which they are overwhelmed, resulting in the occurrence of a few years experiencing cumulated burnt areas higher than 100 ha. Three wild fire scenarios were created based on expert assessment for later analysis of cascading hazards on floods and erosions: (i) an average fire activity of 5.5 burnt ha; (ii) a large fire of 100 ha as already observed three times since 1973 and (iii) a mega fire of the biggest continuous forest units of the catchment, i.e., reaching 700 ha.

An in-depth hydrological study of the catchment has secondly been performed. In addition to existing values taken from archive reports, modelling of runoff with a distributed CCR model and of river discharge using the distributed Shyreg model were performed. Time was taken to

reconstruct the Oct. 2015 disaster hydrograph at city of Biot for its use in calibration and analysis of the hydraulics;

Two methods were used in a third step to appraise the hydraulics of the Brague catchment:

- A simple "0D" analysis focusing on flood excess volumes and way to deal with it was first implemented. It offers a straightforward and educational protocol, for quantified flood-mitigation assessment of protection strategies, targeted for effectiveness analysis and decision-making involving stakeholder participation. It is based on the concept of flood-excess volume (FEV) i.e., volume exceeding a threshold and generating flood damage. The central question is: what fraction of FEV is reduced, and at what cost, by particular flood-mitigation measures?
- An accurate 2D depth-averaged modelling approach is also in progress to study flood hazards in a much more detailed way. The software was selected for its capacity to compute the transport of large wood pieces. The data used to build and calibrate the model, particularly a campaign of data acquisition dedicated to large wood transport processes is described. The calibration of the model is in progress and its principle is only described so far.

The experience proves that all assets located in flooded areas do not experience damages. This is related to what is sometimes called the exposure that consider that only a certain percentage of assets are indeed damaged due to multiple reasons e.g., first floor elevation above the flood level, garden walls diverting the flows but neglected in the models. An analysis of the CCR database and cross controls with several flood mapping method results was performed to analysis this exposure.

Finally, two works were dedicated to the flood reduction capacities of ecosystem services or of comprehensive NBS strategies:

- The first was a retro-analysis on the south of France of burnt catchments to highlight eventual post-fire changes in hydrology. The work is still in progress but the preliminary results presented here showed no clear trends on daily discharges. A refinement on hourly discharges will be presented in a later stage of NAIAD.
- Comprehensive and integrated flood protection scenarios were secondly tailored for the Brague lowlands, i.e., the Biot and Antibes municipalities. Three strategies were defined, the measures and works' location were mapped and their implementations in the model defined on their principles. This actual implementation will be performed during the last year of NAIAD project and presented in subsequent deliverables. The three strategies are:

- o An NBS-based strategy with intermediate ambition that is likely feasible on the short term. It avoids houses and industrial building removal but widen the river bed and corridor wherever possible.
- o An NBS-based strategy of much higher ambition but with a higher impact on real estates and assets and thus likely feasible on a longer term.
- o A strategy based on large retention basins with a cumulated retention volume of more than 1 Mm^3 in order to deal with events similar to Oct. 2015.

These three protection strategies will be studied, model and evaluated in the later stages of the NAIAD project in order to perform cost-benefit analysis and multi-criteria assessments of their benefits, drawbacks and co-benefits.

References

Amatulli, G., A. Camia, and J. San-Miguel-Ayanz. 2013. Estimating future burned areas under changing climate in the EU-Mediterranean countries. Science of The Total Environment 450–451:209–222.

Arnaud, P. ., Y. . Aubert, D. . Organde, P. . Cantet, C. . Fouchier, and N. . Folton. 2014. Hydro-meteorological risk estimation based on a flood generation model: SHYREG approach: The method, its performances and the associated database [Estimation de l'aléa hydrométéorologique par une méthode par simulation: la méthode SHYREG *: présentation - performances - bases de données]. Houille Blanche:20–26.

Arnaud, P., P. Cantet, and Y. Aubert. 2015. Relevance of an at-site flood frequency analysis method for extreme events based on stochastic simulation of hourly rainfall. Hydrological Sciences Journal 61:36–49.

Arnaud, P., P. Cantet, and J. Odry. 2017. Uncertainties of flood frequency estimation approaches based on continuous simulation using data resampling. Journal of Hydrology 554:360–369.

Arnaud, P., J. Lavabre, B. Sol, and C. Desouches. 2006. Rainfall risk of France [Cartographie de l'aléa pluviographique de la France]. Houille Blanche:102–111.

Arnaud, P., J. Lavabre, B. Sol, and C. Desouches. 2008. Regionalization of an hourly rainfall generating model over metropolitan France for flood hazard estimation [Régionalisation d'un générateur de pluies horaires sur la France métropolitaine pour la connaissance de l'aléa pluviographique]. Hydrological Sciences Journal 53:34–47.

Aronica, G., A. Candela, and M. Santoro. 2002. Changes in the hydrological response of two Sicilian basins affected by fire. FRIEND 2002- Regional Hydrology: Bridging the Gap Between Research and Practice:163–169.

Aubert, Y., P. Arnaud, P. Ribstein, and J.-A. Fine. 2014. La méthode SHYREG débit—application sur 1605 bassins versants en France métropolitaine. Hydrological Sciences Journal 59:993–1005.

Bart, R., and A. Hope. 2010. Streamflow response to fire in large catchments of a Mediterranean-climate region using paired-catchment experiments. Journal of hydrology 388:370–378.

Bertrand, M., and F. Liébault. 2018. Active channel width as a proxy of sediment supply from mining sites in New Caledonia. Earth Surface Processes and Landforms.

Bladé, E., L. Cea, G. Corestein, E. Escolano, J. Puertas, E. Vázquez-Cendón, J. Dolz, and A. Coll. 2014. Iber: herramienta de simulación numérica del flujo en rıos. Revista Internacional de Métodos Numéricos para Cálculo y Diseño en Ingenierıa 30:1–10.

Bokhove, O., M.A. Kelmanson, and T. Kent. 2018a. On using flood-excess volume in flood mitigation, exemplified for the River Aire Boxing Day Flood of 2015. Archived at https://eartharxiv.org.

Bokhove, O., M.A. Kelmanson, T. Kent, G. Piton, and JM. Tacnet. 2018b. Communicating nature-based solutions using flood-excess volume, for three extreme UK and French river floods. sub. to River Research and Application.

Cabinet Merlin. 2016a. Mission D'etude Hydraulique Préalable Au Réamenagement De La Brague Et Ses Affluents - Phase 1 : Collecte De Donnees Et Diagnostic En Situation Actuelle. . villes d'Antibes Juan-les-Pins et de Biot.

Cabinet Merlin. 2016b. Mission Complementaire Relative a L'analyse Hydrologique Et Hydraulique Des Intemperies Du 3 Octobre 2015 - Mémoire explicatif. . villes d'Antibes Juan-les-Pins et de Biot.

Cabinet Merlin. 2016c. Mission d'Etude Hydraulique Préalable Au Réamenagement De La Brague Et Ses Affluents - Phase 2 : Modélisation Hydraulique et Diagnostic en Situation Actuelle. . villes d'Antibes Juan-les-Pins et de Biot.

Castillo, C., R. Pérez, and J. A. Gómez. 2014. A conceptual model of check dam hydraulics for gully control: efficiency, optimal spacing and relation with step-pools. Hydrology and Earth System Sciences 18:1705–1721.

CFBR. 2013. Recommandations pour le dimensionnement des évacuateurs de crues de barrages [recommendations for dams' spillway design]. Page 166 (G. de Travail Dimensionnement des évacuateurs de crues de barrages, Ed.). . Comité Français des Barrages et Réservoirs, Le Bourget-Du-Lac.

Couvert, B., and B. Lefebvre. 1994. Contribution de modèles physiques à l'étude du charriage torrentiel. La Houille Blanche 3:81–90.

Dupire, S., T. Curt, and S. Bigot. 2017. Spatio-temporal trends in fire weather in the French Alps. Science of The Total Environment 595:801–817.

Evette, A., S. Labonne, F. Rey, F. Liebault, O. Jancke, and J. Girel. 2009. History of bioengineering techniques for erosion control in rivers in western europe. Environmental Management 43:972–984.

Folléa-Gautier, ., . ECOMED, and C. Merlin. 2017. Élaboration d'un plan-guide d'aménagement et de gestion durable de la plaine de la Brague - étape 1 : diagnostic dynamique et propositions d'aménagement - Définition d'un périmètre de DUP qui s'inscrit dans un projet de territoire - Comité de pilotage du 8 novembre 2017. . Communauté d'Agglomération Sophia Antipolis.

Folléa-Gautier, ., . ECOMED, and C. Merlin. 2018. Devenir de la plaine de la Brague - Comité de pilotage restreint du 30 mars 2018. . Communauté d'Agglomération Sophia Antipolis.

Garrote, J., F. M. Alvarenga, and A. Dıez-Herrero. 2016. Quantification of flash flood economic risk using ultra-detailed stage–damage functions and 2-D hydraulic models. Journal of Hydrology 541:611–625.

Gems, B., B. Mazzorana, T. Hofer, M. Sturm, R. Gabl, and M. Aufleger. 2016. 3-D hydrodynamic modelling of flood impacts on a building and indoor flooding processes. Natural Hazards and Earth System Sciences 16:1351–1368.

Genialp. 2012. Génie végétal en rivière de montangne - connaissance et retour d'expériences sur l'utilisation d'espèces et de techniques végétales: végétalisation de berges et ouvrages bois. (L. Bonin, A. Evette, P.-A. Frossard, P. Prunier, D. Roman, and N. Valé, Eds.). . Europeen Union and Swiss Confederation.

Gilleland, E., and R. W. Katz. 2016. extRemes 2.0: An Extreme Value Analysis Package in R. Journal of Statistical Software 72:1–39.

Guitet, S. 2018. Fourniture de résultats concernant l'inventaire forestier détaillé des zones de production d'embâcles sur la Brague. . Institut national de l'information géographique et forestière (IGN).

Hallema, D. W., G. Sun, P. V. Caldwell, S. P. Norman, E. C. Cohen, Y. Liu, K. D. Bladon, and S. G. McNulty. 2018. Burned forests impact water supplies. Nature Communications 9.

Hunzinger, L. 2014. Freeboard analysis in river engineering and flood mapping-new recommendations. Pages 31–37 Special Session on Swiss Competences in River Engineering and Restoration of the 7th International Conf. on Fluvial Hydraulics, RIVER FLOW 2014.

Lavabre, J., C. Fouchier, N. Folton, and Y. Gregoris. 2003. SHYREG : une méthode pour l'estimation régionale des débits de crue. Application aux régions méditerranéennes françaises. Ingénieries:97–111.

Lebouc, L., and O. Payrastre. 2017. Reconstitution et analyse des débits de pointe des crues du 3 octobre 2015 dans les Alpes Maritimes.Convention DGPR-Ifsttar 2016. Page 18p. . IFSTTAR - Institut Français des Sciences et Technologies des Transports, de l'Aménagement et des Réseaux.

Lindénia. 2012. Plan De Gestion 2011- 2018 Des Cours D'eau Du Bassin De La Brague Études Et Inventaires Complementaires Etude Complementaire Des Zones D'expansion Des Crues Du Bassin Versant. . SIAQUEBA.

Lindénia. 2016. Retour d'Expérience sur l'événement de crue du 3 octobre 2015 : Expertise hydrologique. . SIAQUEBA.

Mazzorana, B., F. Comiti, C. Scherer, and S. Fuchs. 2012. Developing consistent scenarios to assess flood hazards in mountain streams. Journal of Environmental Management 94:112–124.

Moncoulon, D., D. Labat, J. Ardon, E. Leblois, T. Onfroy, C. Poulard, S. Aji, A. Rémy, and A. Quantin. 2014. Analysis of the French insurance market exposure to floods: a stochastic model combining river overflow and surface runoff. Natural Hazards and Earth System Science 14:2469–2485.

Moritz, M. A., P. F. Hessburg, and N. A. Povak. 2011. Native Fire Regimes and Landscape Resilience. Pages 51–86 in D. McKenzie, C. Miller, and D. A. Falk, editors. The Landscape Ecology of Fire. . Springer Netherlands, Dordrecht.

Moritz, M. A., M. E. Morais, L. A. Summerell, J. M. Carlson, and J. Doyle. 2005. Wildfires, complexity, and highly optimized tolerance. Proceedings of the National Academy of Sciences 102:17912–17917.

Naulin, J. P., D. Moncoulon, S. L. Roy, R. Pedreros, D. Idier, and C. Oliveros. 2016. Estimation of insurance-related losses resulting from coastal flooding in France. Natural Hazards and Earth System Sciences 16:195–207.

Owens, P., T. Giles, E. Petticrew, M. Leggat, R. Moore, and B. Eaton. 2013. Muted responses of streamflow and suspended sediment flux in a wildfire-affected watershed. Geomorphology 202:128–139.

Parker, G., P. R. Wilcock, C. Paola, W. E. Dietrich, and J. Pitlick. 2007. Physical basis for quasi-universal relations describing bankfull hydraulic geometry of single-thread gravel bed rivers. Journal of Geophysical Research: Earth Surface 112:1–21.

Pengal et al. 2017. DELIVERABLE 6.1 Catchment Characterization Report. . NAIAD H2020 project (Grant Agreement nᵒ 730497).

Pengal et al. 2018. DELIVERABLE 6.2 From hazards to risk: models for the DEMOs - Part 5: Slovnia - Glinscica catchment DEMO. . NAIAD H2020 project (Grant Agreement nᵒ 730497).

Piégay, H., A. Alber, L. Slater, and L. Bourdin. 2009. Census and typology of braided rivers in the French Alps. Aquatic Sciences 71:371–388.

Piton, G., and A. Recking. 2016. Design of sediment traps with open check dams. II: woody debris. Journal of Hydraulic Engineering 142:1–17.

Piton, G., A. Recking, J. Le Coz, H. Bellot, A. Hauet, and M. Jodeau. 2018. Reconstructing Depth-Averaged Open-Channel Flows Using Image Velocimetry and Photogrammetry. Water Resources Research 54:4164–4179.

Posi, S., L. Montabonnet, A. Recking, A. Evette, H. Bellot, F. Ousset, X. Ravanat, G. Piton, and L. Solari. 2018. Experimental study of riverbank protection with bio-engineering techniques. E3S Web of Conferences 40:05023.

Préfécture des Alpes-Maritimes. 2016. Inondations des 3 et 4 octobre 2015 dans les Alpes-Maritimes - retour d'experience. . République Française.

Préfécture des Alpes-Maritimes. 2017. Suite des intempéries du 3 octobre 2015 - Porter à connaissance communes de Biot et Antibes. . République Française.

Prométhée. 2018. PROMÉTHÉE 2 : La banque de données sur les incendies de forêts en région Méditerranéenne en France.

Puttock, A., H. A. Graham, A. M. Cunliffe, M. Elliott, and R. E. Brazier. 2017. Eurasian beaver activity increases water storage, attenuates flow and mitigates diffuse pollution from intensively-managed grasslands. Science of The Total Environment 576:430–443.

AE-RMC, . 2016. Délimiter l'espace de bon fonctionnement des cours d'eau. . Agence de l'eau Rhône Méditerranée Corse.

RTM06. 2016a. Analyse du phénomène d'embâcle sur la Brague Crue du 3 Octobre 2015. ONF-RTM.

RTM06. 2016b. Etude sur la formation et le transport des embâcles lors d'une crue, Analyse du phénomène sur la crue de la Brague du 03-10-2015. . ONF-RTM.

RTM06. 2018. Inventaire Détaillé Des Zones De Production D'embâcles Sur La Brague Et Estimations Des Coûts De Gestion Du Cours D'eau Des Boisements De Berge Et De Versant - Partie Rtm De L'appel D'offre Irstea 18_gren_35. . ONF-RTM.

Ruiz-Villanueva, V., E. Bladé, M. Sánchez-Juny, B. Marti-Cardona, A. Dɪez-Herrero, and J. M. Bodoque. 2014a. Two-dimensional numerical modeling of wood transport. Journal of Hydroinformatics 16:1077.

Ruiz-Villanueva, V., J. M. Bodoque, A. Dɪez-Herrero, and E. Bladé. 2014b. Large wood transport as significant influence on flood risk in a mountain village. Natural Hazards 74:967–987.

Ruiz-Villanueva, V., E. B. Castellet, A. Dɪez-Herrero, J. M. Bodoque, and M. Sánchez-Juny. 2013. Two-dimensional modelling of large wood transport during flash floods. Earth Surface Processes and Landforms 39:438–449.

Ruiz-Villanueva, V., B. Wyzga, H. Hajdukiewicz, and M. Stoffel. 2016a. Exploring large wood retention and deposition in contrasting river morphologies linking numerical modelling and field observations. Earth Surface Processes and Landforms 41:446–459.

Ruiz-Villanueva, V., B. Wyzga, P. Mikus, H. Hajdukiewicz, and M. Stoffel. 2016b. The role of flood hydrograph in the remobilization of large wood in a wide mountain river. Journal of Hydrology 541:330–343.

Ruiz-Villanueva, V., B. Wyzga, P. Mikus, M. Hajdukiewicz, and M. Stoffel. 2017. Large wood clogging during floods in a gravel-bed river: the Dlugopole bridge in the Czarny Dunajec River, Poland. Earth Surface Processes and Landforms.

Ruiz-Villanueva, V., B. Wyzga, J. Zawiejska, M. Hajdukiewicz, and M. Stoffel. 2016c. Factors controlling large-wood transport in a mountain river. Geomorphology 272:21–31.

Saxe, S., T. S. Hogue, and L. Hay. 2018. Characterization and evaluation of controls on post-fire streamflow response across western US watersheds. Hydrology and Earth System Sciences 22:1221–1237.

Schloerke, B., J. Crowley, D. Cook, F. Briatte, M. Marbach, E. Thoen, A. Elberg, and J. Larmarange. 2018. GGally: Extension to 'ggplot2.

Schmocker, L., and Weitbrecht. 2013. Driftwood: Risk analysis and engineering measures. Journal of Hydraulic Engineering 139:683–695.

Seibert, J., and J. J. McDonnell. 2010. Land-cover impacts on streamflow: a change-detection modelling approach that incorporates parameter uncertainty. Hydrological Sciences Journal 55:316–332.

Strosser, P., G. Delacámara, H. Hanus, H. Williams, and N. Jaritt. 2015. A guide to support the selection, design and implementation of Natural Water Retention Measures in Europe. Capturing the multiple benefits of nature-based solutions. . Publications Office of the European Union.

Te Chow, V. 1959. Open-channel hydraulics. McGraw-Hill, New York.

Vidal, J.-P., E. Martin, L. Franchistéguy, M. Baillon, and J.-M. Soubeyroux. 2010. A 50-year high-resolution atmospheric reanalysis over France with the Safran system. International Journal of Climatology 30:1627–1644.

Van Wagner, C. 1987. Development and structure of the Canadian Forest Fire Weather Index System. . Canadian Forestry Service, Forestry Technical Report 35.

Wohl, E. 2006. Human impacts to mountain streams. Geomorphology 79:217–248.

Appendix

Appendix 1. Rainfall and discharge data
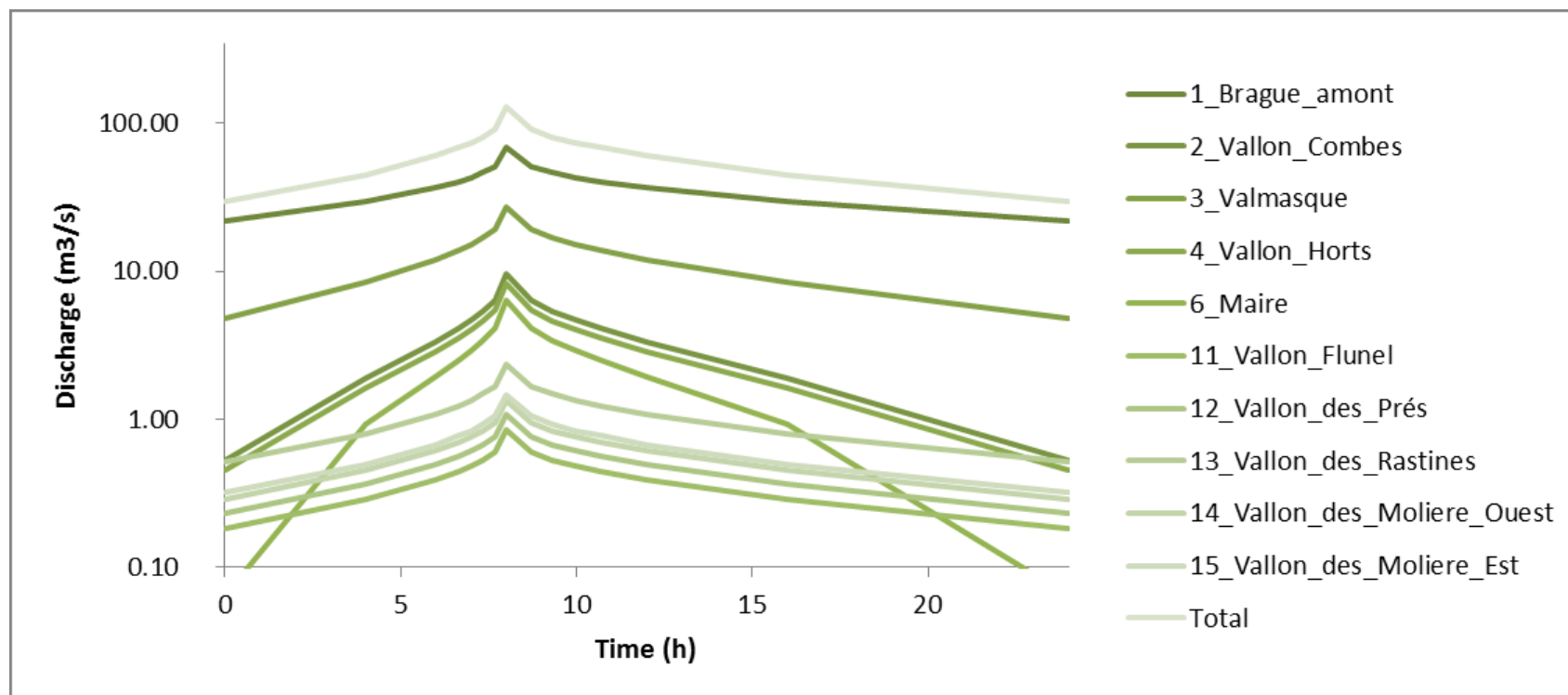
A 10 years return period hydrographs

t(h)	1_Brague_amont	2_Vallon_Combes	3_Valmasque	4_Vallon_Horts	6_Maire	11_Vallon_Flunel	12_Vallon_des_Prés	13_Vallon_des_Rastines	14_Vallon_des_Moliere_Ouest	15_Vallon_des_Moliere_Est	Total
0	22.07	0.52	4.85	0.45	0.06	0.18	0.23	0.51	0.29	0.32	29.50
4	29.65	1.88	8.47	1.61	0.93	0.29	0.36	0.80	0.45	0.50	44.93
6	36.79	3.32	11.98	2.85	1.92	0.39	0.49	1.08	0.61	0.67	60.11
6.67	40.61	4.13	13.89	3.55	2.51	0.44	0.56	1.24	0.70	0.77	68.40
7	43.24	4.67	15.09	4.02	2.90	0.48	0.61	1.34	0.75	0.84	73.94
7.33	46.50	5.38	16.79	4.63	3.42	0.53	0.67	1.48	0.83	0.92	81.14
7.67	51.38	6.41	19.23	5.52	4.17	0.60	0.76	1.68	0.94	1.04	91.73
8	**69.48**	**9.56**	**27.50**	**8.23**	**6.43**	**0.84**	**1.07**	**2.36**	**1.33**	**1.47**	**128.28**
8.7	51.38	6.41	19.23	5.52	4.17	0.60	0.76	1.68	0.94	1.04	91.73
9.3	46.50	5.38	16.79	4.63	3.42	0.53	0.67	1.48	0.83	0.92	81.14
10	43.24	4.67	15.09	4.02	2.90	0.48	0.61	1.34	0.75	0.84	73.94

10.7	40.61	4.13	13.89	3.55	2.51	0.44	0.56	1.24	0.70	0.77	68.40
12	36.79	3.32	11.98	2.85	1.92	0.39	0.49	1.08	0.61	0.67	60.11
16	29.65	1.88	8.47	1.61	0.93	0.29	0.36	0.80	0.45	0.50	44.93
24	22.07	0.52	4.85	0.45	0.06	0.18	0.23	0.51	0.29	0.32	29.50

Note the log y axis.

B   100 years return period hydrographs

t(h)	1_Brague _amont	2_Vallon_ Combes	3_Valmas que	4_Vallon_ Horts	6_Maire	11_Vallon _Flunel	12_Vallon _des_Prés	13_Vallon _des_Rast ines	14_Vallon _des_Mol iere_Oues t	15_Vallon _des_Mol iere_Est	Total
0	46.6	1.1	8.6	0.8	0.5	0.4	0.5	1.1	0.6	0.7	60.7
4	61.3	3.4	16.2	2.7	1.9	0.6	0.7	1.6	0.9	1.0	90.4
6	75.4	6.2	24.3	5.1	3.7	0.8	1.0	2.2	1.2	1.4	121.2
6.67	83.8	7.9	29.2	6.6	4.9	0.9	1.1	2.5	1.4	1.6	139.9
7	89.5	9.1	32.4	7.7	5.7	1.0	1.3	2.8	1.6	1.7	152.7
7.33	96.8	10.7	36.7	9.1	6.8	1.1	1.4	3.1	1.7	1.9	169.3
7.67	108.7	13.5	43.8	11.5	8.6	1.3	1.6	3.6	2.0	2.2	196.7
8	**175.5**	**25.0**	**74.2**	**21.6**	**16.6**	**2.2**	**2.8**	**6.1**	**3.4**	**3.8**	**331.1**
8.7	108.7	13.5	43.8	11.5	8.6	1.3	1.6	3.6	2.0	2.2	196.7
9.3	96.8	10.7	36.7	9.1	6.8	1.1	1.4	3.1	1.7	1.9	169.3
10	89.5	9.1	32.4	7.7	5.7	1.0	1.3	2.8	1.6	1.7	152.7
10.7	83.8	7.9	29.2	6.6	4.9	0.9	1.1	2.5	1.4	1.6	139.9
12	75.4	6.2	24.3	5.1	3.7	0.8	1.0	2.2	1.2	1.4	121.2
16	61.3	3.4	16.2	2.7	1.9	0.6	0.7	1.6	0.9	1.0	90.4
24	46.6	1.1	8.6	0.8	0.5	0.4	0.5	1.1	0.6	0.7	60.7

Note the log y axis.